Development of Climate Change Scenarios for the South Nation Watershed

Abdullah Alodah

A Thesis submitted under the supervision of
Dr. Ousmane Seidou

Presented to the University of Ottawa in Partial Fulfillment of the Requirements for Master of Applied Science in Civil Engineering

Under the auspices of the Ottawa-Carleton Institute for Civil Engineering

uOttawa

University of Ottawa

Ottawa, Ontario, Canada

Abstract

Climate change studies are crucial to assist decision-makers in understanding future risks and planning adequate adaptation measures. In general, Global/Regional Climate Models (GCMs/RCMs) achieve coarse resolutions, and are thus unable to provide sufficient information to conduct local climate assessments. Downscaling, defined as a method that derives local to regional-scale (10 to 100 km) information from larger-scale models or data analyses, is used to address this deficiency. In this thesis, a particular downscaling technique, known as the Quantile-Quantile transformation, was used to adjust the statistical distribution of RCM variables to match the statistical distribution of the observed variables generated by two RCMs: the Canadian Regional Climate Model version 3.7.1 and the ARPEGE model, on the historical period (1961-2001). The analyses presented in this study were applied to daily precipitation as well as maximum and minimum temperatures in the South Nation watershed in Eastern Ontario, Canada. The two-sample Kolmogorov–Smirnov test indicated that the Quantile-Quantile transformation improved the shape of the PDF of RCM-simulated climate variables. The results suggest that, under the A1B scenario, temperatures in the watershed would rise significantly and there would be an increment in precipitation occurrence and intensity. Trend analysis was performed on the 1961 to 2001 and 2041 to 2081 timeframes, using the Mann-Kendall test and the Sen's slope estimator. Discernible, often significant, increases of maximum and minimum temperatures were found for the 1961 to 2001 period, and stronger ascending slopes

for the 2041 to 2081 period. However, there was marginal evidence of changes in the time series of maximum and accumulated annual precipitation for both periods. The study also outlined how the frequency and intensity of some extreme weather events will evolve in the 2041-2081 period in response to the rise in atmospheric GHG concentrations. Projected impacts were investigated by tracking future changes in four extreme temperature indices and three precipitation indices. It was predicted that heavy precipitation events and warm spells will occur more frequently and intensely, while extreme cold events will be weaker, and some will be hardly observed.

***Keywords*:** Climate change, Statistical downscaling, Quantile-Quantile transformation, Extreme events analysis

Acknowledgment

All Praises and Thanks are due to Allah; the Creator and the Lord of the Heavens and the Earth. "Indeed! He has power over all things."

I owe a great debt of gratitude to my wonderful parents, Sulaiman and Sharifah, whose inseparable support and prayers are always my greatest motivation. I intend to always do my best to make them proud and meet their expectations. I deeply appreciate the persistent support of my lovely wife Ruba, whose dedication, understanding and tireless confidence in me have lightened the load. I greatly appreciate her encouragement and patience towards myself and our little one, Khallad. Many thanks also go to my siblings, who keep encouraging me to reach my objectives. My brother Ahmad deserves special thanks for his help with Khallad's official documents.

It has been a privilege to work closely with my thesis supervisor Professor Ousmane Seidou, who helped me tremendously throughout this research. I am so grateful for his boundless support and encouragement. Thanks are extended to my thesis committee members, Dr. Ioan Nistor, Dr. Mohammad Rayhani and Dr. Sai Vanapalli, for their constructive input and guidance. I also wish to express my appreciation to my colleagues, Gado Djibo Abdouramane and Ali Hussein, for their invaluable support.

Finally, I am very grateful to Qassim University, the Ministry of Education and the Saudi Arabian cultural bureau in Canada for sponsoring my educational journey.

Abdullah,
Jan 25th, 2015

Table of Contents

List of Figures

List of Tables

List of Acronyms

Acronym	Definition
AD	Anderson Darling test
ARPEGE	Action de Recherche Petite Echelle Grande Echelle
CDD	Consecutive Dry Days
CDF	Cumulative Distribution Function
CDF	Probability Distribution Function
CRCM	Canadian Regional Climate Models
CWD	Consecutive Wet Days
ETCCDMI	Expert Team on Climate Change Detection Monitoring and Indices and/or the European project
FD0	Frost Days
GCM	Global Climate Models or General Circulation Model
GEV	Generalized Extreme Value distribution
GHG	Greenhouse Gases
ID0	Icing Days
IDF	Intensity- Duration- Frequency curves
IPCC	the Intergovernmental Panel on Climate Change
KS	the Kolmogorov–Smirnov test (K–S test)
MK	Mann-Kendall Trend Test

ML	Maximum Likelihood method
mm	Millimeter
Obs	Observations
PRCP	Daily Precipitation
PRCPTOT	the annual total precipitation
Q-Q	Quantile-Quantile downscaling
R20	Count of very heavy precipitation days (PRCP > 20mm)
RClimDex	Climate indices estimation package in R software
RCM	Regional Climate Models
RCPs	Representative Concentration Pathways
SRES	Special Report on Emissions Scenarios
SNW	The South Nation Watershed
STARDEX	Statistical and Regional Dynamical Downscaling of Extremes for European Regions
SU25	Summer Days
T_{MAX}	Daily Maximum Temperature
T_{MIN}	Daily Minimum Temperature
TR20	Tropical Nights
α	Significance Level
°C	The degree Celsius

Chapter 1. INTRODUCTION

1.1 Overview

Extensive investigation of the potential adverse effects of global climate change is required, to help the scientific community, stakeholders and decision-makers plan adequate adaptation measures. Concerns about the impact of climate change on the environment and key sectors of the economy have grown significantly, particularly among scientific researchers, social activists, economic analysts and other concerned parties.

Climate change over the next century is unavoidable due to the existing level of greenhouse gases (GHG), and all we can do now is limit the impact and adapt to the adverse consequences. It is widely accepted that climate change will have major effects on certain essentials, such as water, food and general health (Campbell-Lendrum & Corvalan, 2007). Long term strategies in water resource management require sufficient knowledge of how key hydrometeorological variables will change. Predicting changes in climate involves investigating the two most important input parameters: temperature and precipitation. Awareness of projected shifts and their impact can lead to selection of the most effective mitigation and adaptation options.

Climate change was initially defined by the UNFCCC (1992) as, "a change of climate which is attributed directly or indirectly to human activity that alters the composition of the global atmosphere and which is in addition to natural climate variability observed over comparable time periods". There is broad scientific agreement that increased concentration of global GHG in the atmosphere accelerates the increase of air temperatures. Substantial anthropogenic GHG increased dramatically over the last three decades of the twentieth century, and are expected to continue to increase in the future. Consequently, the higher air temperatures will undoubtedly alter the hydrological cycle.

The primary evidence of climate change is obtained from observations of global atmospheric fluctuations. According to the Intergovernmental Panel on Climate Change (IPCC, 2007), the average global air temperature increased by approximately 0.6 ± 0.2 °C over the last century, which is considered to be the greatest increase over the past thousand years. Historical records prove that there is no uniform rate of global change due to variations in location and anthropogenic forcings (IPCC, 2007). In Canada specifically, the average annual temperature has increased by 1.1 °C over the last century, one of the highest rates of warming on the planet (Cunderlik & Simonovic, 2005; Lemmen & Warren, 2004). When compared to previous records, Canada has generally had a warmer and wetter climate over the last half of the 20th century. Moreover, depending on emission scenarios, the IPCC projects a further increase in global air temperature of between 1 and 5 °C for the 21st century. Various globally

projected trends in precipitation predict a wetter climate in the northern hemisphere, particularly in the fall and winter. A decrease in precipitation in the tropic and subtropical regions of both hemispheres is also expected (Cunderlik & Simonovic, 2005).

Temperature changes in the future will be accompanied by other fluctuations, including the occurrence and intensity of rainfall, snow and ice, which can lead to increased risk of extreme weather events such as heat waves, hurricanes, cyclones, floods, droughts and forest fires (IPCC, 2007). Such severe events can also result in extensive physical damage. Some believe we are already witnessing the impacts of global warning, as there are more reported incidents of extreme anomalies such as Hurricane Katrina in the US in 2005, which caused the loss of over 1500 lives and severe economic consequences.

Extensive historical compilation of three hundred years of temperature measurements has informed the current knowledge of climate change (Bosetti & Lubowski, 2010). Anthropogenic contribution to climate change is widely recognized, and societies must act accordingly to adapt to its effects, even if mitigation is successful (New *et al*., 2009). Therefore, comprehensive understanding of climate change (i.e. how to evaluate and respond) is highly important for engineers, policy-makers and other involved parties. Potential climate changes are likely to affect numerous sectors, including food and agriculture, ecosystems, energy and infrastructure. Most regions of Canada are potentially affected by water-related difficulties such as floods, droughts and water quality deterioration. Thus, as asserted by Lemmen and Warren (2004), the impact

of climate change on Canadian water resources should be considered one of the highest-priority adaptation areas.

This study will investigate some possible 21st century climate patterns in the South Nation watershed in Ontario, Canada. Temperatures and precipitation extremes, and the subsequent potential future changes, are evaluated and compared under the A1B scenario, using two regional climate models. One of the innovations of this study is that it is the first to analyze and evaluate the anticipated impacts of climate change on the study area.

1.2 Thesis Objectives

The essential goal of this study is to generate a projection of the meteorological variables of precipitation and maximum and minimum temperatures that corresponds to a given scenario of future climate (A1B SERS), based on two regional climate models: the Canadian Regional Climate Model and the ARPEGE Regional Climate Model; ARPEGE refers to Action de Recherché Petite Echelle Grande Echelle, which translates as research project on small and large scales, as stated by Déqué *et al*. [1994]). The South Nation watershed is the study area, and the specific objectives of the study are to perform the following analysis using these two regional climate models:

i. Bias correction of the RCM outputs using the Quantile-Quantile transformation;

ii. Investigation of changes in the frequency and intensity of precipitation;

iii. Examination of changes of maximum and minimum temperatures;

iv. Comparison of the projections of the two different climate models, and formation of an understanding of climate change impact on temperature and precipitation variability; and,

v. Study of the impact of projected climate change on extreme temperature and precipitation events.

1.3 Thesis Organization

The thesis is organized into six chapters. Chapter 1 provides a brief introduction to the topic, the main objectives and the thesis structure. Chapter 2 includes a climate change literature review, forms the scientific basis required to perform the study, describes downscaling methods and provides examples of previous studies conducted using different approaches. Chapter 3 summarizes the geographic and historical features of the study area, and describes the source of the meteorological and climate model data. Chapter 4 explains the methodology. Chapter 5 presents and discusses the corrected climate model outputs, including the results of trend analysis and extreme values analysis of current and future precipitation, and maximum and minimum temperatures projections. Finally, Chapter 6 provides a summary of the findings, and presents several recommendations for further study.

Appendices are included to describe the performance of the model based on p-values of KS test, and the results of the four CRCM variables described in this research.

Chapter 2. LITERATURE REVIEW

2.1 Introduction

Recognition of the importance of climate change assessments has gradually increased in the scientific community over the past twenty years (e.g. UNFCCC 1992; Hewitson and Crane 1996; Wilby and Wigley 1997; Wilby *et al*., 1998; Xu 1999; Giorgi *et al*., 2001; Bosetti and Lubowski 2010). It was motivated by the observed and growing evidences of global atmospheric changes (Hook *et al*., 2010). Climate change influences must be taken into consideration in order to develop effective adoption and mitigation plans.

This chapter provides an overview of the literature on observed climate change, its triggers, and potential future climate scenarios. It also describes techniques used to generate data sets that are representative of the future climate, such as global and regional climate models simulations, downscaling and bias correction.

2.2 Climate Change Overview

The term ‘climate change’ was recently defined by the Intergovernmental Panel on Climate Change as, "a change in the state of the climate that can be identified (e.g. using statistical tests) by changes in the mean and/or the variability of its properties, and that persists for an extended period, typically decades or longer" (IPCC, 2007). The observations of global temperatures and average sea levels, for example, indisputably

show differences that are mainly due to human activities in the last century (IPCC, 2007). Figure 2.1 displays observed changes in the global temperature, sea level and northern hemisphere snow cover.

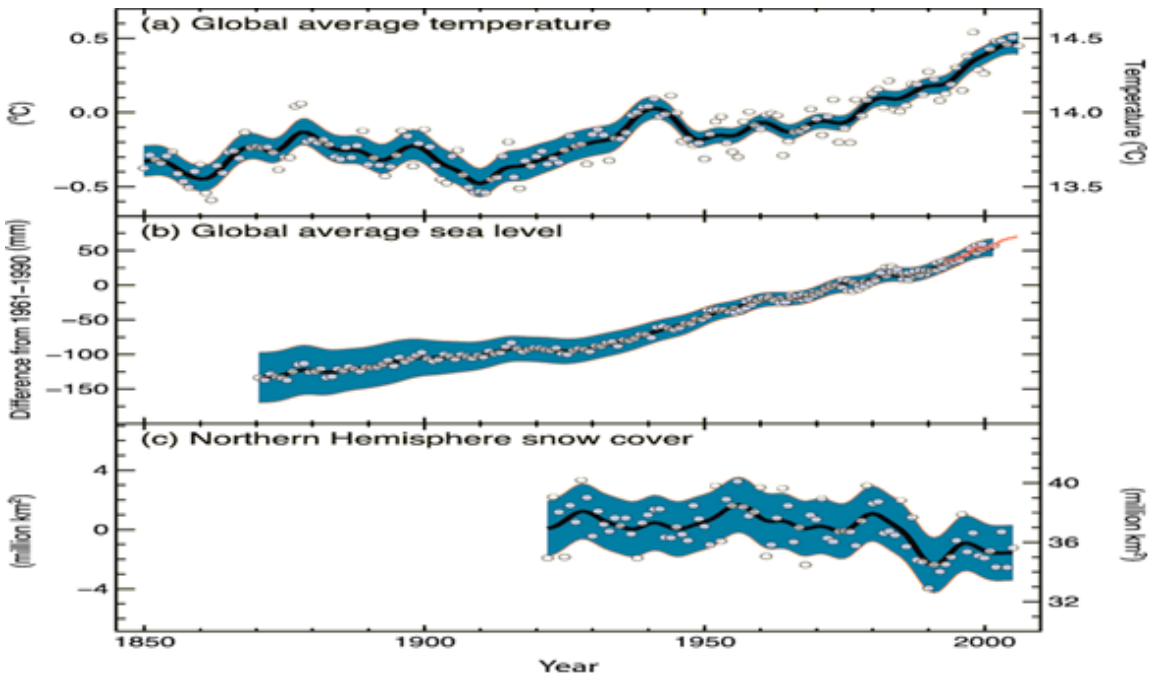

Figure 2.1 Observed increase in (a) global temperature and (b) sea level as well as (c) observed decrease in Northern Hemisphere snow cover relative to corresponding averages for the period 1961 to 1990 (IPCC, 2007).

2.2.1 Causes of Climate Change

Global emissions of long-lived Green House Gases (GHG) are the fundamental cause of climate change. GHGs are substances in the atmosphere that absorb and emit radiation, which traps heat and subsequently alters the climate.

According to IPCC (2007), GHGs emitted solely by human activities increased 70% over the last thirty years of the twenty century, as shown in Figure 2.2. Carbon dioxide (CO_2) is considered the most substantial anthropogenic GHG, due to its long lifetime (up to thousands of years) and being the largest contributor to radiative forcing (Goosse *et al.*, 2010). In 2004, CO_2 added approximately 38 gigatonnes (Gt), over 77% of the total anthropogenic GHG emissions.

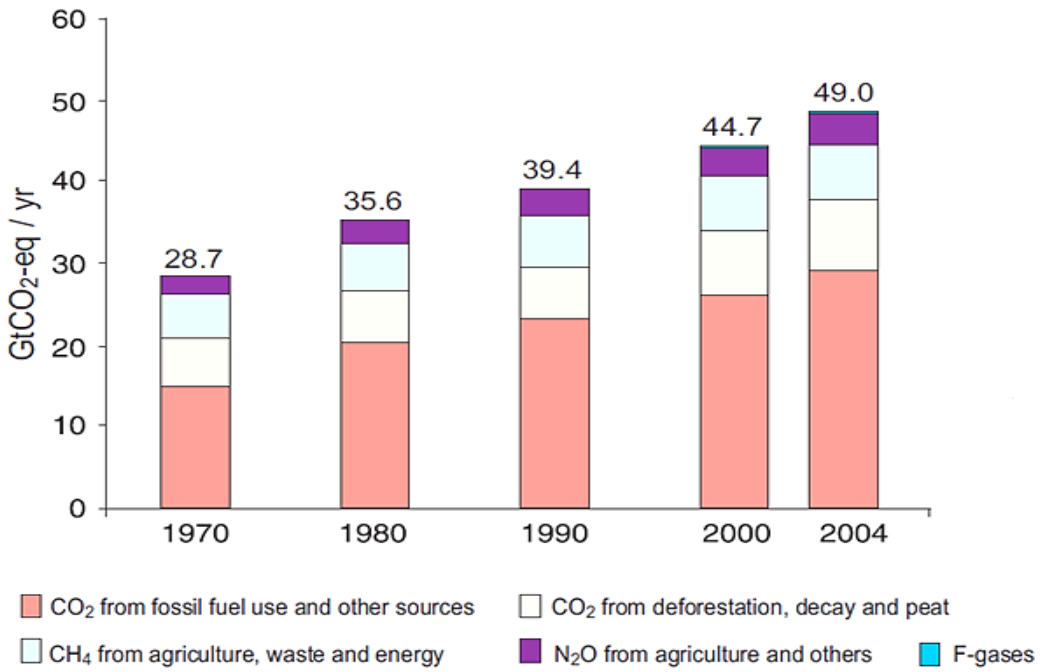

Figure 2.2 Global annual emissions of anthropogenic GHGs (1970 to 2004) (IPCC, 2007).

The large rise in GHG emissions is due to many factors, including meeting high energy demands by burning fossil fuel, transportation and industry (Canadell *et al.*,

2007). However, minor emissions caused by other sectors, such as residential and commercial buildings, forestry and agriculture, have increased as well, though at a lower rate (IPCC, 2007). Thus, the vast majority of GHG emissions are produced by anthropogenic sources.

2.2.2 Climate Change Scenarios

The extent of future climate change depends heavily on the choice of GHG emission scenario. Climate scenarios are used to estimate changes in the climate patterns of the 21st century and beyond by applying various assumptions. Various socio-economic, demographic and technological changes assumptions are used to obtain future GHG emissions of aerosols as well as various pollutants in the atmosphere (Goosse *et al.*, 2010). Scenarios were established to symbolize the range of driving forces and emissions. The Special Report on Emissions Scenarios (SRES) was introduced by the IPCC, and has been used in climate change studies since 2000. However, a new set of scenarios with some amendments by expert groups (known as Representative Concentration Pathways (RCPs)) is replacing the SRES scenarios (Moss *et al*., 2008, 2010; Van Vuuren *et al.*, 2012). Both scenario sets will be briefly discussed in this section.

2.2.3 Special Report on Emissions Scenarios (SRES)

SRES is a set of four families (A1, B1, A2 and B2) that comprise 40 scenarios encompassing various possibilities. These families can be characterized as follows (IPCC 2000, IPCC 2007):

- The A1 family proposes very rapid economic growth, an increase in the global population peaking in 2050, and rapid introduction of efficient technologies. A1 is categorized into three main directions of technological change: A1F, A1T and A1B. The latest, A1B SRES, has received significant attention in recent years, considering that it represents a balance across all fossil and non-fossil energy sources.
- The B1 family proposes similar population growth and world convergence as A1, but with economic growth based more on efficient service technologies.
- The A2 family proposes an extremely heterogeneous world and high population growth, with no shift toward efficient technologies.
- The B2 family proposes intermediate population and economic growth, with local economically sustainable solutions and a more gradual introduction of new technologies than B1 and A1.

SRES scenarios rely on GHG emissions from 2000 to 2100, without any changes or developments of current climate policies. Figure 2.3 illustrates the projected emissions of CO_2 (the dominant anthropologically generated GHG) of the SRES scenarios, as well as CO_2 concentrations. Nonetheless, SRES scenarios have been criticized for being

exaggerating resource availability, and for having unrealistic expectations of the future use of fossil fuels (Hook *et al.*, 2010).

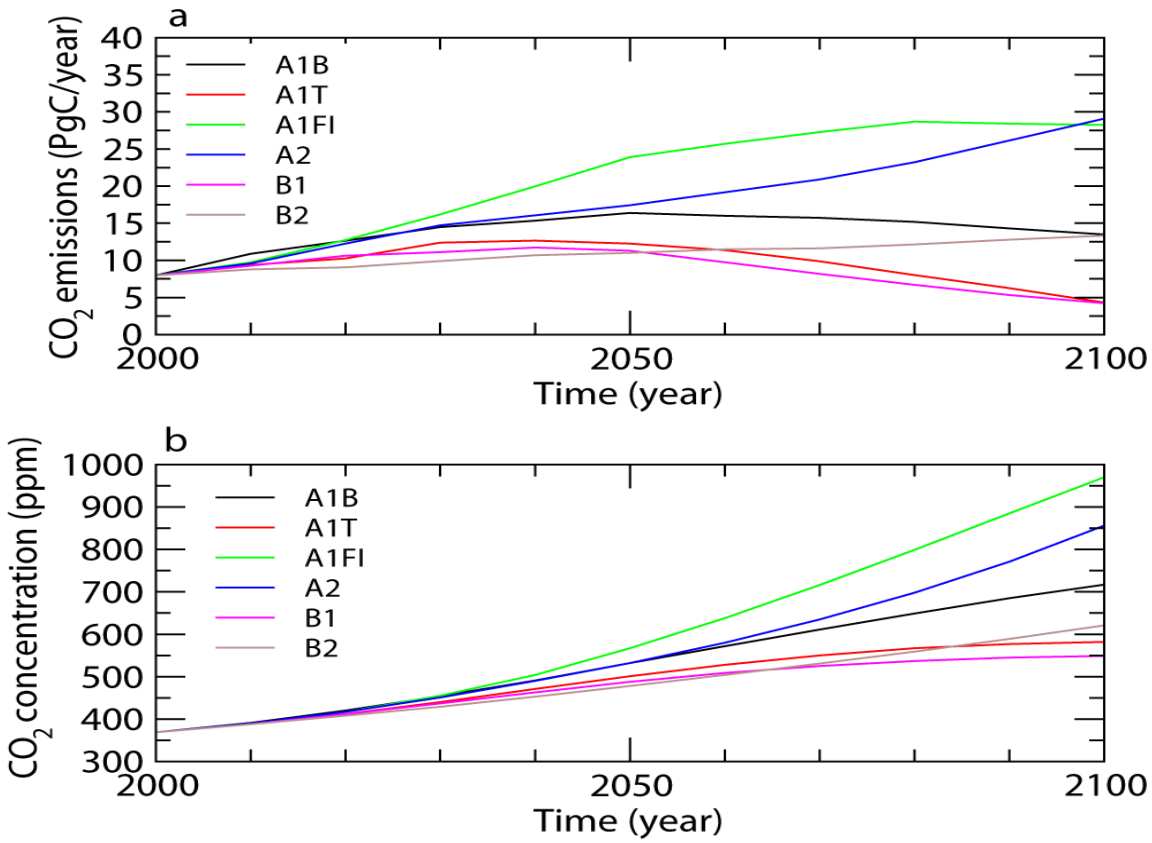

Figure 2.3 Global GHG emissions (a) and atmospheric concentrations (b) of SRES scenarios (in $GtCO_2$-eq / year) (Goosse *et al.*, 2010).

2.2.4 Representative concentration pathways (RCPs)

A new set of scenarios, known as Representative Concentration Pathways (RCPs), that implement some mitigation policies has been developed by four different modeling groups for AR5, the newest IPCC assessment report (see Clarke *et al*., 2007; Riahi *et al*.,

2011; Masui *et al*., 2011; Van Vuuren *et al.*, 2011). Although this fifth IPCC assessment report was scheduled to be published in 2014, the final draft in 2013 suggested these scenarios have different goals, in terms of radiative forcing to the end of the 21st century and beyond.

Since RCP scenarios have been recently approved by IPCC, a limited number of sources have discussed them in depth. Moreover, social-economic projections are not fully covered. However, the radiative forcing, an important component in terms of climate modeling, is known. Radiative forcing and GHGs concentration of RCP scenarios are described in Table 2.1.

Table 2.1 The four RCPs radiative forcing pathway (Adopted from Moss *et al.*, 2010)

RCP Scenario	Radiative Forcing (W/m²)	Concentration (ppm)
RCP 8.5	Peaking up to 8.5 in 2100	1,370 CO_2-equiv. in 2100
RCP 6	Stabilization without overshoot pathway to 6 W/m² at stabilization after 2100	~ 850 CO_2-equiv. at stabilization after 2100
RCP 4.5	Stabilization without overshoot pathway to 4.5 W/m² at stabilization after 2100	~ 650 CO_2-equiv. at stabilization after 2100
RCP 3-PD2 (or RCP2.6)	Peak in radiative forcing at ~ 3 W/m² before 2100 and decline instance, (i.e. nearly no emission of CO_2 after 2080)	~ 490 CO_2-equiv. before 2100, and then declines

The projected CO_2 emissions (the dominant anthropologically generated GHGs) of the RCP scenarios, as well as CO_2 concentrations are illustrated Figure 2.4. It is important

to note that neither the SRES nor the RCPs will necessarily be the best future scenario (Goosse *et al.*, 2010).

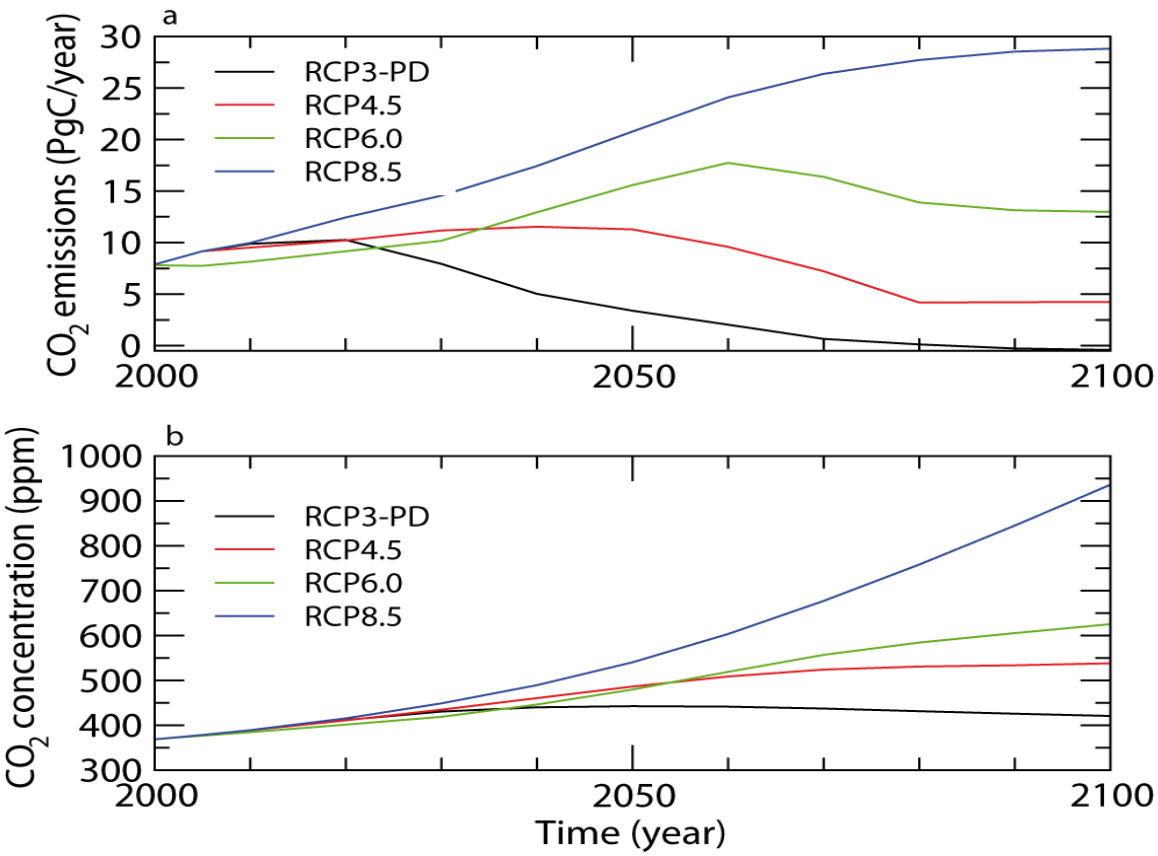

Figure 2.4 Global GHG emissions (a) and atmospheric concentrations (b) of RCP scenarios (in $GtCO_2$-eq / year) (Goosse *et al.*, 2010).

2.4 Global Climate Models (GCMs)

Global climate models (GCMs) are numerical coupled models that play a critical role in the assessment of climate change impact. They are developed to represent different earth

systems, containing atmosphere, oceans and land surface (Xu, 1999). By using IPCC emission scenarios, GCMs can link the effect of GHGs on present and future climate at global and regional scales. GCMs run at a coarser resolution grid of 2° or more latitude and longitude (Salathe, 2003) and a spatial resolution of 50,000 km^2 (Wilby *et al*. 2002). However, the observational grids usually have much higher spatial resolution (e.g. ~ 4000 km^2 in the case of the South Nation Watershed, Ontario).

As noted above, the accuracy of GCMs is decreased due to low spatial resolution for capturing local geographic characteristics (i.e. topography, land/water-distributions, and vegetation), which could lead to weak projections (Wilby *et al*., 2002). In terms of precipitation projections, Salathe (2003) showed that GCMs are unable to resolve crucial mesoscale processes and surface topographies that dominate local precipitation. Though GCMs are important for the assessment of climate change, a transformation process to bridge the gaps between large-scale climate model variables and local-scale meteorological variables is required (Fowler *et al*., 2007). Such refining approaches can be conducted by using climate 'downscaling' techniques, which are discussed in the next section. Selecting one of the various global climate models for a particular terrain depends on many factors, including the study purpose, data availability and other considerations (Xu, 1999).

2.5 Downscaling

Despite substantial development, GCMs do not provide perfect simulations or details on small spatial scales. Applying GCMs at local scales and predicting future climate

variable time series requires a means of refining large-scale GCM outputs to a finer resolution. However, inaccuracies in the GCM simulation can easily be overcome by fine-scale modelling through the boundary conditions (Wheater, 2002). As determined by Hayhoe (2010), even a simple downscaling method will achieve better estimations than using raw output from the current generation of GCM simulations. Downscaling techniques have been widely utilized in recent studies to acquire the local watershed scales needed for climate change effect evaluations. The term downscaling denotes, "methods by which local to regional-scale (10–100km) climate information is derived from coarse resolution (>100km) atmospheric data or global climate model (GCM) output" (Fowler *et al*., 2007) as shown in Figure 2.5. The two fundamental atmospheric parameters required for assessment studies are daily temperature and precipitation. These can be adequately simulated at a spatial resolution of 0.125° latitude and longitude for mountainous river basins more than 10000 km^2 in size (Salathe, 2003).

The two fundamental methods conventionally used in downscaling are 'Statistical (or Empirical) downscaling' and 'Dynamical downscaling'. Many studies have reviewed the various downscaling methodologies (see Hewitson and Crane 1996; Wilby and Wigley 1997; Wilby *et al*., 1998; Xu 1999; Giorgi *et al*., 2001; Christensen *et al*., 2007; Fowler *et al*., 2007 ; Wilby & Fowler, 2011) and recently by (Sachindra *et al*.,2013).

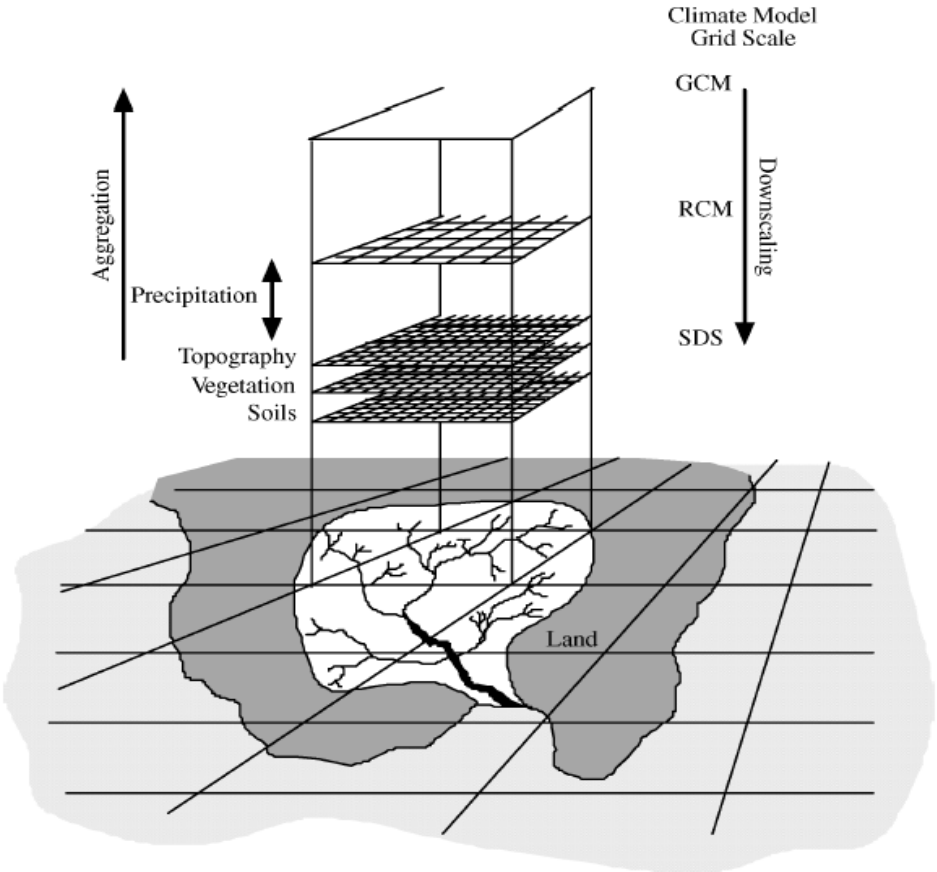

Figure 2.5 The concept of downscaling approaches (GCM: global climate model; RCM: regional climate model; SDS: statistical downscaling) (Wilby & Fowler, 2011).

2.5.1 Dynamical downscaling

Dynamical downscaling models simulate sub-GCM grid scale climate variables, using large-scale lateral boundary conditions from GCMs. These models, also known as Regional Climate Models (RCMs), have spatial resolutions of 20 to 50 km. Thus, dynamical downscaling models can simulate local climate features better than large-scale GCMs (Frei *et al.*, 2006). Salathe *et al*. (2004) stated that RCM is the best downscaling

technique, and it reproduces historical climate more accurately. The main improvement of RCMs is their capability to capture regional climate reactions to alterations in land-surface vegetation or atmospheric chemistry (Wilby & Fowler, 2011). Several studies have evaluated dynamical downscaling methods (e.g. Frei *et al*., 2006; Wilby & Fowler, 2011; Sharma *et al*., 2011).

When converting the GCM grid-spacing to RCM grid-spacing, the study area should not be in the vicinity of the lateral buffer zone, in order to avoid the relatively-high model noise at the lateral boundaries (Wilby & Fowler, 2011). Murphy (2000) suggested using dynamical downscaling to simulate rainfall in regions with summer dominated rainfall.

However, RCMs have some drawbacks. They are computationally demanding, time consuming, and not easily applied to other regions due to their sensitivity to the initial conditions selected at the start of experiments (Wilby & Fowler, 2011). Also, inherited systematic errors (bias) from global models could affect the quality of regional climate simulations (IPCC, 2007). (Boyer *et al*., 2010) stated that, "the overall added value of RCMs is small for areas weakly influenced by topographical forcing". Therefore, an apparent improvement in the simulation results was found after further downscaling RCMs outputs over the raw RCM outputs (Wood *et al*., 2004; Samuel *et al*., 2011; Sharma *et al*., 2011).

Chen *et al*. (2012) recently showed that high-resolution global GCMs are able now to run at a resolution that is compatible with the resolution of many RCMs. For example, the JMA-GSM can simulate at a resolution of 20 km, as stated by Mizuta *et al*. (2006).

2.5.2 Statistical Downscaling

The statistical downscaling approach relies on empirical relationships between large-scale atmospheric variables (i.e. predictors) and local variables (i.e. predictands) such as precipitation and temperature (Wilby *et al*., 1998; Boyer *et al*., 2010). Statistical downscaling is commonly used as it less expensive and consumes minimal computation resources, although it does require a large, high-quality dataset for calibration and validation. Furthermore, Wilby & Fowler (2011) showed that statistical downscaling is relatively easy to transfer between regions. However, as discussed by Wilby and Wigly (2000), all downscaling techniques depend on the assumption that GCM outputs and observed local-scale variables are also valid for a changing future climate. In other words, stationarity assumption is highly questionable in the presence of climate change (Sachindra *et al*.,2013).

Predictors and predictands in statistical downscaling could share the same variables on different spatial scales; however, they are usually different (Giorgi *et al*., 2001). Predictor variables, which typically include sea-level pressure, specific/relative humidity, and temperature variables, are derived from reanalysis climate models, such as the National Centers for Environmental Prediction/National Center for Atmospheric Research (NCEP/NCAR) which has resolution of 300 to 500km (Wilby & Fowler, 2011).

Statistical techniques have been reviewed several times (Giorgi *et al*., 2001; Wilby *et al*., 2004; Fowler *et al*., 2007; Wilby & Fowler, 2011; Chen *et al*., 2012). The main statistical downscaling techniques can be classified as Regression methods (transfer functions), Weather typing (weather classification schemes) and Weather generators (Wilby & Fowler, 2011). Each technique has strengths and weaknesses.

2.5.2.1 Regression methods

Hessami *et al*. (2008) stated that among current statistical techniques, regression methods are more widely used due to their ease of implementation and low computational requirements. These methods are a simple way to represent a linear or non-linear relationship between a predictand and a set of predictor variables (Giorgi at al., 2001; Fowler *et al*., 2007). Previous studies have used a variety of regression methods; for example, multiple regression was applied by Murphy (2000). Crane and Hewitson (1998) used an Artificial Neural Networks (ANN) method that is classified as being close to non-linear regression. ANN is a machine learning tool that imitates a biological nervous system, and can be defined as a non-linear multivariate regression approach (Wilby & Fowler, 2011).

Additionally, Wilby *et al*. (2002) established a Statistical DownScaling Model known as SDSM. It uses multiple linear regression to create a relationship between predictors and predictands, then generates local-scale climate variables (precipitation and temperature) for current and future periods. Automated Statistical Downscaling (ASD), an alternative tool developed by Hessami *et al*. (2008), operated within the MATLAB

environment. Seidou *et al*. (2012) investigated ASD at the Ontario Kemptville watershed, and found that it cannot estimate the number of wet days correctly, and the precipitation processes (occurrence and intensities) must be modified.

Precipitation uncertainty in all regression-based methods is a serious issue, due to the relatively low predictability of local amounts when using large-scale forcing alone (Burger 2002; Wilby & Fowler, 2011). To address this, Burger and Chen (2005) forced the regression model to maintain local covariance (a measure of how much two random variables change simultaneously). Apparently, because of the low resolution models, regression-based methods are unable to accurately capture hydrological extremes, which are highly weighted to particular locations and short-lived events. This limitation can be resolved by applying approaches such as the quantile-quantile method (Wilby & Fowler, 2011) (see 2.5.4).

2.5.2.2 Weather typing

In weather typing (also known as weather classification schemes), climate change is determined by estimating changes in the frequency of the weather patterns simulated by the GCM (Fowler *et al*., 2007). "Before downscaling can begin, atmospheric data are divided by their similarity with 'nearest neighbours' or reference types. The local variable(s) of interest are then assigned to the prevailing weather state, and replicated under changed climate conditions by resampling or regression functions" (Wilby & Fowler, 2011). This method assumes that the attributes of the weather patterns will remain the same in the future and (Brinkmann, 2000). Weather typing also assumes

stationary properties of the weather patterns, and cannot simulate events which are not included in this set of data (Chen *et al*., 2012).

2.5.2.3 Weather generators (WGs)

Weather generators (WGs) are designed to predict synthetic time series of weather data for a particular location, by replicating the statistical characteristics of a local climate variable (e.g. mean, variance) (IPCC, 2007). However, similar sequences of observed events are not expected (Wilby & Fowler, 2011). Brissette *et al*. (2007) stated that studies about using weather generators for climate change impacts have been limited, compared to other downscaling methods.

Similar to weather typing, a weather generator can simulate events according to the calibration data set. Precipitation, minimum and maximum temperatures and solar radiation are the most commonly modelled variables in WGs (Brissette *et al*., 2007). WGs can only be implemented at a single point, or independently at several points (Brissette *et al*., 2007). Fowler *et al*. (2007) criticized WGs for poor modeling of inter-annual variability in monthly means, as well as for being strictly localized; thus, they may not be useful in other climates. Nonetheless, Wilby & Fowler (2011) suggested that WGs are beneficial in sparse situations, such as the count of rainy days and accumulated monthly precipitation for hydrological applications in developing nations.

2.5.3 Bias correction methods

In the downscaling process, two sets of input datasets are obtained: climate model data and historical data from observations. These sources do not have similar degrees of accuracy (i.e. they are not homogenous in terms of quality). Sachindra *et al*. (2013) stated that bias in global/regional climate model outputs are due to various assumptions and approximations employed in the structure of these models. In other words, global climate models do not perfectly simulate climatology, as they deviate from observed atmospheric variables. Therefore, bias correction to adjust global/regional climate models is required (Maraun *et al*., 2010).

Bias correction methods have been widely used as alternative means of downscaling large-scale climate models data to local-scale. (Christensen *et al*., 2008) downscaled monthly mean temperatures and precipitation by forcing a group of thirteen regional climate models (RCMs) over the entire Europe, at a horizontal grid spacing of 25 km. They demonstrated that only a simple bias correction was needed for each of these models. (Samuel *et al*., 2011) estimated the climate projections of 90 basins across Ontario, using a multi-model approach of bias correction and regional climate models. By comparing non-corrected RCM outputs, corrected RCM data, and downscaled GCM outputs, it was determined that bias corrected RCM data is the most accurate predictor, as it reduces errors in monthly precipitation and daily temperatures of regional climate models by approximately 90%.

2.5.3.1 Quantile-based approaches

A quantile-quantile plot is a basic graphical approach for checking normality by comparing sample quantiles against population quantiles. Q-Q plots are also used to compare two or more data distributions (Helsel & Hirsch, 2002). Thus, quantile-quantile downscaling consists of a probability plot of model outputs against observed values, with both corresponding to the same probability (Déqué, 2007) or using empirical distribution functions (Amadou *et al.*, 2014). It assumes that although the two time series are independent, they describe the same variable at approximately the same location and, therefore, must have similar probability density functions (PDFs).

Quantile-quantile transformation (also known as quantile matching, cumulative distribution function matching and quantile-based mapping) was used on the host GCM by Wood *et al*. in (2004) to adjust coarse-resolution to the observed monthly climatology (mean temperature and total precipitation). Also, Sulis *et al*. (2009) used a bias-correction scheme based on quantile mapping to compel the Canadian General Circulation Model (CGCM, version 3.1) to agree with observations. More recently, work by Sachindra *et al*. (2013) determined that using the equidistant quantile mapping technique corrected the outputs of used GCMs for the minimum and maximum monthly precipitation. Leider (2012) used quantile regression with time series methods for temperature changes, and found that Q-Q is more resistant to extremes than least-squares methods. Moreover, Li *et al*. (2010) showed that bias-correction improvement when using a quantile-matching method was better than traditional CDF mapping methods.

Based on a real-world evaluation of different quantile methods by Gudmundsson *et al*. (2012), most quantile methods can remove biases in RCM precipitation. However, it was noted that the performance of quantile methods differs substantially. The nonparametric transformation methods were found to be the best at minimizing biases in RCM precipitation through the entire range of the distribution.

However, Q-Q cannot overcome the limitation of all downscaling techniques: the assumption of a stationary relationship between decades. This issue leads to setting predictor values outside the original range of the historic extreme (Wilby and Fowler, 2011). Nonetheless, uncertainties related to the choice of climate models and emission scenarios are higher than those related to the choice of calibration period (Chen *et al*., 2011).

Chapter 3. STUDY AREA AND DATA COLLECTION

3.1 Introduction

This chapter covers the study site in terms of location, social context and climate patterns over the last decades. Meteorological data and reanalysis data used in the study are also presented.

3.2 Study Area

3.2.1 Geographic Location

The South Nation watershed of approximately 4000 km^2 is located in Eastern Ontario, Canada, at 75°32′ W to 74°22′ W longitude and 44°44′ N to 45°38′ N latitude (Figure 3.1). It is used mostly for agriculture, and is drained by the 175 km South Nation River which runs northeast from Brockville to Plantagenet, where it merges with the Ottawa River. The watershed is relatively flat; the South Nation River has a topographic gradient of only 80 m between its headwaters and the confluence with the Ottawa River. Hence, the South Nation watershed is poorly drained, which maximizes flood risk and increases the erosion of riverbanks and topsoil on farmlands. The peak flow of the South Nation River occurs in March and April during spring thaw. Soil types vary from light sand to clay and clay loam (El Khoury, 2012), and this generally impermeable soil requires

extensive artificial drainage (e.g. deep open drains and buried pipe drains) to avoid the formation of pools which can consequently causes damage to the crops (SNC, 2012a).

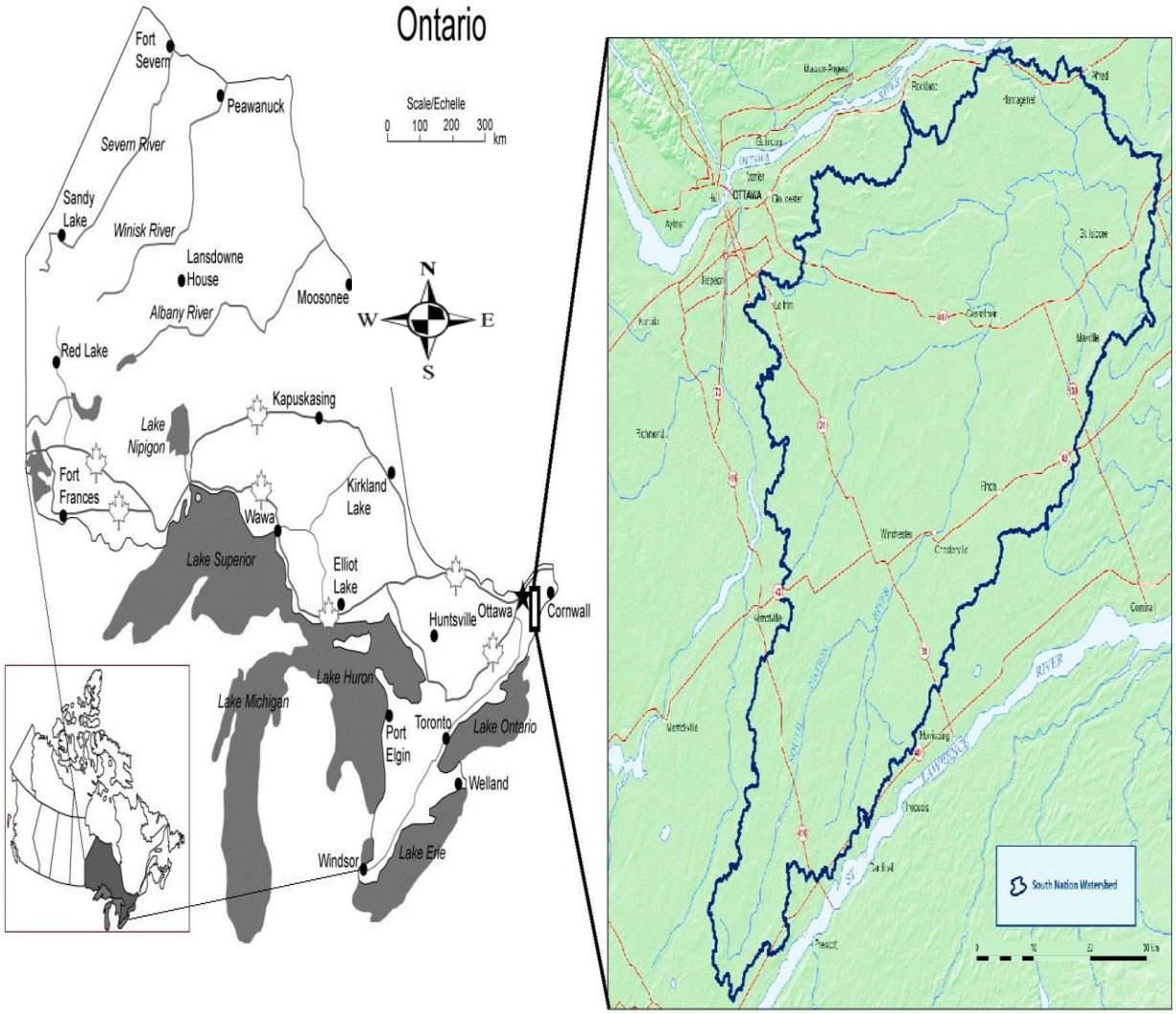

Figure 3.1 The South Nation watershed (Modified from: Agriculture and Agri-Food Canada, 2013).

3.2.2 Social Context

The rich natural resources of the South Nation watershed initially attracted people to the area. The aboriginal peoples were the first to benefit from the forests, wildlife and waters. Europeans came later, and they used the land for agriculture, the forests to build towns and ships, and the river for transportation (El Khoury, 2012). Agricultural activity increased after the introduction of electrical power in the 20th century, and this brought many changes to the area (Coyne, 2001). The population increased significantly (21%) between 1981 and 2001 (Coyne, 2001). The current population of approximately 120,000 is in 15 local municipalities managed by the South Nation Conservation (SNC), and the average population density is 39.4 people per km^2. The region has a rural economy based chiefly on agriculture (54% of the land use area) (Cummings and Russell, 2007). The history of the South Nation watershed highlights how important the area is, largely due to its rich natural resources.

3.2.3 Climate Context

The region typically has warm summers with an average annual rainfall of 733 mm, and cold snowy winters with an average annual snowfall of 203 cm. Fluctuations in weather conditions have been observed over the past few decades, and various natural occurrences have affected the watershed dramatically. In 1902, a severe storm passed through the area in a southeasterly direction, causing the loss of many human lives and much damage to infrastructures (Coyne, 2001). Two massive ice storms hit the area in 1942 and 1998, and the latter destroyed communication grids and power lines and caused

long-term power outages for millions of homes in Eastern Ontario and Southern Quebec (Coyne, 2001). Two landslides occurred in 1971 and 1993, with the displacement of 70 and 50 acres of land, respectively (Coyne, 2001).

After a dry winter, record-breaking high temperatures and 30% decreases in the monthly river flows occurred between July and November 2012. In response, the South Nation Conservation Authority issued a Level 2 low water alert, and asked landowners, businesses and industries to voluntarily reduce their water consumption by 20% and conserve non-essential water. This drought period resulted in recorded impacts on fish migration, and some economic losses in local communities and businesses, particularly for meat producers. Also, discolouration and shedding of tree leaves occurred earlier than usual. In terms of groundwater, SNC received the most complaints about dry wells in the watershed since they were last monitored in 2001 (SNC, 2012b).

3.3 Data Collection

Three data sets were compiled for the purposes of climate scenarios generation: meteorological data, reanalysis data and regional climate model outputs.

3.3.1 Meteorological Data

The availability of reliable meteorological data is key to the success of any climate impact study. In this work, the relevant data from all meteorological stations with long-term records (i.e. over 20 years) were obtained, at the daily time scale. The data in this study include daily records of precipitation, and maximum and minimum temperatures. Some stations within the study area did not have sufficient records, namely the newly established and others with less than 20 years of recording. Seven stations were considered, as shown in Figure 3.2. The Russell, South Mountain, Ottawa Int'l Airport, Avonmore and St. Albert stations are within the study area, and the Brockville station is near the southern borders of the watershed. Though it is located outside the watershed borders, the Pointe Au Chene station was used due to a shortage of available data in the northern area of the watershed. The basic characteristics of these meteorological stations are listed in Table 3.1. The data from the stations were collected by Environment Canada.

3.3.2 Meteorological Data Analysis

As shown in Table 3.2, the watershed stations have some similar climate characteristics: a mean maximum temperature of 11 ± 0.28 °C, a mean minimum temperature of 0.86 ± 0.20 °C and accumulated precipitation of 945 ± 60 mm per

year. The only significant difference is Brockville's mean minimum temperature of 2.71 °C, almost 2 °C higher than the watershed average.

Table 3.1 Meteorological Stations in the Study Area

Meteorological Station	Latitude	Longitude	Climate Identifier	Elevation (m)	Obs. Data Interval	Missing Data %
Russell	45°15'46.008" N	75°21'34.032" W	6107247	76.2	1978 - 2012	4 %
South Mountain	44°58'00.000" N	75°29'00.000" W	6107955	84.70	1960 -1996	1 %
Ottawa Int'l Airport	45°19'21.000" N	75°40'09.000" W	6106000	114.00	1960 – 2011	0 %
Avonmore	45°10'12.042" N	74°58'15.024" W	6100398	91.40	1976 - 2006	1 %
St. Albert	45°17'14.004" N	75°03'49.026" W	6107276	80.00	1986 - 2006	1 %
Brockville	44°36'00.000" N	75°40'00.000" W	6100971	96.00	1966 - 2006	1%
Pointe Au Chene	45°39'00.000" N	74°48'00.000" W	7036063	51.00	1960 - 2006	11%

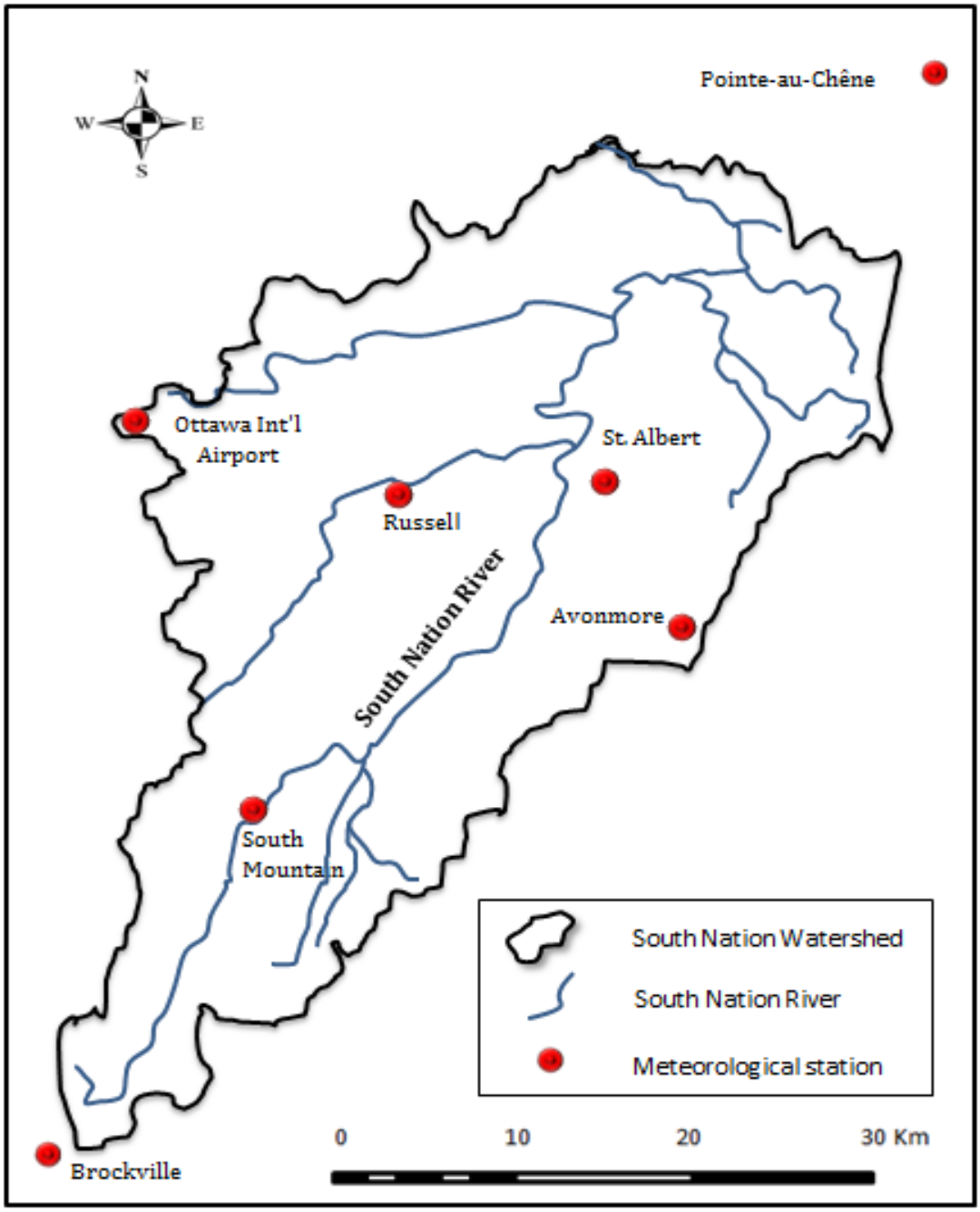

Figure 3.2 Location of Meteorological stations used in the study within the South Nation watershed of Ontario, Canada.

Table 3.2 Average observed monthly precipitation (PRCP), maximum temperatures (T_{MAX}) and minimum temperatures (T_{MIN}) in the SN watershed.

	Jan	Feb	Mar	Apr	May	Jun	Jul	Aug	Sep	Oct	Nov	Dec	Annual
South Mountain (1986 – 2006)													
T_{MAX} (°C)	-5.24	-4.08	2.19	10.73	18.27	23.11	25.74	24.30	19.33	12.93	5.31	-2.50	10.84
T_{MIN} (°C)	-14.56	-13.75	-6.81	0.71	6.75	11.62	14.18	12.93	8.37	3.12	-2.14	-10.67	0.81
PRCP (mm)	70.17	62.54	63.24	71.48	68.49	68.57	80.87	82.73	81.80	72.80	84.02	83.66	890.34*
Russell (1977 – 2006)													
T_{MAX} (°C)	-5.13	-3.05	2.77	11.35	18.83	23.26	25.80	24.49	19.69	12.58	5.66	-1.62	11.22
T_{MIN} (°C)	-14.27	-13.14	-7.05	0.78	6.97	11.97	14.43	13.13	8.63	3.03	-2.11	-9.66	1.06
PRCP (mm)	74.36	55.51	65.65	74.54	78.89	90.33	86.90	82.16	90.59	82.61	82.99	74.05	938.57*
Avonmore (1977-2006)													
T_{MAX} (°C)	-5.45	-3.38	2.64	10.92	18.37	22.90	26.28	25.03	20.24	12.75	5.70	-1.89	11.18
T_{MIN} (°C)	-14.72	-13.38	-7.08	0.54	6.77	11.33	14.13	12.97	8.45	2.78	-2.46	-10.46	0.74
PRCP (mm)	78.17	59.23	67.02	77.49	83.83	88.32	94.27	88.88	91.22	88.64	89.07	78.08	984.23*

Ottawa Int'l Airport (1960-2011)													
T_{MAX} (°C)	-5.99	-4.07	1.98	10.88	18.50	23.46	25.84	24.50	19.65	12.53	5.00	-2.93	10.78
T_{MIN} (°C)	-14.80	-13.31	-7.06	0.53	7.20	12.35	14.92	13.73	9.09	3.12	-2.47	-10.70	1.05
PRCP (mm)	61.78	55.81	64.45	70.70	74.32	82.93	89.50	84.62	83.47	77.43	81.30	76.62	902.93*
St. Albert (1986 – 2006)													
T_{MAX} (°C)	-4.99	-3.62	1.96	10.66	18.03	22.95	24.97	24.03	19.39	12.16	5.33	-1.84	10.75
T_{MIN} (°C)	-14.34	-13.86	-7.40	0.56	6.39	11.61	13.79	12.46	8.19	2.65	-2.48	-9.82	0.64
PRCP (mm)	79.73	56.99	65.94	79.13	86.67	96.38	94.96	91.63	98.61	89.95	91.19	75.56	1006.76*
Brockville (1966 – 2006)													
T_{MAX} (°C)	-3.82	-2.42	3.11	10.76	17.43	22.28	25.13	24.22	19.72	12.91	6.46	-0.47	11.28
T_{MIN} (°C)	-12.07	-10.99	-5.40	1.56	7.51	12.79	15.78	15.14	10.99	5.08	-0.17	-7.74	2.71
PRCP (mm)	77.93	62.88	67.12	72.09	78.12	85.83	81.34	80.80	95.49	83.59	91.45	87.90	964.53*
Pointe au Chene (1966 – 2006)													
T_{MAX} (°C)	-6.26	-3.96	2.31	10.65	18.72	23.69	26.00	24.66	19.84	12.75	5.06	-2.59	10.91
T_{MIN} (°C)	-16.15	-14.48	-7.41	0.21	6.86	12.16	14.72	13.56	9.38	3.64	-2.21	-10.84	0.79
PRCP (mm)	64.16	54.40	56.41	68.30	77.35	90.81	91.35	89.70	95.24	79.74	85.84	74.35	927.63*

* Mean Annually Accumulated Precipitation

As shown in Table 3.3, there was an overall increase over all the variables throughout the four seasonal data intervals: winter (December, January and February), spring (March, April and May), summer (June, July and August) and fall (September, October and November). It is notable that the mean maximum and minimum temperatures for all seasons has risen slightly over the past 20 to 50 years, while total precipitation has increased significantly at most stations in the spring, summer and fall, and decreased in the winter.

Table 3.3 Historic Linear Trends for precipitation (PRCP), maximum (T_{MAX}) and minimum temperatures (T_{MIN}) in the South Nation Watershed.

Station	Variable	Winter	Spring	Summer	Fall	Annual
Avonmore	T_{MAX}	2.85%	1.60%	1.73%	1.77%	1.99%
	T_{MIN}	2.69%	0.78%	1.77%	1.21%	1.61%
	PRCP	-0.94%	24.29%	9.40%	13.36%	11.53%
Brockville	T_{MAX}	2.41%	1.80%	1.23%	0.85%	1.57%
	T_{MIN}	2.99%	1.62%	0.89%	0.65%	1.54%
	PRCP	-12.23%	9.89%	6.78%	13.51%	4.49%
Russell	T_{MAX}	2.85%	1.55%	0.78%	1.43%	1.65%
	T_{MIN}	2.94%	1.09%	1.71%	1.35%	1.77%
	PRCP	-1.95%	12.74%	6.61%	16.95%	8.59%
St. Albert	T_{MAX}	2.84%	2.55%	2.30%	2.69%	2.60%
	T_{MIN}	3.80%	2.40%	2.76%	2.62%	2.90%
	PRCP	13.22%	38.15%	-6.02%	24.95%	17.58%
Ottawa Airport	T_{MAX}	1.38%	1.46%	0.62%	2.90%	1.15%
	T_{MIN}	1.70%	1.09%	0.91%	2.90%	1.23%
	PRCP	-1.64%	9.15%	11.32%	11.41%	7.56%
Pointe au Chene	T_{MAX}	3.06%	1.53%	0.87%	-0.25%	1.30%
	T_{MIN}	0.98%	0.31%	0.87%	-0.38%	0.45%
	PRCP	-0.68%	-3.93%	0.53%	18.66%	3.65%
South Mountain	T_{MAX}	1.50%	1.61%	0.65%	-0.81%	0.74%
	T_{MIN}	1.72%	1.83%	1.29%	-0.46%	1.10%
	PRCP	-0.72%	28.00%	17.83%	8.01%	13.28%

3.3.3 Reanalysis Data

Reanalysis data provides concurrent climate representation to support the requirements of future climate projection studies. The National Centres for Environmental Prediction (NCEP) reanalysis dataset provides retroactive gridded data with a horizontal resolution of 2.5° × 2.5°. The real time NCEP dataset derives the data from monitoring systems, historical records and forecasts from numerical models (Kistler *et al*., 2001). NCEP data are used by scientists around the world, and are considered to be the best global climate reference of the current state of the earth systems (Alansari *et al*., 2014). In this study, daily data derived from the NCEP reanalysis datasets are used to replenish gaps in the observed data for the same period of records. They are available from 1948 to the present. The NCEP reanalysis data is available at http://wesley.wwb.noaa.gov/Reanalysis.html.

Chapter 4. METHODOLOGY

4.1 Introduction

Although current regional climate models can provide a general idea about how the climate could change over the twenty first century, higher resolution models are required for future water management. To assess the climate change impacts on the South Nation watershed, RCM raw data were transformed to match observations and provide afterward corrected climate projections.

Producing climate change scenarios for the South Nation Watershed requires an approach consisting of several steps, as shown in Figure 4.1. First, as discussed in Chapter 3, missing observational data were replenished by NCEP reanalysis data, and the raw data of two climate models with the same temporal and spatial observed data were extracted. Quantile-Quantile transformation was then applied to the daily precipitation and maxima and minima temperature data to adjust the RCMs. Finally, corrected historical and future simulations were run to assess the effect of climate change on extreme events. Detailed description of these steps follows.

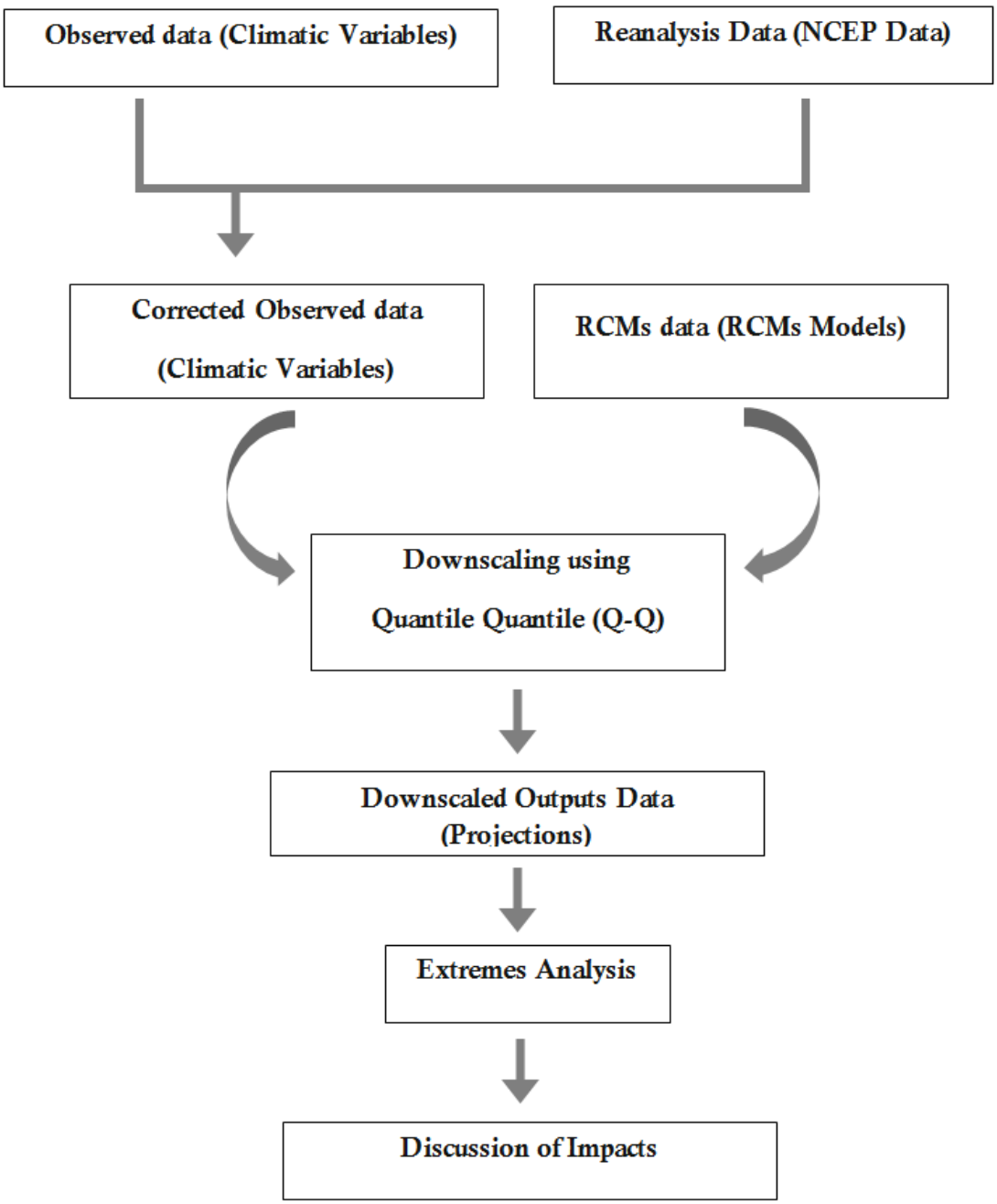

Figure 4.1 Flow Chart illustrating the methodology used to produce climate change scenarios for the South Nation watershed.

4.2 Quantile-Quantile downscaling

The purpose of this downscaling process is to correct the simulated data of two RCMs, and thereby improve projections of future precipitation and temperature data. This was done on a small scale for practical local management of the South Nation River region. CRCM and ARPEGE simulated data were run under the SRES A1B emission scenario. The downscaling methodology applied in this study is based on transformation of the RCMs' outputs, to make them robust and reliable.

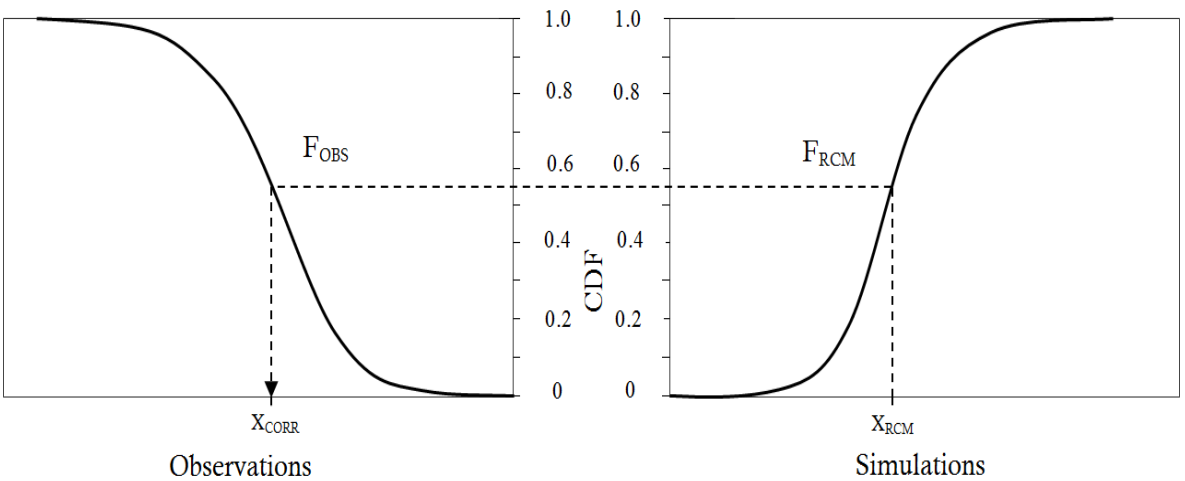

Figure 4.2 Schematic exemplifying the Quantile-Quantile transformation.

The methodology of bias correction herein is the same as that used by Amadou *et al.* (2014). An empirical statistical technique, commonly denoted as 'quantile-quantile', was applied to compare probability density functions for RCM-simulated daily precipitation and maximum and minimum temperature with historical observed data (Figure 2.4; Maurer *et al*., 2002; Maurer and Hidalgo, 2008). The simulated gridded precipitation (PRCP), maximum temperature (T_{MAX}) and minimum temperature (T_{MIN}) over the SNW were obtained at a daily

scale. The quantile-quantile transformation was applied on a monthly basis to a minimum of 20 years of historical records. The Q-Q transformation procedure for a given variable in a given month is conducted following four steps, as explained by Amadou *et al*. (2014):

i. First, the daily time series of observation and RCM simulation data are divided into two periods for calibration and validation. A half of the historical data were used for the calibration period (i.e. biennial data are used in the observations), and the remaining data for the validation period. The historical and simulated daily time series for a particular month are obtained for the corresponding periods.

ii. Two empirical cumulative distribution functions, F_{OBS} and F_{RCM} , were generated by using the observations and RCM simulations on the calibration period, respectively.

iii. Corrected RCM simulations, X_{CORR}, for validation and future periods are then produced by applying the following transformation:

$$X_{CORR} = F_{OBS}^{-1}(F_{RCM}(X_{RCM})) \qquad \text{Equation 4.1}$$

where X_{RCM} refers to the climate variable extracted from simulated RCM data, and X_{CORR} refers to the corrected climate variable.

iv. For precipitation intensity, maxima and minima temperatures, empirical probability distribution functions (PDFs) of the three variables, the observed data, raw- and corrected-RCM, are plotted for visual comparison on both the calibration and validation periods. For precipitation occurrence (i.e. wet/rainy days when precipitation intensity is greater than 1mm day^{-1}), the probability mass function (PMF) was used instead of PDF. The PDF or PMF of the corrected variable should match the PDF or PMF of the associated observed variable, and provide better results

when compared to the raw variable. Then the Quantile-Quantile transformation is applied to produce improved (corrected) future RCM simulations of that climate variable.

ARPEGE has available outputs from 1970 to 2001 and future from 2041 to 2081, and CRCM has available outputs from 1970 to 2100. Thus, the 1970 to 2001 period was used for training (calibration and validation) and 2041 to 2081 for future projections.

4.3 Model performance

The PDF of the following five sets of data were plotted and compared: observations (OBS), raw or non-corrected RCM data on calibration/validation period, corrected RCM data on calibration/validation period, raw or non-corrected RCM data on future period (2041-2081), and corrected RCM data on future period (2041-2081).

In addition to visual comparison, the two-sample Kolmogorov-Smirnov test (K-S) was used to determine if two data samples were from a common distribution. This test is a nonparametric test that is very sensitive to both location and shape parameters of the empirical cumulative distribution functions of both samples (Chakravart *et al.*, 1967). Simply put, the two-sample K–S test statistic measures the distance between the empirical distribution functions of two samples. The test is defined as follows:

H_0: The two samples are drawn from the same continuous distribution (P1 = P2).

H_1: The two samples are not drawn from the same continuous distribution (P1 ≠ P2).

At a 5% significance level, this results in Similar Distribution (SD) if H_0 is accepted, and Not Similar Distribution (NSD) otherwise.

4.4 Extreme Values Analysis

Assessment of climate extremes provides insight into changes that could potentially causes stress to humankind or the environment. Extreme values analysis describes data located mostly in the tails of the distributions of meteorological variables, as shown in Figure 4.1. It is applied to two types of time series: annual maximum series and over-threshold extreme indices.

4.4.1 Frequency Analysis

Frequency analysis refers to widely used procedures to describe the behaviour of hydro-meteorological variables, such as precipitation, temperature, wind speed, flooding and river level. To estimate the frequency analysis of an event, a broad approach used for designing municipal infrastructures can be conducted to the variable of interest, using its annual maximum series. Needless to say, the availability of sufficient recorded data is essential for frequency analysis.

Frequency analysis includes estimating the return period of an extreme event of a given magnitude at a particular location. This is done by fitting a statistical theory to the historical data to predict return period precipitation that might occur once every 5, 10, 20… n years, known as return periods (T). This approach deals with only one value per year, namely the annual maximum value of a hydro-meteorological variable (precipitation in our case).

Determining the magnitude (x) for a given return period (T) is then used for hydrologic design, which is usually specified by a local agency.

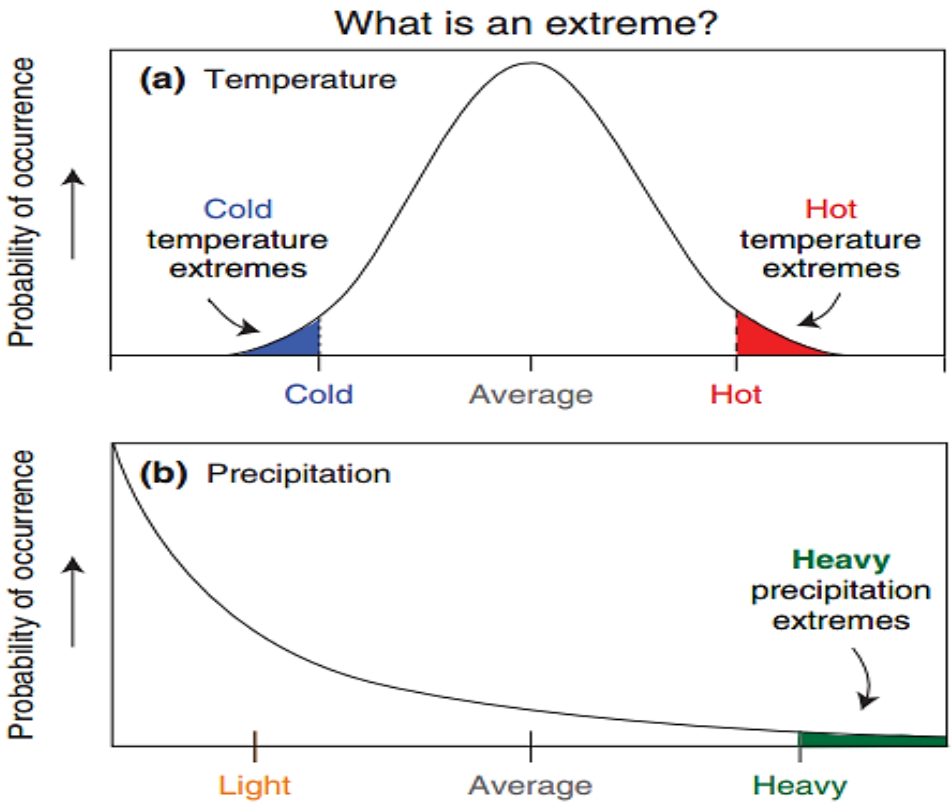

Figure 4.3 Illustration of extreme events using the probability distributions of (a) daily temperature (upper figure) and (b) precipitation (lower figure). The higher the black line, the more often weather with those attributes occurs. Extremes are denoted by the shaded areas (Zhang *et al*., 2011).

In the study, we found that the maximum values of all variables cannot exceed the historical maximum records, due to how the Q-Q algorithm was written. In other words, the used technique is unable to predict values beyond the historical values because of the assumption of stationary between decades. Therefore, any data falling outside those observed

will be adjusted to the historic extreme. This mainly effects the distribution of extreme values, particularly with respect to temperatures which are expected to rise significantly. Thus, we did not perform frequency analysis of temperatures, due to the slight time change in maximum recorded values. In other words, repeating the highest temperature when the predicted values are beyond the historical values results in virtually the same records of maximum values for all future periods of interest, which leads to the failure of any subsequent statistical distribution.

4.4.2 Selection of a Statistical Distribution

'Goodness of fit' tests can play a role in selecting the best underlying distribution to fit given data (e.g. Khaliq *et al.*, 2004; Millington and Simonovic, 2013). Based on previous works, we analyzed a group of 2-parameter and 3-parameter statistical distributions, though not comprehensively. The 2-parameter distributions encompass the Normal (NOR) and Lognormal (LN2), and the 3-parameter distributions encompass the Generalized Extreme Value (GEV), Lognormal (LN3) and Log Pearson Type III (LP3). The selection of a best fitting distribution was achieved using the following three goodness of fit tests: the Anderson-Darling (AD), the Kolmogorov-Smirnov (KS) and the Chi-Squared. The theory behind these tests is defined in (Solaiman, 2011). Based on how they performed in the tests, the five statistical distributions were ranked best to worst (1 to 5) according to their test statistic values, with the lowest statistic value being the best fitting distribution. This replicates the methodology of Millington and Simonovic (2013) of ranking the distributions and selecting the one ranked best, and it can be done by comparing the ranks of all

distributions for each test. As expected, GEV distribution was found to be the best fitting for annual extreme precipitation events. The goodness of fit tests were performed using EasyFit software, available at http://www.mathwave.com/easyfit-distribution-fitting.html.

4.4.3 The GEV distribution

The generalized extreme-value (GEV) distribution is widely used for estimating extreme values of given data sets. It is a 3-parameter distribution family that integrates three extreme-value distributions into a single form: the Gumbel, Frechet and Weibull. GEV comprises three parameters: location (ξ), scale (α) and shape (κ). The location parameter (ξ) determines the left or right shift of a distribution on the horizontal axis, the scale parameter (α) determines how the distribution disperses and spreads out, and the shape parameter (κ) represents the data that lies at the right end, which creates the tail of the distribution. The latter (κ) plays a major role in determining the shape and size of the tail of each distribution (i.e. $\kappa = 0$, $\kappa < 0$ and $\kappa > 0$, corresponds to EV1 (Gumbel), EV2 (Frechet), and EV3 (Weibull) distribution, respectively)

The CDF and PDF of GEV as defined in Hosking (1997) are given by:

$$F(x) = exp[-\left(1 - \frac{\kappa(x-\xi)}{\alpha}\right)^{\frac{1}{\kappa}}] \qquad \text{Equation 4. 2}$$

$$f(x) = \alpha^{-1}\ exp[-(1-\kappa\ )y - exp\ (-y)] \qquad \text{Equation 4. 3}$$

where $y = -\kappa^{-1} \log\left[1 - \frac{\kappa(x-\xi)}{\alpha}\right], when\ \kappa \neq 0$ Equation 4. 4

where, ξ, α and κ are the location parameter, the scale parameter, and the shape parameter, respectively.

4.4.4 Parameters estimation

There are several methods to estimate the parameters of the GEV distribution. The maximum likelihood method (ML) is statistically considered to be the most efficient parameter estimation technique used in hydrology for large samples, as stated by Millington and Simonovic (2013). Theoretical formulation in terms of ML can be obtained from Kotz and Nadarajah (2000). All calculations to estimate GEV parameters were conducted using MATLAB functions. The value of each parameter estimated using ML lies in the confidence interval of 95%.

The structure should provide a certain degree of safety against high wind seed, which are determined based on the probability of occurrence and speeds exceeding the design values.

4.4.5 Return Period

Infrastructures should provide a certain degree of safety against extreme precipitation events, which are determined based on the probability of occurrence and exceeding of the design values. In hydrological studies, fitting data to underlying statistical distributions is mainly done to predict how frequently an extreme precipitation event might occur for given return periods (T). A return period (T) is defined as the average length of time in years for an event

(e.g. 24-hour precipitation depth) of a given magnitude to occur or be exceeded. It has an inverse relationship to the probability of occurrence (p) (i.e. p = 1/T and thus T = 1/p). The value of the random variable X_T corresponding to a return period T (in years), can be computed as follows (Millington and Simonovic, 2013):

$$X_T = \xi + \left(\frac{\alpha}{\kappa}\right)\left\{1 - \left(-\log\left(\frac{T-1}{T}\right)\right)^{\kappa}\right\} \qquad \text{Equation 4. 5}$$

In this study, six time intervals (2-, 5-, 10-, 25-, 50- and 100- years) were chosen as return periods, in order to be consistent with those used by Environment Canada, as presented in Table 4.1.

Table 4.1 Applied return periods (in years) and their probability of occurrence (%)

Return period (years)	**2**	**5**	**10**	**25**	**50**	**100**
Probability of occurrence (%)	50%	20%	10%	4%	2%	1%
(percentile)	(50^{th})	(80^{th})	(90^{th})	(96^{th})	(98^{th})	(99^{th})

4.4.6 Extreme events Indices

Extreme event indices have been applied in several studies to detect changes in temperature and precipitation extremes (e.g., Frich *et al*., 2002; Zhang *et al*., 2011). These indices assessments are generally based on certain thresholds, such as the number of days below a specific temperature in a given month or year. This is done to obtain a more precise evaluation of how climate change may influence certain human and natural systems in the

study area. The less frequent events are usually more likely to cause severe damage to surrounding areas.

To analyze climate variability and climatic extremes, a set of statistically robust indices will allow fundamental, straightforward monitoring. Seven indices were chosen to represent the projected effects of global warming on the study area. As defined in Table 4.1, four indices deal with maxima and minima temperatures, and the other three monitor precipitation. These indices to detect changes in climate extremes were established and defined by recognized research teams: the Expert Team on Climate Change Detection Monitoring and Indices (ETCCDMI) and/or the European Statistical and Regional Dynamical Downscaling of Extremes for European Regions (STARDEX) (Frich *et al*., 2002, Zhang *et al*., 2011; Sarr *et al.*, 2013).

Table 4.2 List of extreme indices applied as defined by the Expert Team on Climate Change Detection and Indices (ETCCDI) (Sillmann & Roeckner, 2008)

	ID	Indicator Name	Indicator Definition	Unit
Temperature Indices	**FD0**	Frost days	Annual count when T_{MIN} (daily minima temperature)<0ºC	Days
	SU25	Summer days	Annual count when T_{MAX} (daily maximum temperature)>25ºC	Days
	ID0	Icing days	Annual count of days when T_{MAX} (daily maximum temperature) < 0 ºC	Days
	TR20	Tropical Nights	Annual count of days when T_{MIN} (daily minimum temperature) > 20 ºC	Days
Precipitation Indices	**CDD**	Consecutive dry days (The maximum length of dry spell)	Maximum number of consecutive days with PRCP <1mm	Days
	CWD	Consecutive wet days (The maximum length of dry spell)	Maximum number of consecutive days with PRCP ≥ 1mm	Days
	R20	Number of very heavy precipitation days	Annual count of days when PRCP ≥ 20mm	Days

These indices were applied to current and future periods, to help explain how the frequency or intensity of extreme events might change and which could potentially affect humans and/or the environment. R software (version 3.1.0) was used to compute the indices, by implementing the RClimDex (1.0) package provided by the Climate Research Branch of the Meteorological Service of Canada. Definitions for indicators as defined by the ETCCDI are listed below (Sillmann & Roeckner, 2008):

1. Frost days **(FD0)**
Let Tn_{ij} be the daily minimum temperature on day i in period j. Count the number of days where $Tn_{ij} < 0°C$

2. Summer days **(SU25)**
Let Tx_{ij} be the daily maximum temperature on day i in period j. Count the number of days where $Tx_{ij} > 25°C$

3. Icing days **(ID0)**
Let Tx_{ij} be the daily maximum temperature on day i in period j. Count the number of days where $Tx_{ij} < 0°C$

4. Tropical Nights **(TR20)**
Let Tn_{ij} be the daily minimum temperature on day$i$ in period j. Count the number of days where $Tn_{ij} > 20°C$

5. Consecutive dry days **(CDD)**
Let RR_{ij} be the daily precipitation amount on day i in period j. Count the largest number of consecutive days where $RR_{ij} < 1mm$

6. Consecutive dry days **(CWD)**
Let RR_{ij} be the daily precipitation amount on day i in period j. Count the largest number of consecutive days where $RR_{ij} \geq 1mm$

7. Heavy precipitation days **(R20)**
Let RR_{ij} be the daily precipitation amount on day i in period j. Count the number of days where $RR_{ij} \geq 20mm$

4.5 Trend Analysis

The analysis of trends in prolonged series of climatological data can help distinguish between actual impacts of climate change and short term fluctuations. Nonparametric trend tests are the preferred technique to detect trends in time series climatic variables without an assumption of normal distribution. The study of rates of trends is also of practical significance in determining the magnitude and direction of such changes. In this study, trend detection was attempted by checking PRCP, T_{MAX} and T_{MIN} in the chosen location. Daily precipitation data and maximum annual precipitation data were checked in terms of occurrence of positive or negative trends by applying the Mann-Kendall and the seasonal Mann-Kendal tests. To accomplish this task, the XLSTAT statistical software package was used. The Mann-Kendall trend test was used to check the maximum and minimum temperatures in the SNW at the station level, to establish the presence of trends. Sen's Slope Estimator was applied to determine the slope of trends, as well as a modified version for data with seasonality patterns.

4.5.1 Mann-Kendall Trend Test

The Mann-Kendall Test to search for trends in time series was devised by Mann (1945) and further developed by Kendall (1975), and hydrologists have been applying the test in metrological studies since then. The Mann-Kendall Test is a nonparametric trend test that can avoid problems associated with highly skewed meteorological data (U.S. EPA, 2006). It does not assume any particular distribution, and is robust against outliers and large data gaps.

Using Man-Kendall trend testing is specifically recommended when different stations are analyzed in a single study, as stated by Hirsch *et al*. (1991).

The test is used to assess if a hypothesis has an upward or downward trend, or if no trend was detected in the time series of climatological variables. The null hypothesis (H_o) and the alternative hypothesis (H_1) are defined as follow:

H_o : There is no trend in the series (i.e. the variation of the data is random)

H_1 : There is a trend in the series (i.e. a trend exists and can be either upward or downward)

For a time series of an atmospheric variable $\{x_1 \ldots x_N\}$, statistic S is computed as follows:

$$S = \sum_{i=1}^{N-1} \sum_{j=i+1}^{N} sgn(x_j - x_i) \qquad \text{Equation 4.6}$$

$$\text{where } sgn(x_j - x_i) = \begin{cases} \mathbf{1} & (x_j - x_i > 0) \\ \mathbf{0} & (x_j - x_i = 0) \\ \mathbf{-1} & (x_j - x_i < 0) \end{cases} \qquad \text{Equation 4.7}$$

A result with a large positive S indicates that an upward trend is detected, and a large negative S indicates detection of a downward trend. These variations are caused by either later-subsequently measured values tend to be larger or smaller than those measured previously. The value of S tends to be close or equal to 0 when there is no trend. The test statistic ($\boldsymbol{\tau}$) can be calculated as follows (Meals *et al*., 2011):

$$\boldsymbol{\tau} = \frac{S}{n(n-1)/2} \qquad \text{Equation 4.8}$$

and can be a range of values from +1 to -1 (i.e. $+1 \leq \boldsymbol{\tau} \leq -1$). There is no trend when the values of S and $\boldsymbol{\tau}$ are significantly away from zero.

When a trend is detected, the direction and rate of change can be captured using a non-parametric method known as the Sen Slope estimator, which can avoid miscalculations due to outliers (Helsel and Hirsch 2002).

4.5.2 Seasonal Mann-Kendall Trend Test

The original Mann-Kendall test presented earlier assumes no cyclical pattern in the time series. However, daily temperature data could exhibit a seasonal pattern, so average values of each day over all years are tested for trends. To overcome the issue of leap years, all Feb 29th values are removed from time series. The seasonal Mann-Kendall test, as developed by Hirsch *et al*. (1982), is an extension of the Mann-Kendall, and deals with seasonality in the data. This test was used to examine trends in daily precipitation, and maxima and minima temperature time series. Seasonality analysis was not required for maximum annual precipitation data neither performed, as these do not have seasonal variations. The XLSTAT statistical software package was used to apply the seasonal Mann-Kendall test.

4.5.3 Sen's Slope Estimator

Although linear slop estimator is a widely used and relatively easy screening tool, it has limitations that could reflect on the accuracy of results. Simple linear regression is less

helpful, as it cannot discount the effects of extreme values (outliers) and could lead to low quality results (U.S. EPA, 2006). More accurate rate of trend estimates can be achieved using Sen's Slope Estimator as an alternative to linear trend results. This method uses an overall slope by calculating the median of slopes for all the pairs of time points, so it can handle the issue of sensitivity to outliers. With n time points, and $X_{i,j}$ denoting the data value for the i^{th} and j^{th} time point, Sen's slope estimator β can be computed as follows (Helsel and Hirsch 1992):

$$\beta = median\left(\frac{y_j - y_i}{x_j - x_i}\right) \qquad \text{Equation 4.9}$$

where i > j and i = 1, 2, …, n-1 and j = 2, 3,…, n.

An underlying trend is detected when the latter X_j points are higher or lower than the previous X_i points, whereas no trend is detected when the values of the slope are near zero, as X_i is likely to be close to the latter X_j when positive slopes cancel negative ones. On account of the number of calculations needed, Sen's estimator requires some computational effort, thus the XLSTAT statistical software package was used.

4.5.4 Seasonal Kendall Slope Estimator

For data with cyclic trends, a modified version of the Sen's Slope Estimator known as the Seasonal Kendall Slope Estimator can be applied. As with the Sen's Slope Estimator, due to the number of calculations this estimator also requires some computational effort, so the same XLSTAT statistical software package was used. In our case, daily data exhibited annual

cycles. The Seasonal Kendall Slope Estimator uses 365 separate sets of slopes to calculate the median slope, as stated by U.S. EPA (2006).

Chapter 5. RESULTS AND DISCUSSION

5.1 Introduction

The previous chapter presented details of the approach used to produce climate scenarios under greenhouse conditions of SRES A1B. As the main interest of this study is to develop improved climate change scenarios for the study area, this chapter covers the results of the downscaling of precipitation and temperatures. It also presents several analysis indicators for the future time period of 2041 to 2081, relative to the current time period of 1960 to 2010.

5.2 Model Performance

The two-sample Kolmogorov-Smirnov test was used to evaluate the performance of the applied model, in addition to visual comparisons. It was observed that better maximum and minimum temperature results were achieved using quantile-quantile transformation, whereas corrected precipitation is not highly compatible with observations. This issue was examined in previous studies (Burger, 2002; Boe *et al*., 2007; Wilby & Fowler, 2011), and was found to be due to the inherited lower efficiency of large-scale forcing to predict comparable small-scale values of daily precipitation. Mehrotra (2005) suggested that including a predictor variable that represents atmospheric moisture (e.g. specific humidity, relative humidity) can play a major role in improving simulation results.

To better identify improvements when applying Q-Q downscaling, the observed raw and corrected data of two time periods are plotted in juxtaposition to each other. By

comparing the PDF of the data sets, the majority of downscaling results of temperature variables for all stations showed acceptable agreement in the calibration and validation periods. As precipitation and temperatures are downscaled independently at each station, results of the downscaled variables of one station (Airport) are included herein for comparison. Figures 5.1, 5.2, 5.3 and 5.4 present the ARPEGE model, and the CRCM model results are presented in Appendix B: Figures B.1, B.2, B.3 and B.4). The PDF monthly results are presented, compared and discussed.

As shown in Figure 5.4, with respect to precipitation occurrence it is apparent that the raw ARPEGE model outputs underestimate the number of wet days (i.e. precipitation $\geq$ 1 mm) in the winter season, and overestimate the number of wet days in the summer season. On the other hand, the raw CRCM outputs found more rainy days throughout all seasons than were in the historical records. After correction, both models produce results that are comparable to the observations, and adjust projections in terms of precipitation occurrence.

In terms of p-values, comparison using the two-sample KS test is significantly improved after applying Q-Q downscaling to the calibration and validation periods of all the stations, as shown in Table 5.1. For example, the p-values of non-corrected ARPEGE were p=1.2e-036 (N.S.D.) in the calibration period, and p=1.6e-037 (N.S.D.) in the validation period for the month of January, whereas after correction they were p=1 (S.D.) and p=0.84 (S.D.) respectively. For more details see the KS Test results for Airport station in Appendix A. Maximum and minimum temperatures have good agreement with observed data in calibration period and acceptable results for the validation period. However, the model did not perform as well in predicting precipitation, as explained previously. Table 5.1 also

indicates that the performance of both RMCs was similar, and that minimum temperature variable produced better results than maximum temperature variable.

Table 5.1 Average number of months when the PDF of corrected RCM and observed data are similar before and after applying Q-Q downscaling using the two-sample KS test.

Variable	RCM	Calibration Period		Validation Period	
		Non-Corrected RCM	Corrected RCM	Non-Corrected RCM	Corrected RCM
T_{MAX}	ARPEGE	3	11	1	3
	CRCM	2	11	1	3
T_{MIN}	ARPEGE	2	11	2	5
	CRCM	2	11	1	4
PRCP	ARPEGE	0	0	0	0
	CRCM	0	0	0	0

(a) **Calibration** (b) **Validation**

Jan

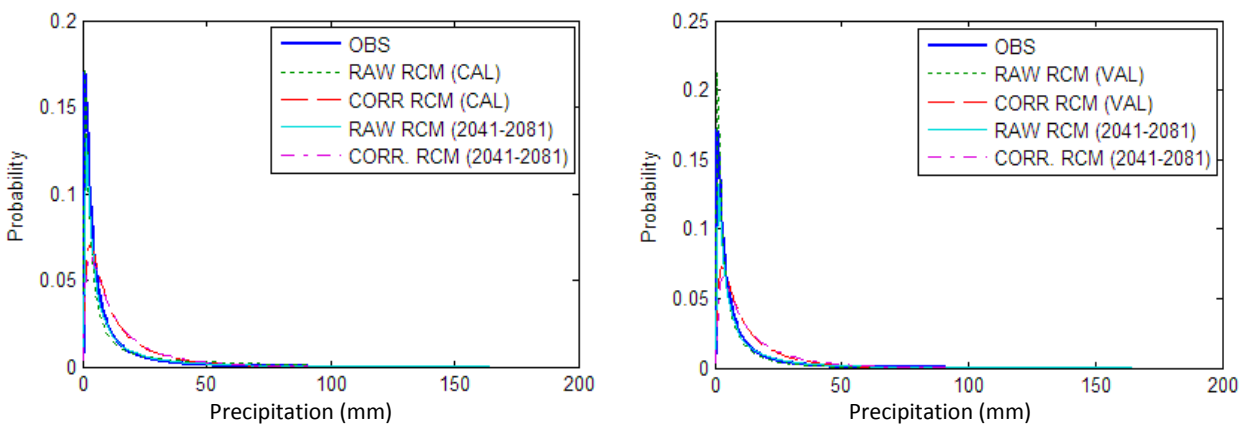

Feb

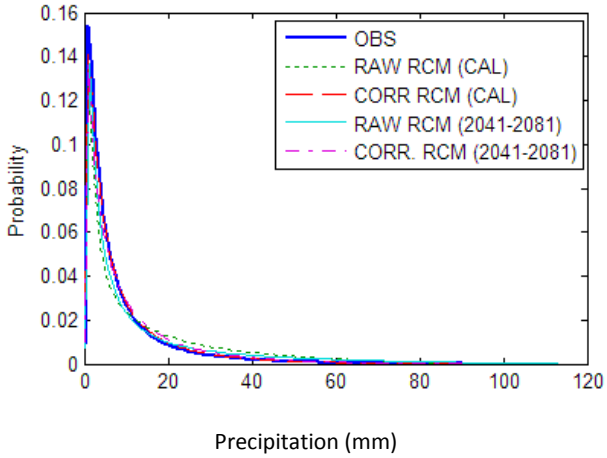

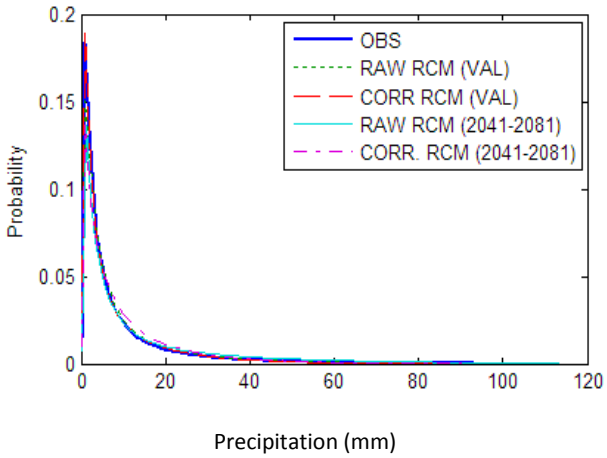

March

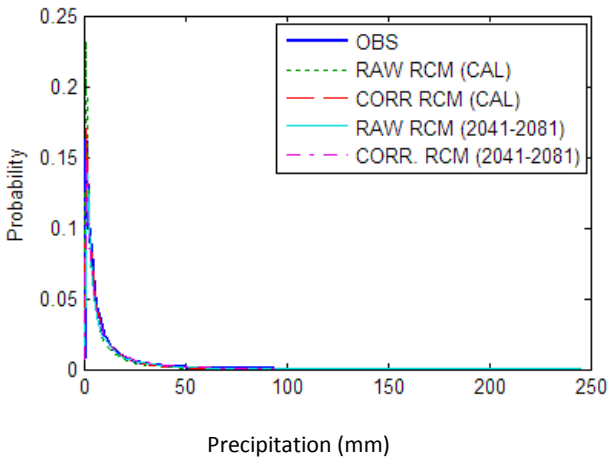

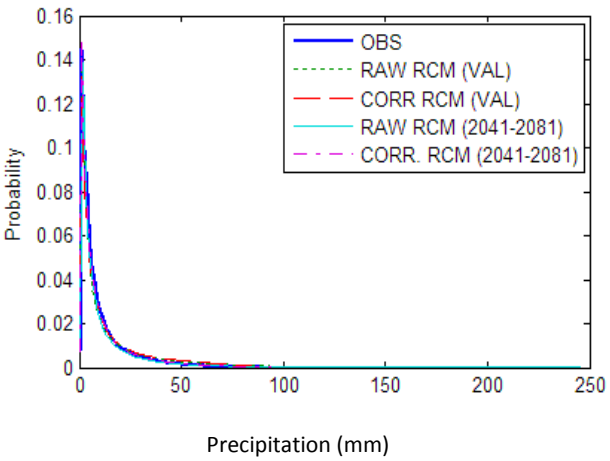

April

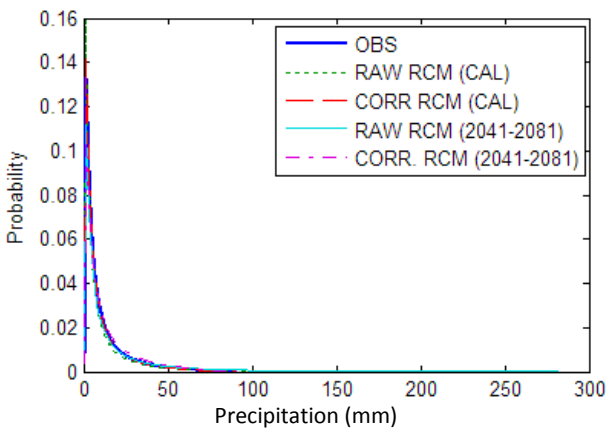

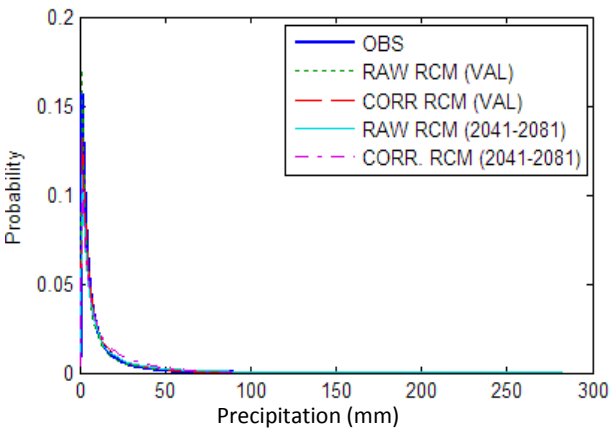

May

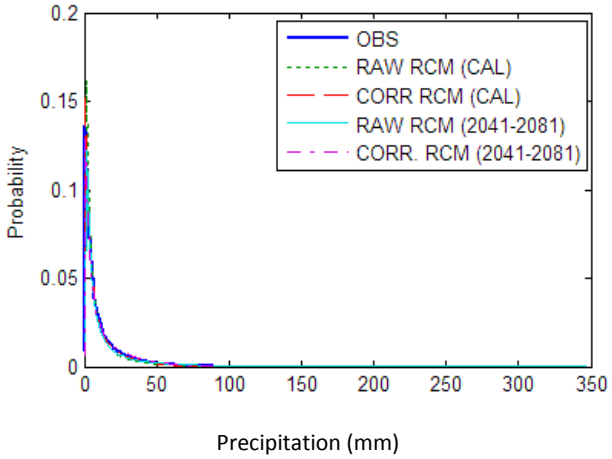

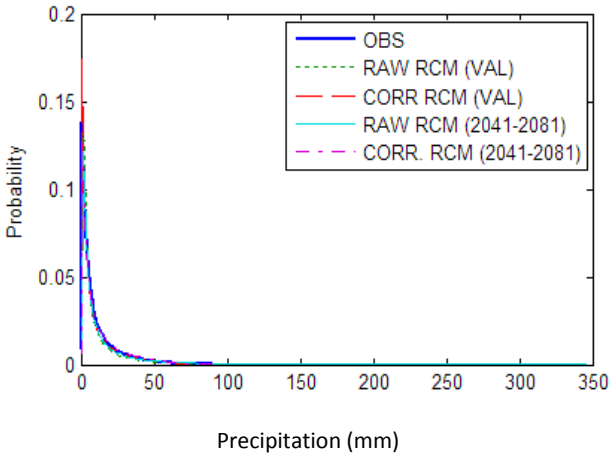

June

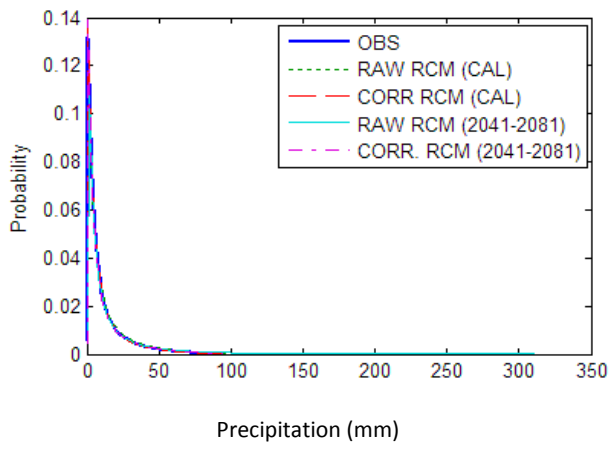

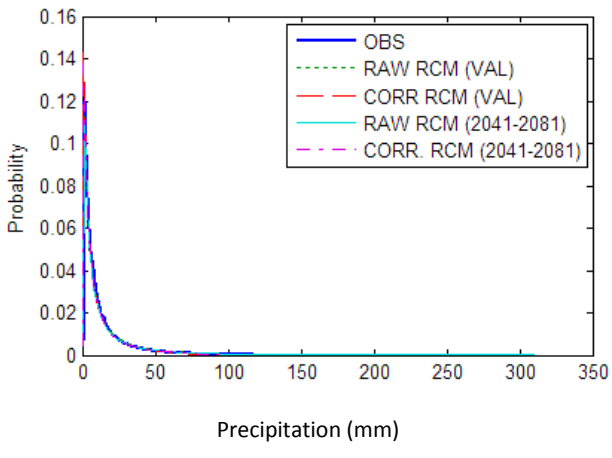

July

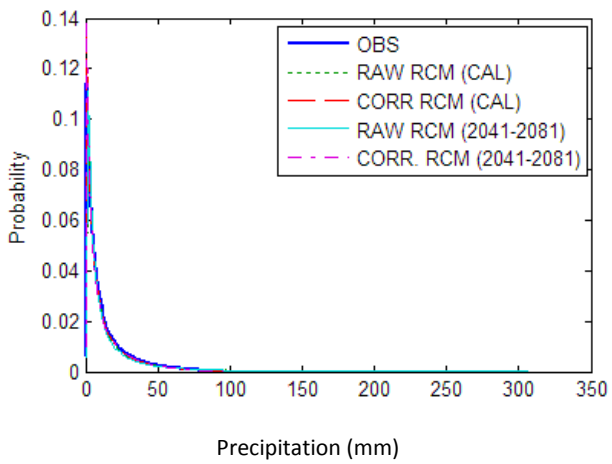

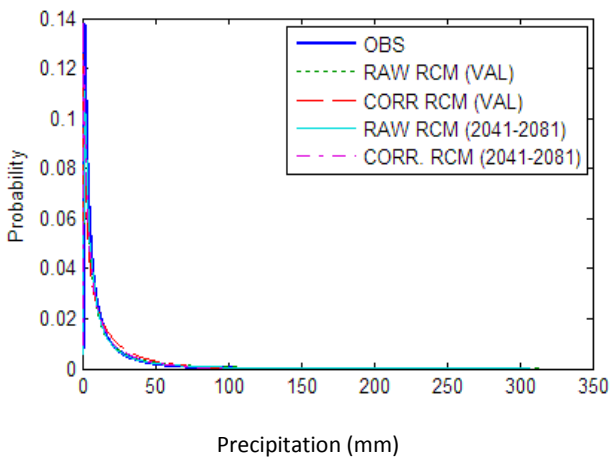

Aug

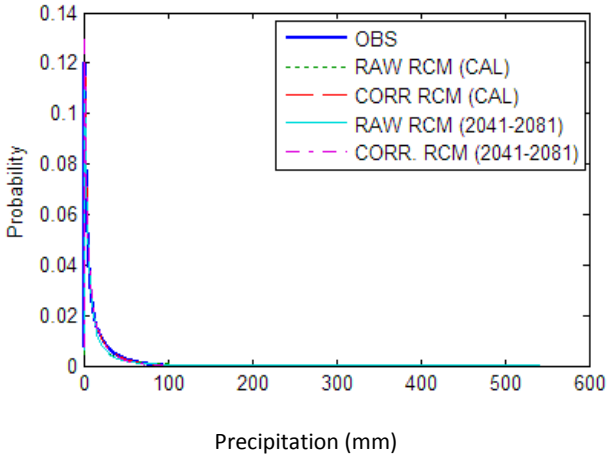
OBS
RAW RCM (CAL)
CORR RCM (CAL)
RAW RCM (2041-2081)
CORR. RCM (2041-2081)
Probability
Precipitation (mm)

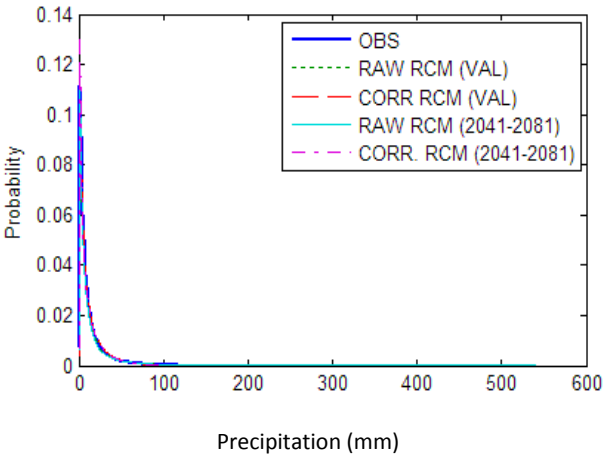
OBS
RAW RCM (VAL)
CORR RCM (VAL)
RAW RCM (2041-2081)
CORR. RCM (2041-2081)
Probability
Precipitation (mm)

Sep

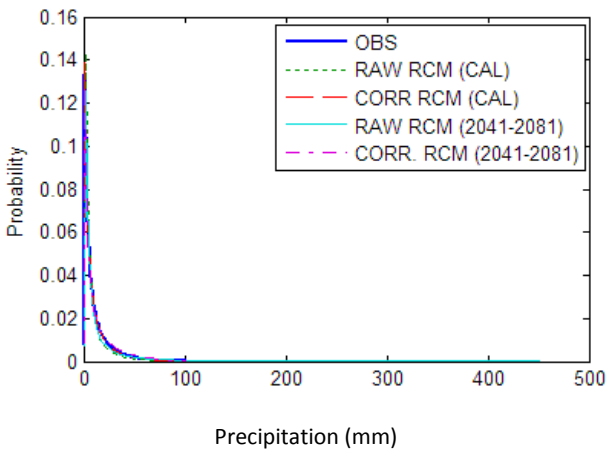
OBS
RAW RCM (CAL)
CORR RCM (CAL)
RAW RCM (2041-2081)
CORR. RCM (2041-2081)
Probability
Precipitation (mm)

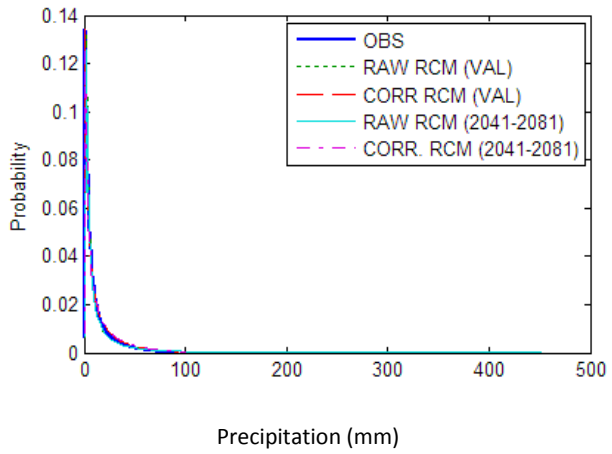
OBS
RAW RCM (VAL)
CORR RCM (VAL)
RAW RCM (2041-2081)
CORR. RCM (2041-2081)
Probability
Precipitation (mm)

Oct

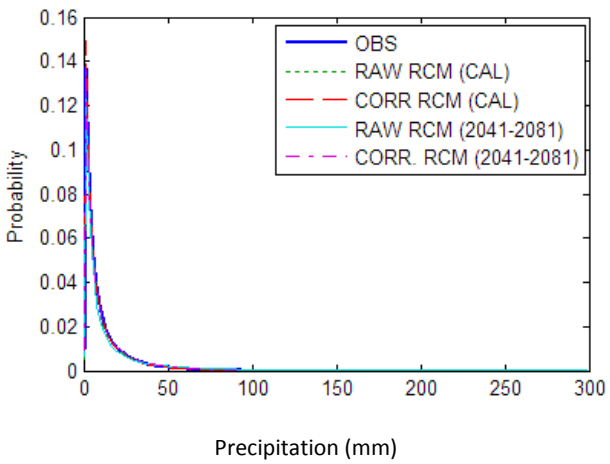
OBS
RAW RCM (CAL)
CORR RCM (CAL)
RAW RCM (2041-2081)
CORR. RCM (2041-2081)
Probability
Precipitation (mm)

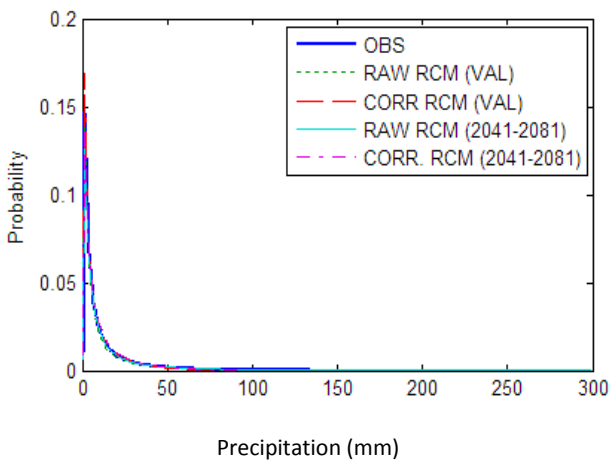
OBS
RAW RCM (VAL)
CORR RCM (VAL)
RAW RCM (2041-2081)
CORR. RCM (2041-2081)
Probability
Precipitation (mm)

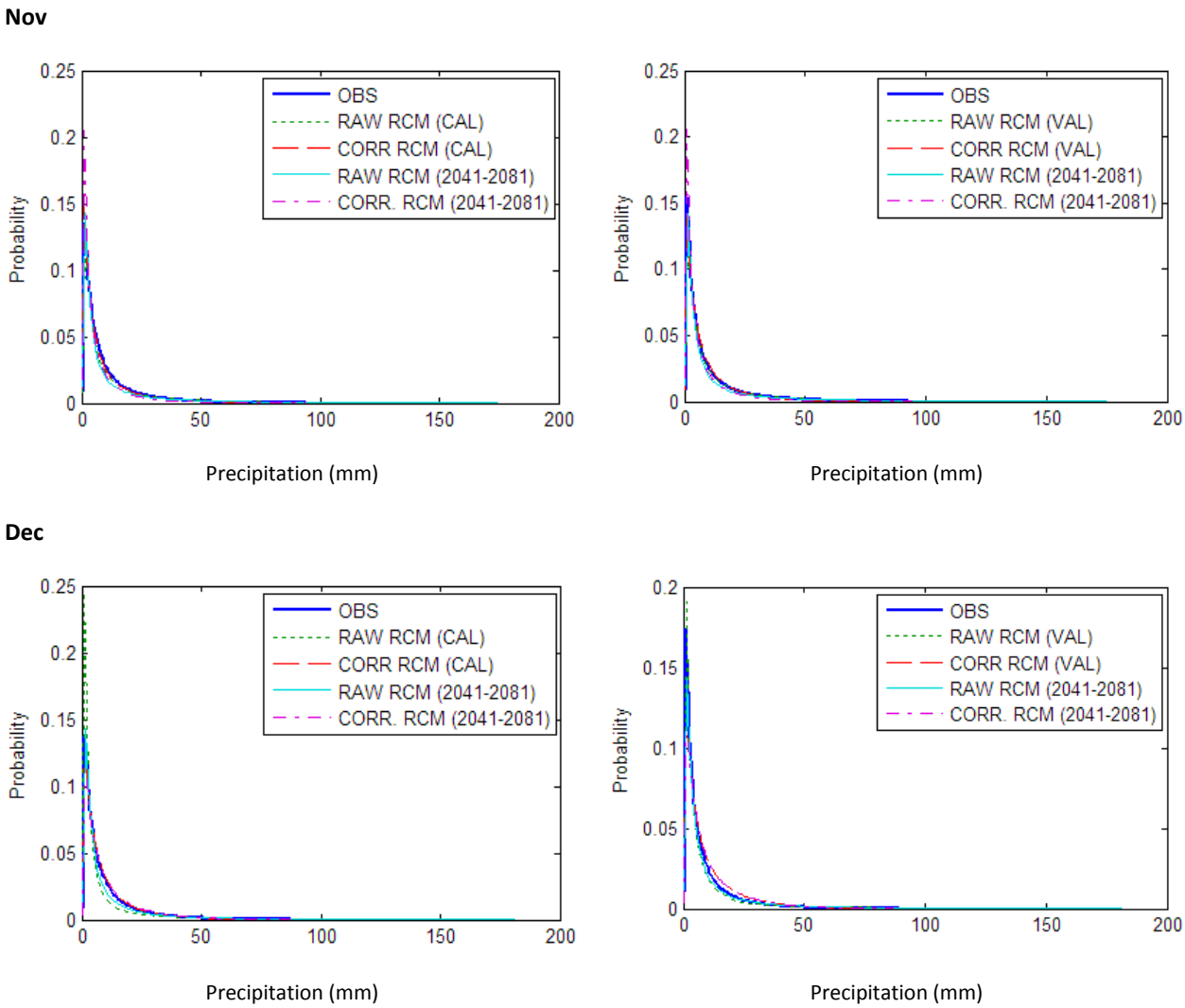

Figure 5.1 Empirical monthly PDF of observed, raw and corrected ARPEGE precipitation (mm d^{-1}) and future raw and corrected RCM precipitation (2041 to 2081) over two periods: (a) calibration (left side) and (b) validation (right side) of the Ottawa Airport station.

(a) **Calibration**

(b) **Validation**

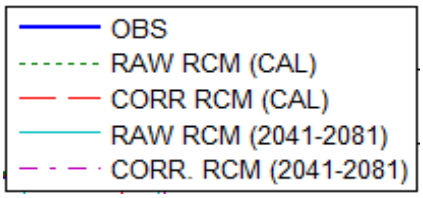

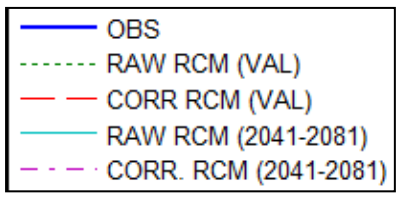

Jan

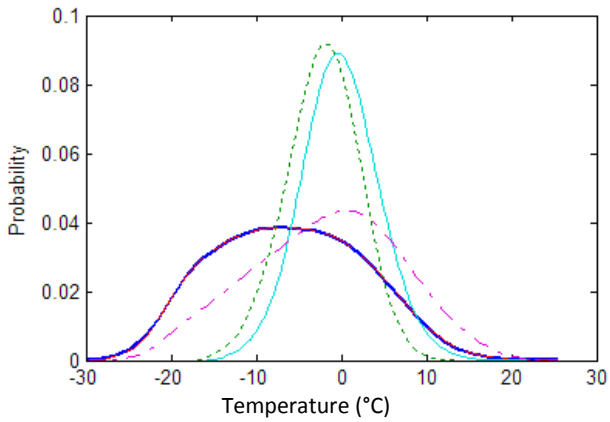

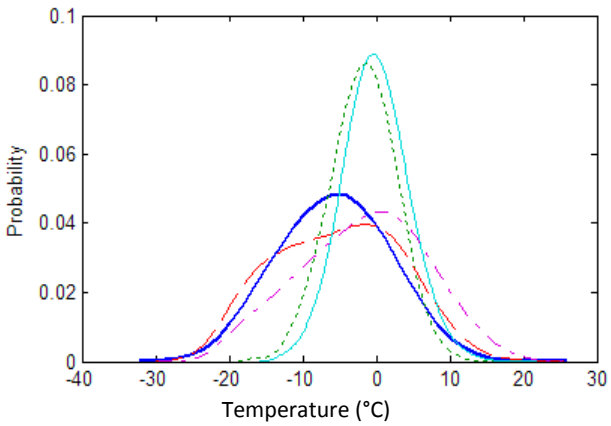

Feb

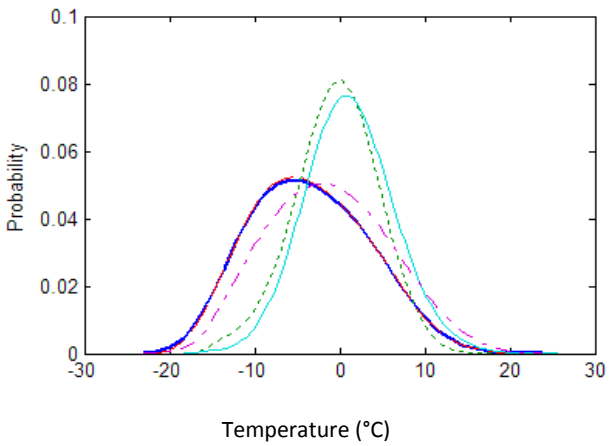

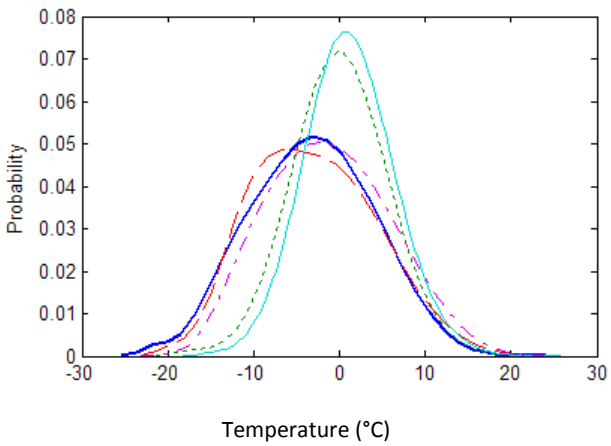

March

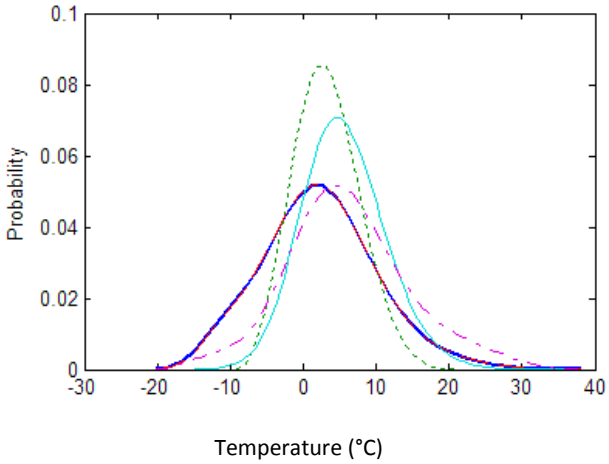

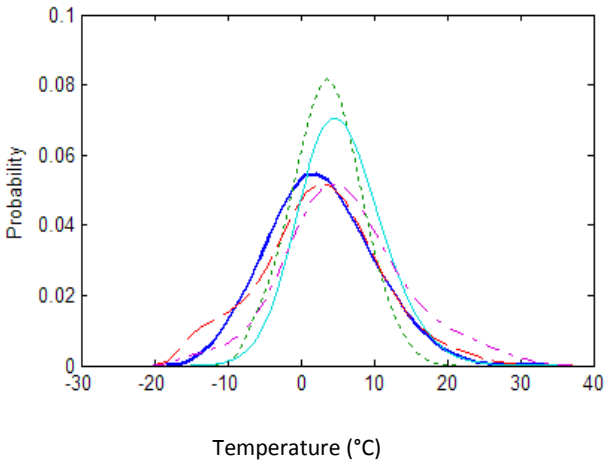

April

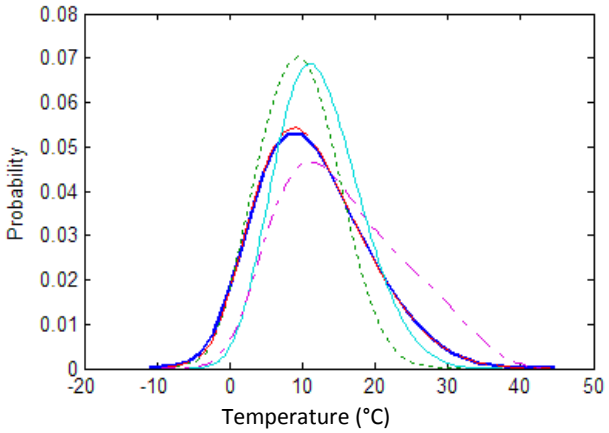

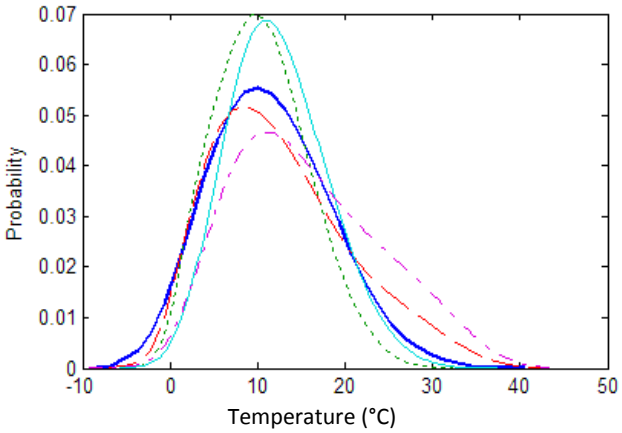

May

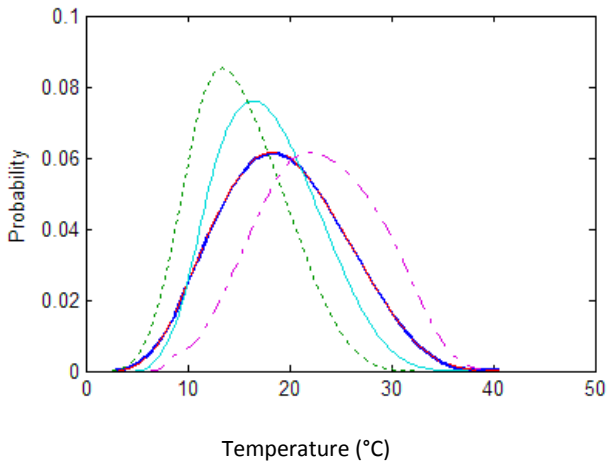

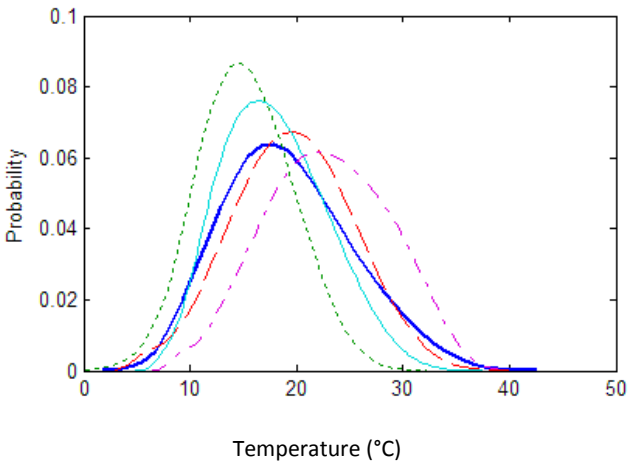

June

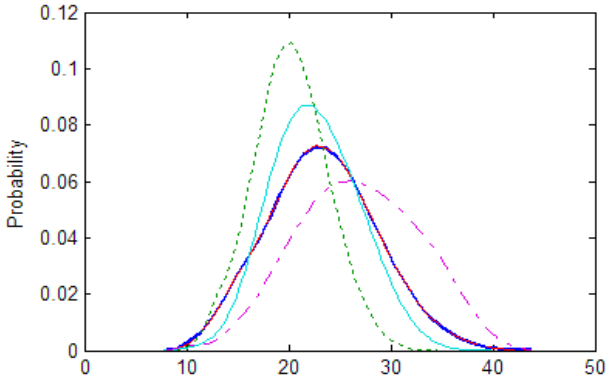

Temperature (°C)

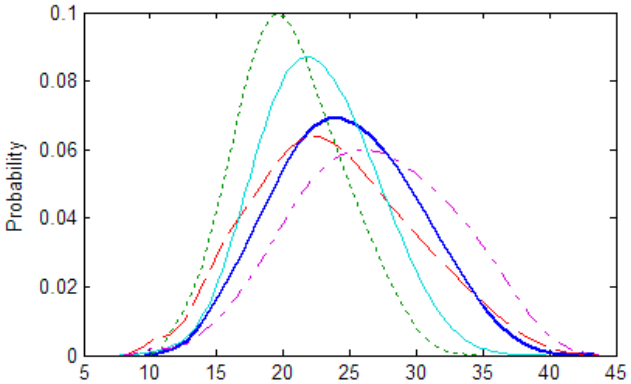

Temperature (°C)

July

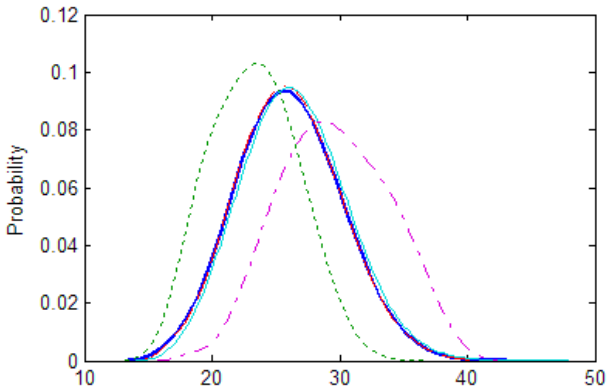

Temperature (°C)

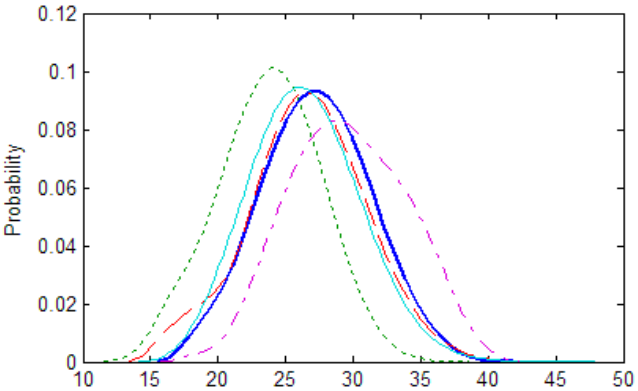

Temperature (°C)

Aug

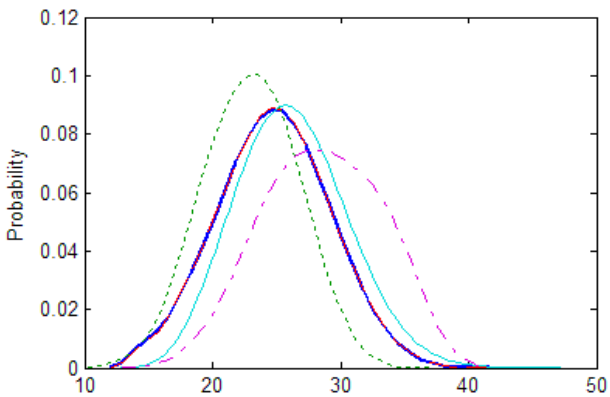

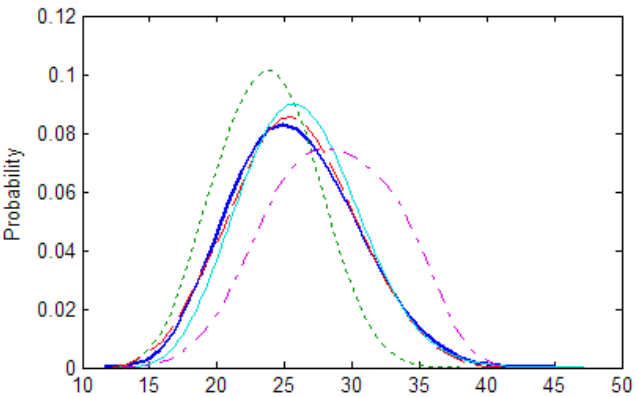

Sep

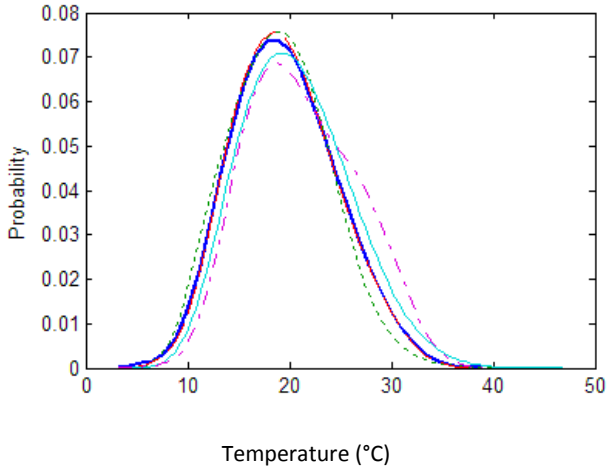
Probability
0.08
0.07
0.06
0.05
0.04
0.03
0.02
0.01
0
0
10
20
30
40
50
Temperature (°C)

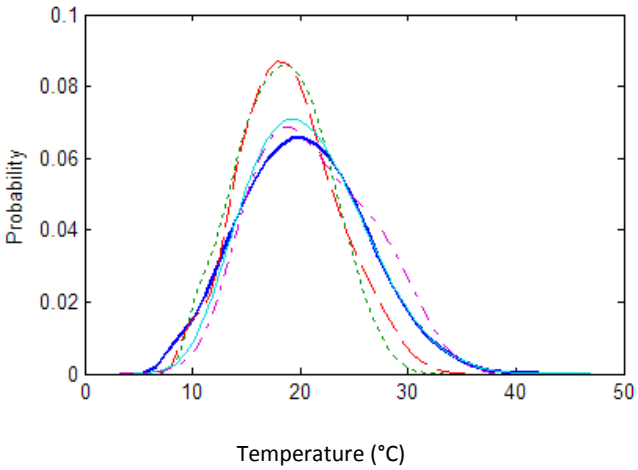
Probability
0.1
0.08
0.06
0.04
0.02
0
0
10
20
30
40
50
Temperature (°C)

Oct

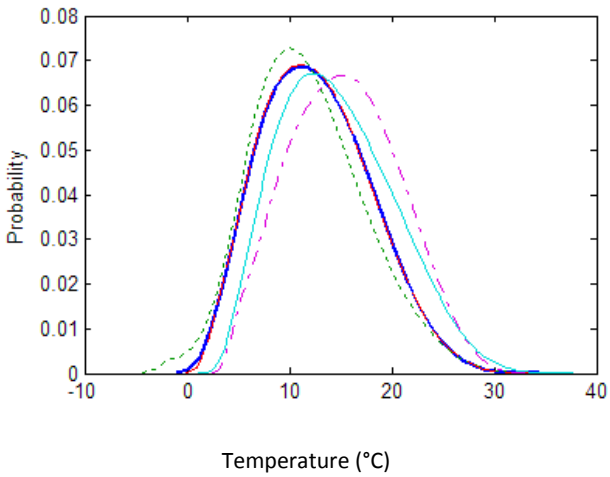
Probability
0.08
0.07
0.06
0.05
0.04
0.03
0.02
0.01
0
-10
0
10
20
30
40
Temperature (°C)

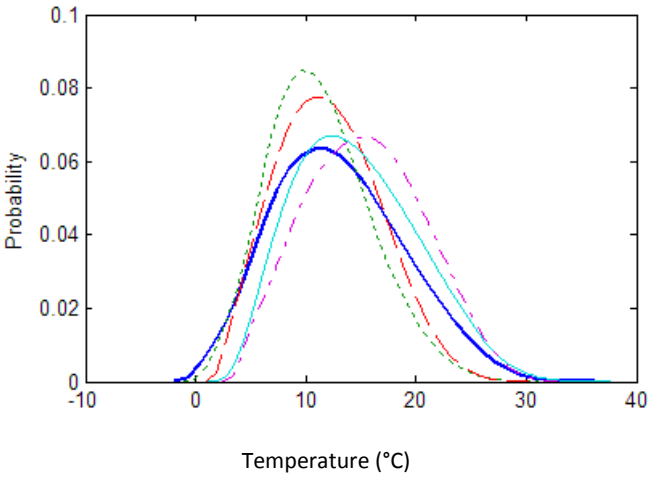
Probability
0.1
0.08
0.06
0.04
0.02
0
-10
0
10
20
30
40
Temperature (°C)

Nov

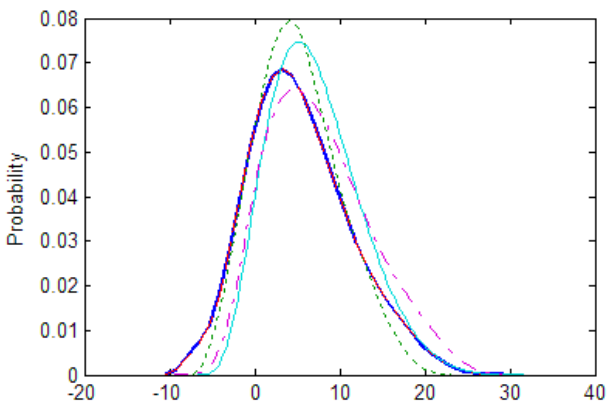
Probability
0.08
0.07
0.06
0.05
0.04
0.03
0.02
0.01
0
-20
-10
0
10
20
30
40

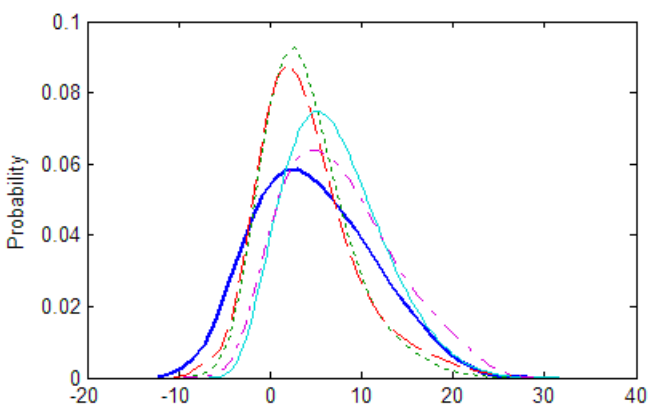
Probability
0.1
0.08
0.06
0.04
0.02
0
-20
-10
0
10
20
30
40

Dec

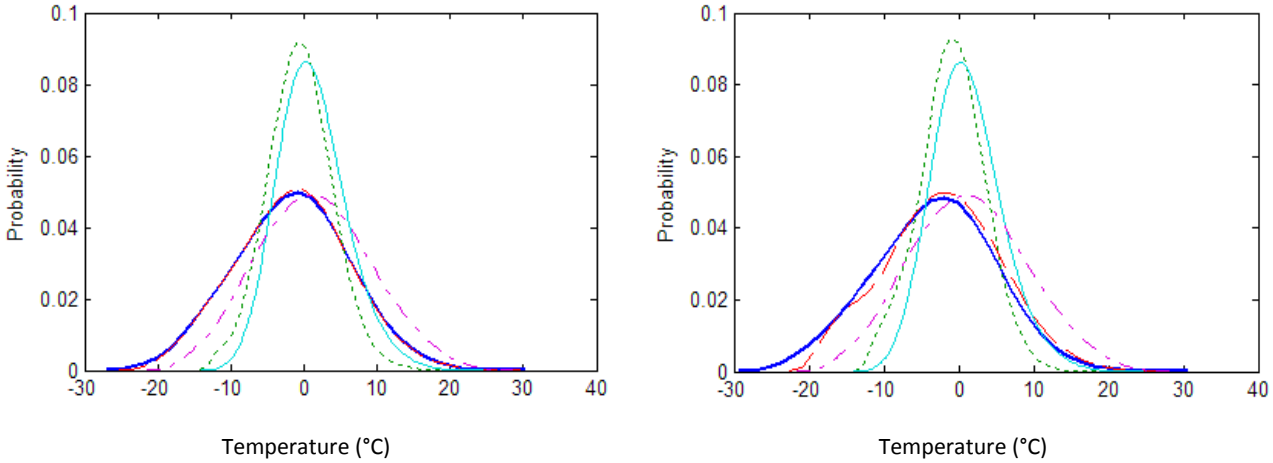

Figure 5.2 Empirical monthly PDF of observed, raw and corrected ARPEGE maximum temperature and future raw and corrected RCM maximum temperature (2041 to 2081) over two periods: (a) calibration (left side) and (b) validation (right side) of the Ottawa Airport station.

(a) **Calibration** (b) **Validation**

Jan

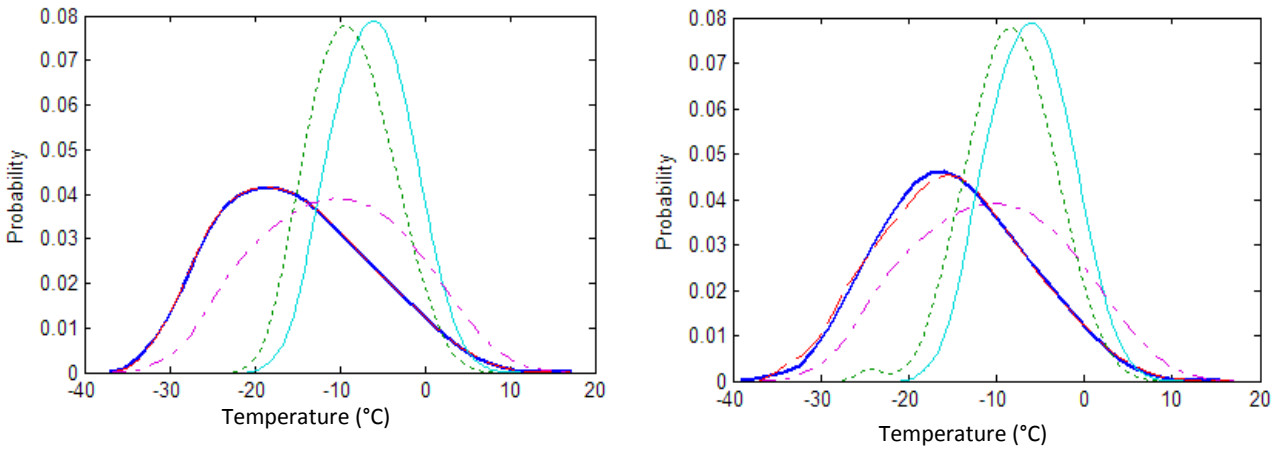

Feb

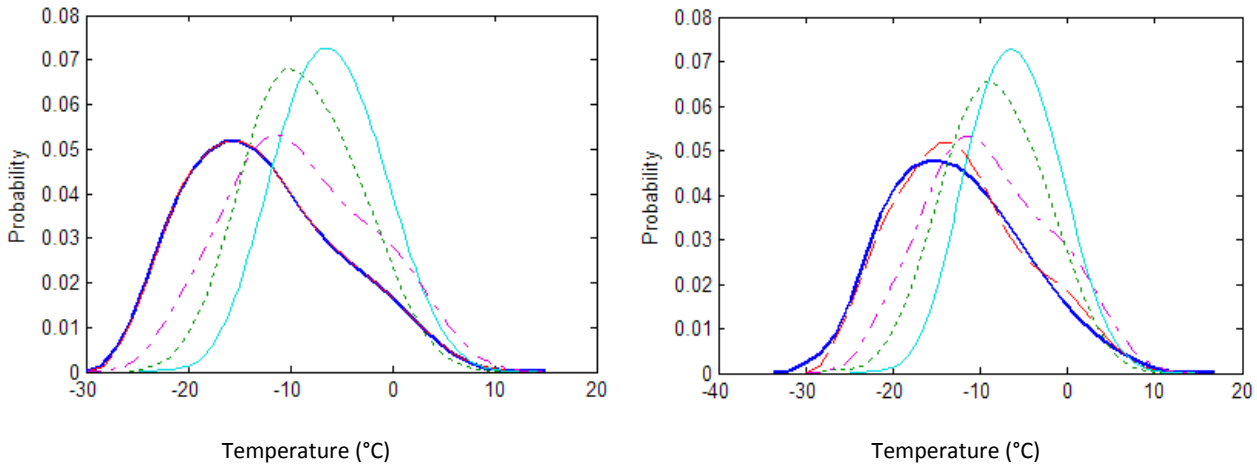

March

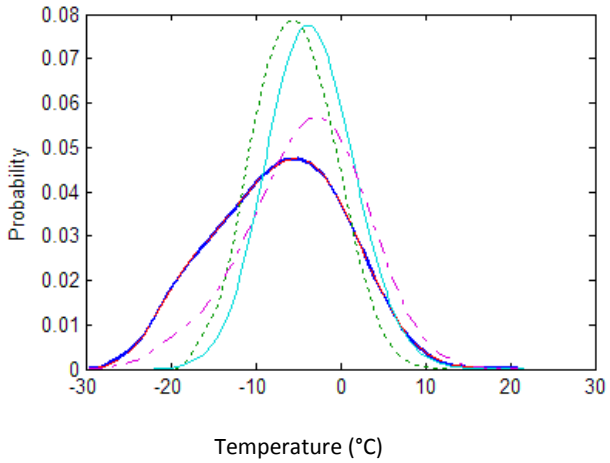

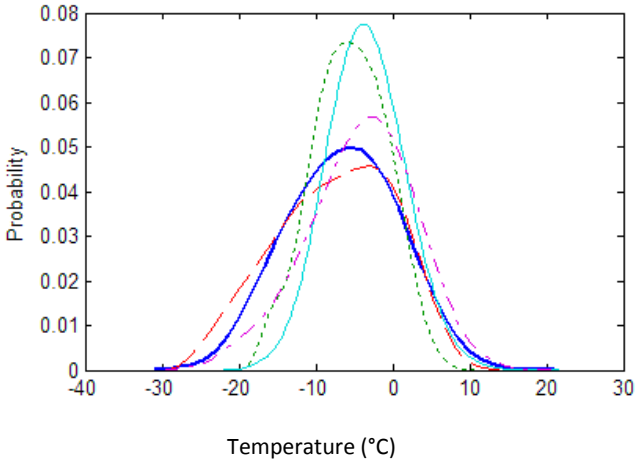

April

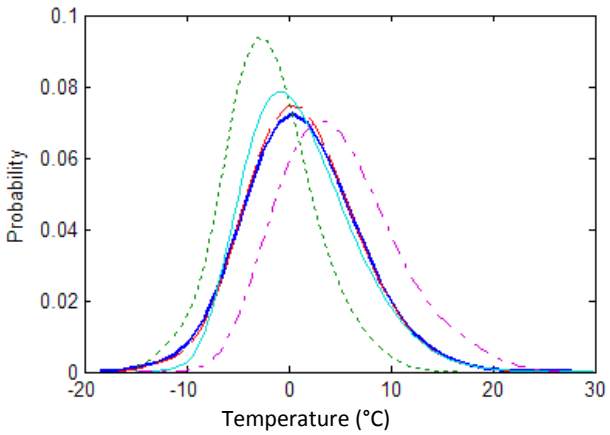

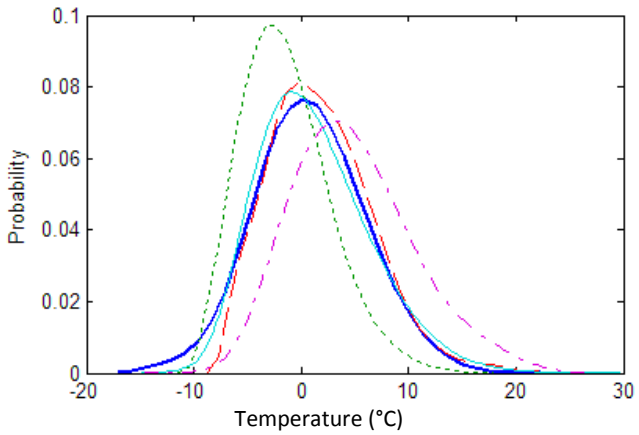

May

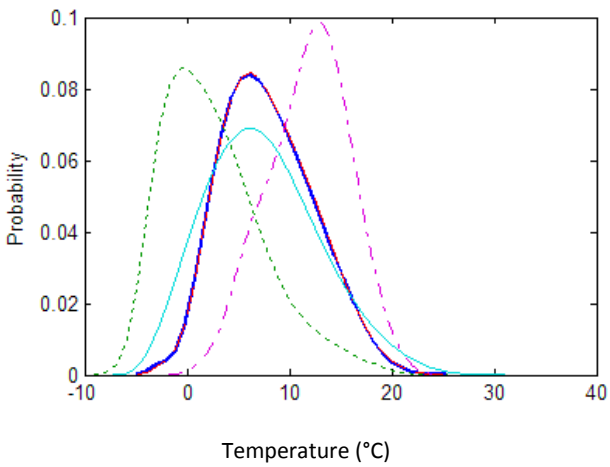

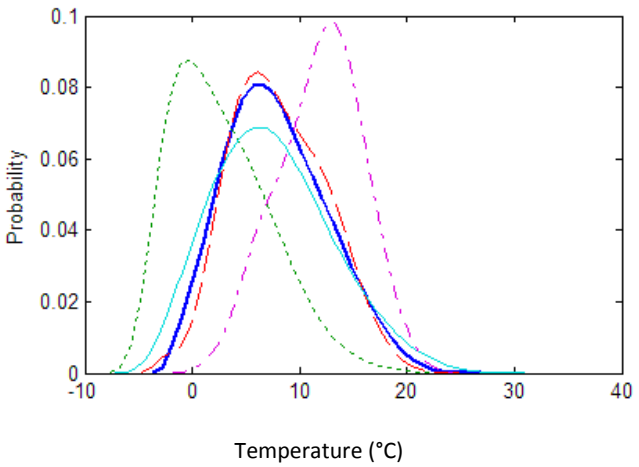

June

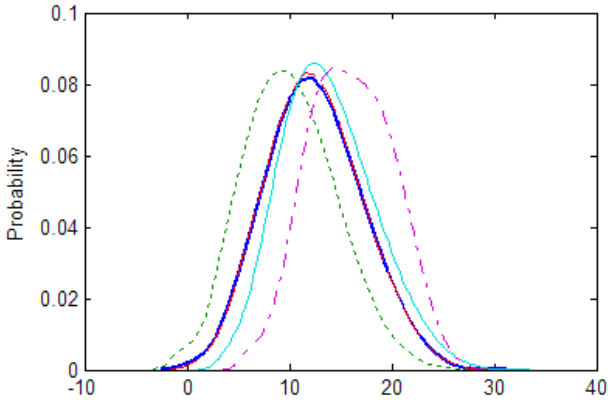

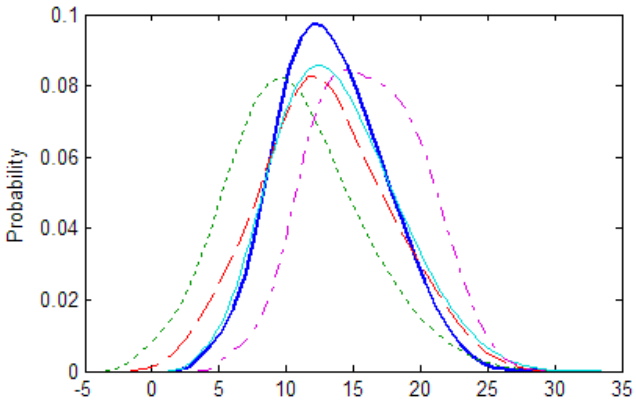

July

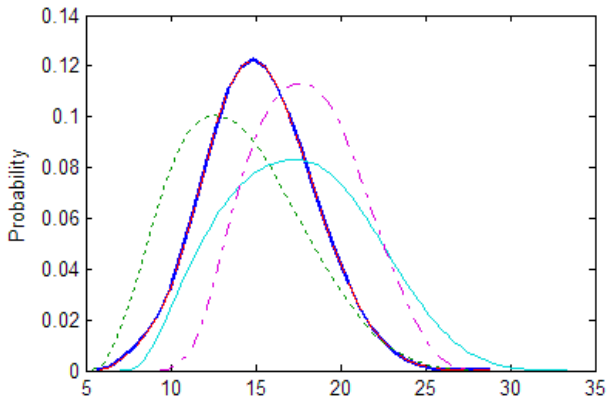

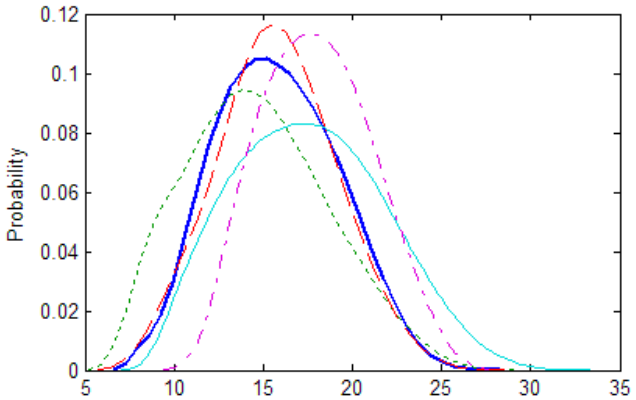

Aug

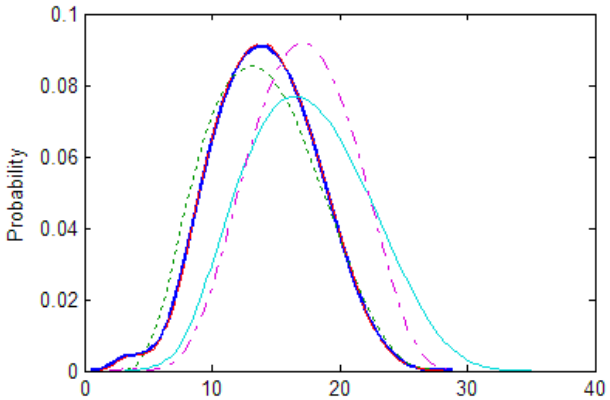

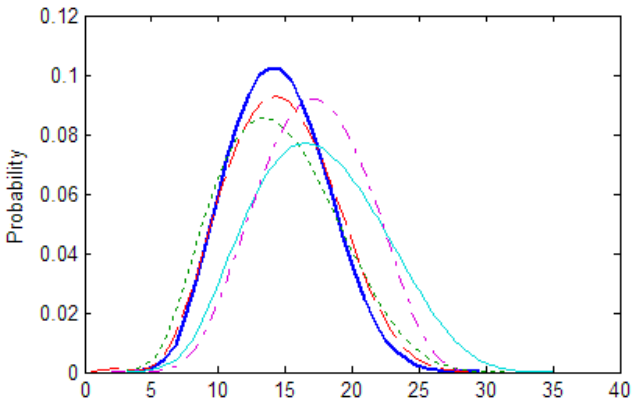

Sep

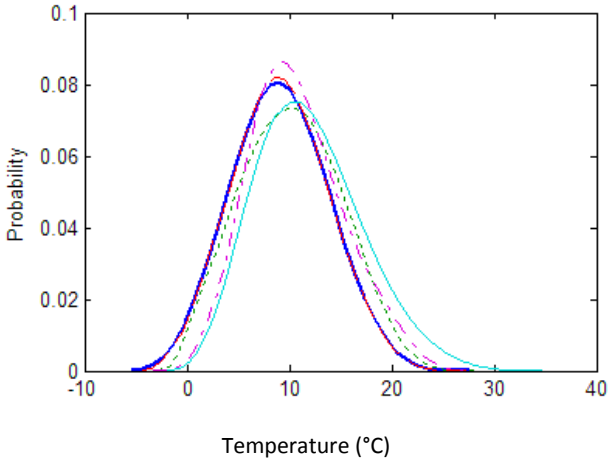
Probability
Temperature (°C)

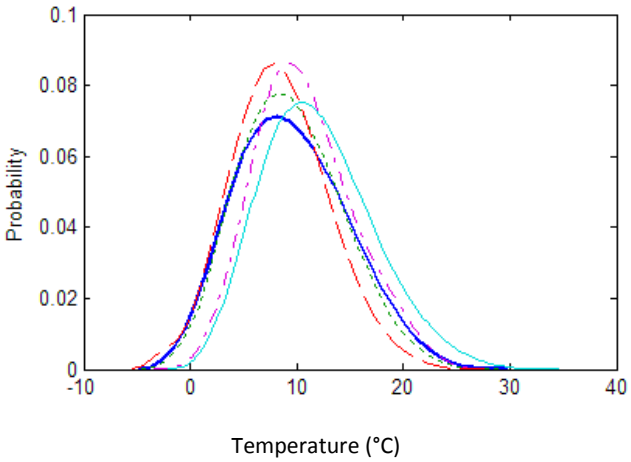
Probability
Temperature (°C)

Oct

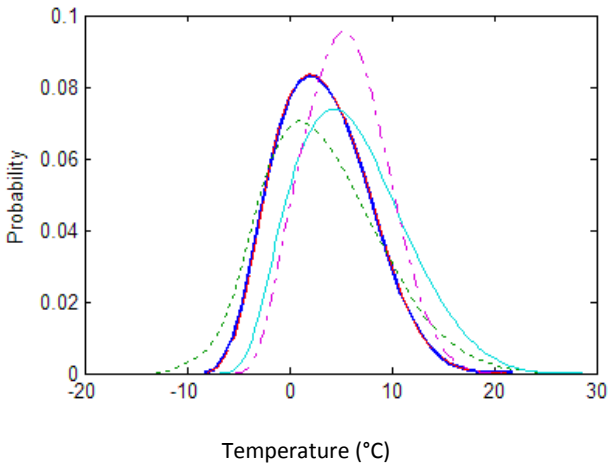
Probability
Temperature (°C)

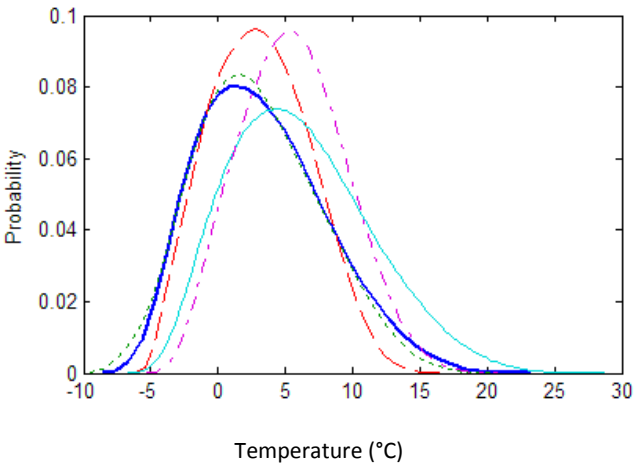
Probability
Temperature (°C)

Nov

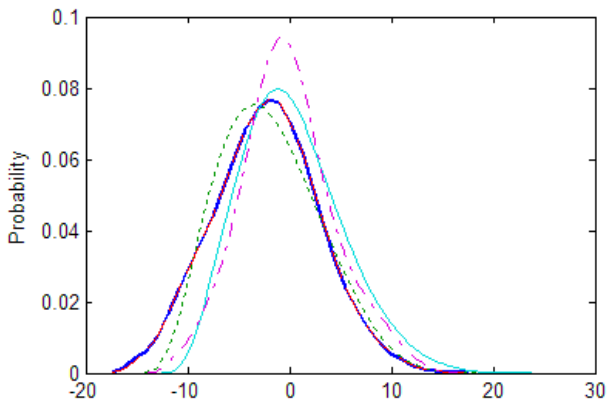
Probability

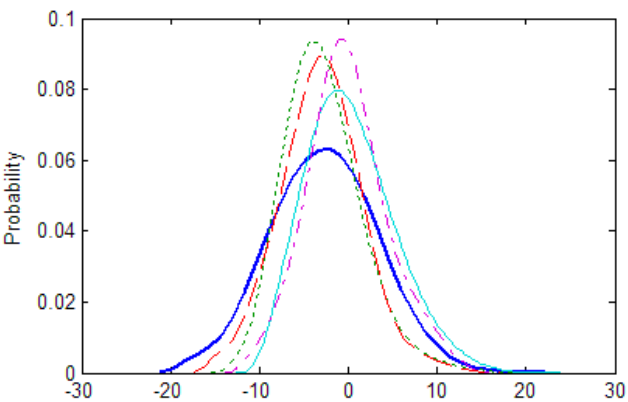
Probability

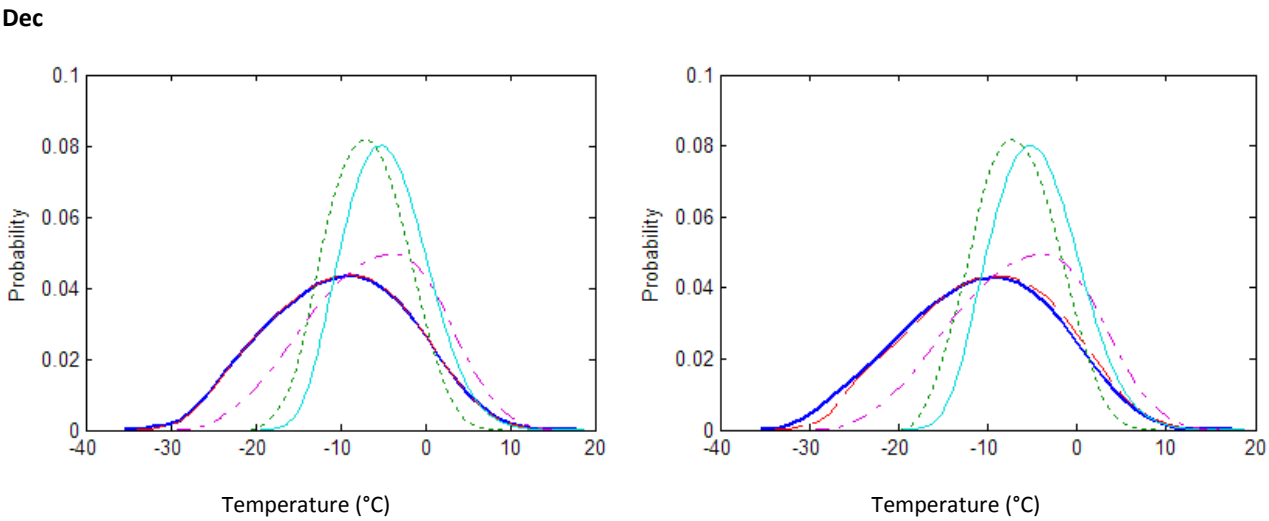

Figure 5.3 Empirical monthly PDF of observed, raw, and corrected ARPEGE minimum temperature and future raw and corrected RCM minimum temperature (2041-2081) over two periods: (a) calibration (left side) and (b) validation (right side) of the Ottawa Airport station.

(a) **Calibration** (b) **Validation**

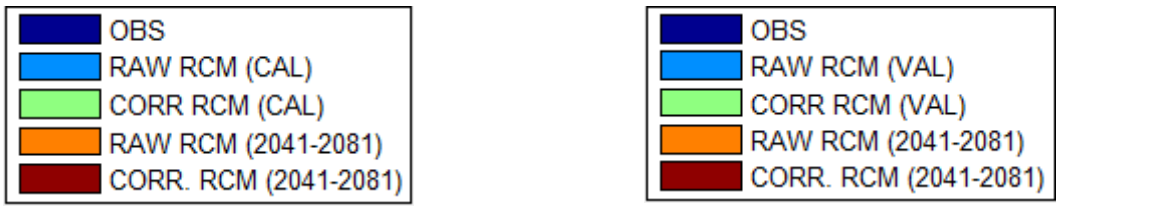

Jan

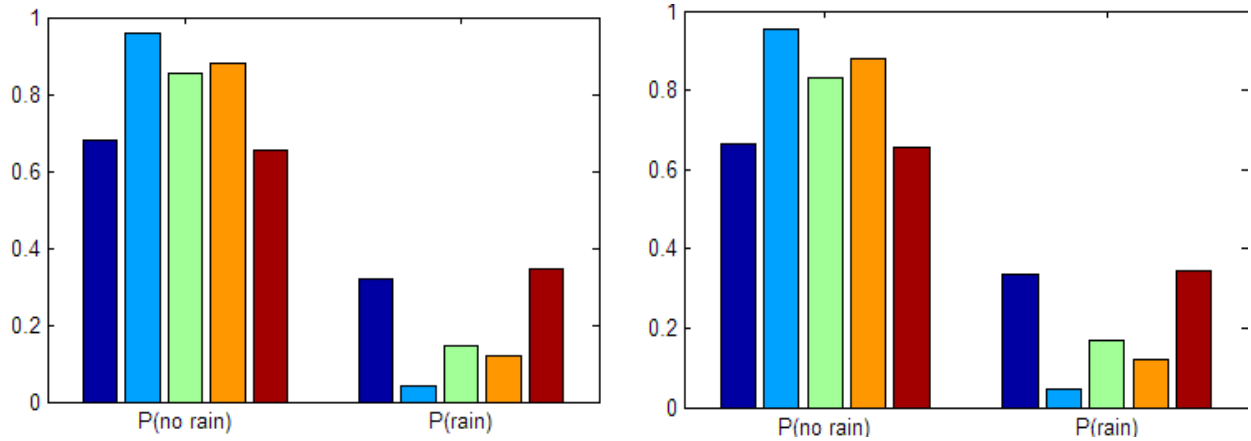

Feb

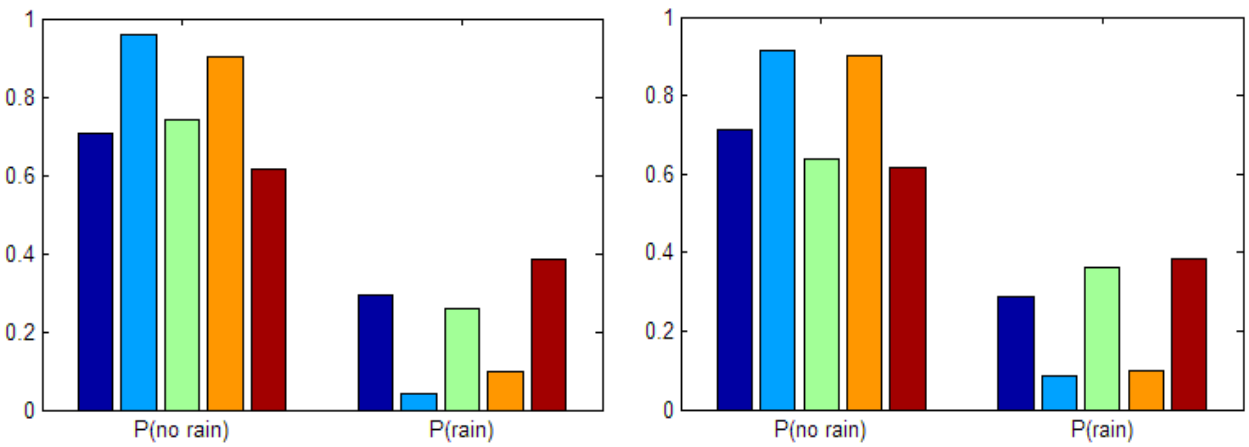

March

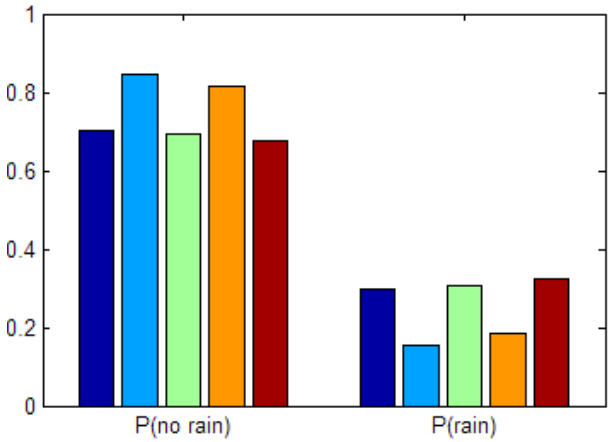

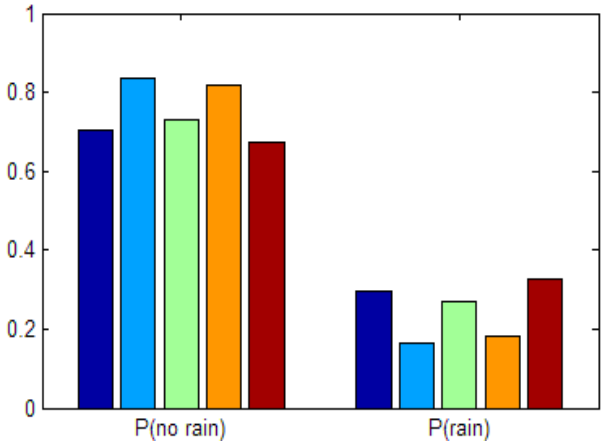

April

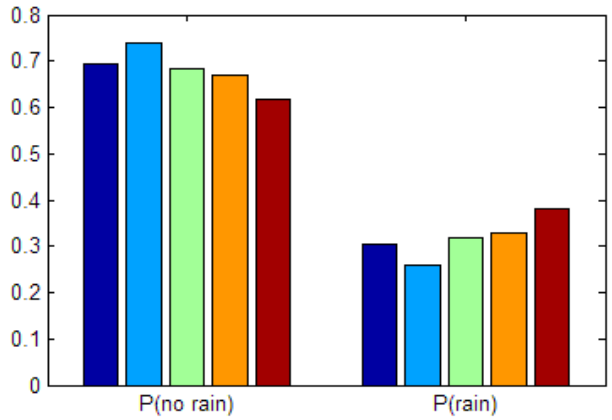

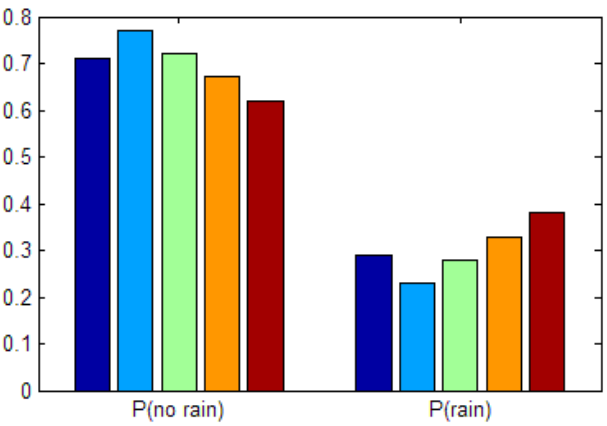

May

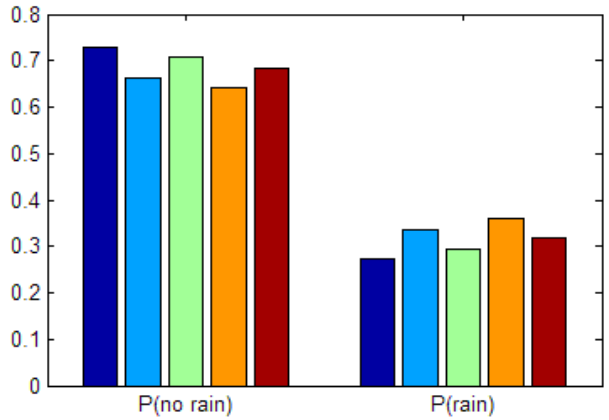

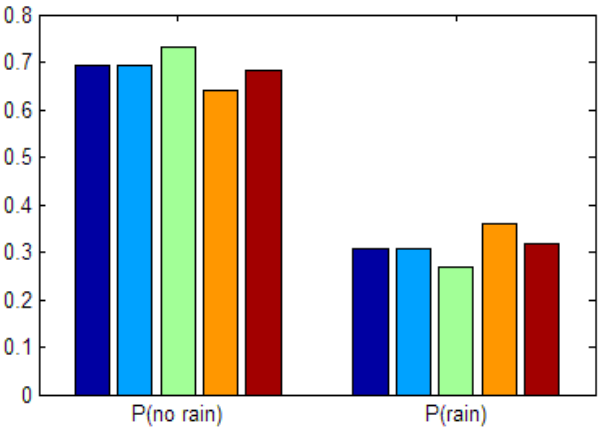

June

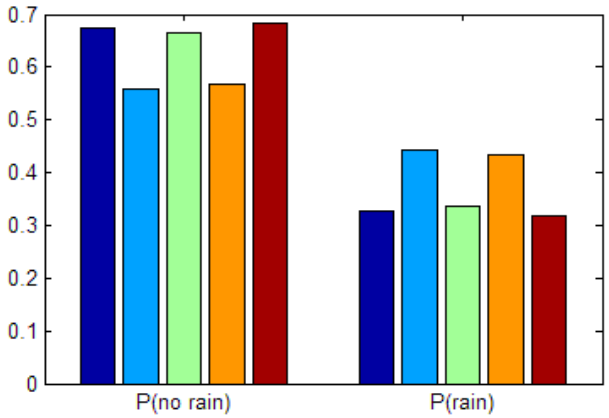

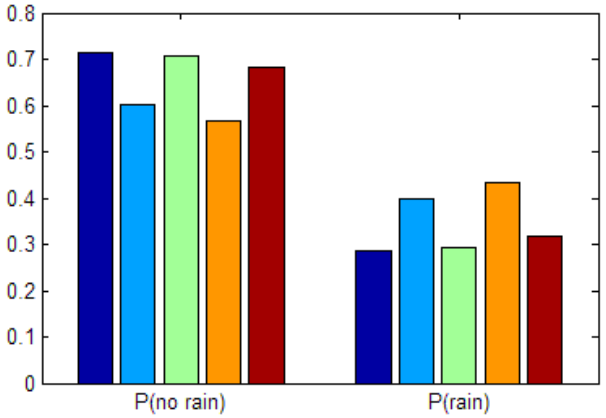

July

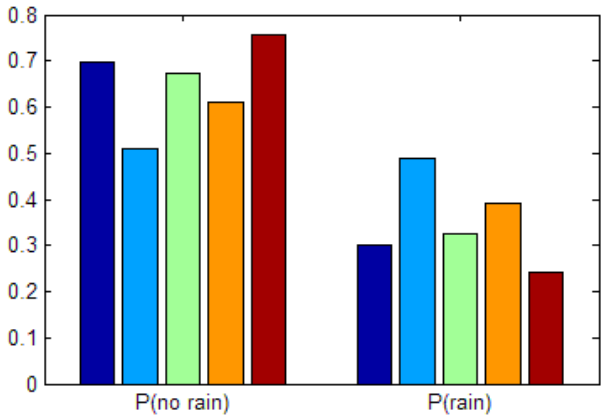

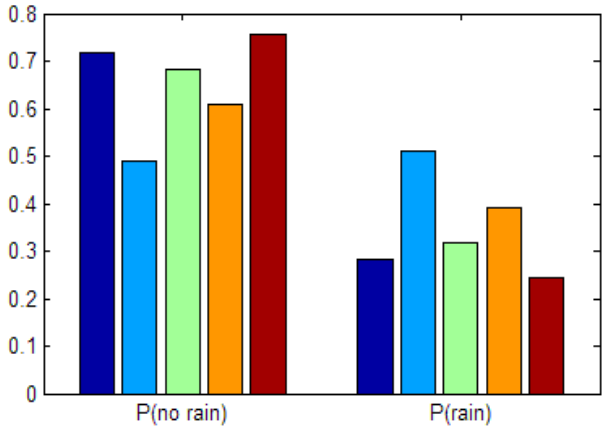

Aug

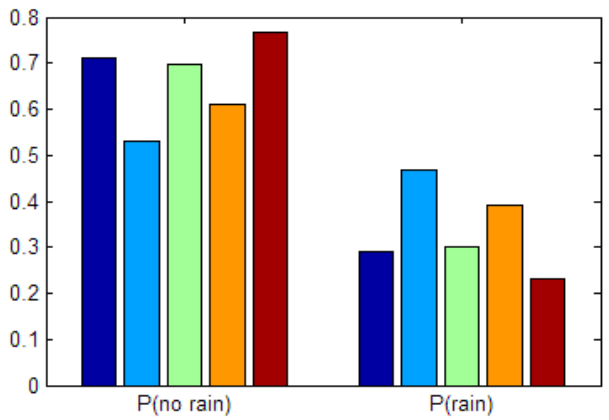

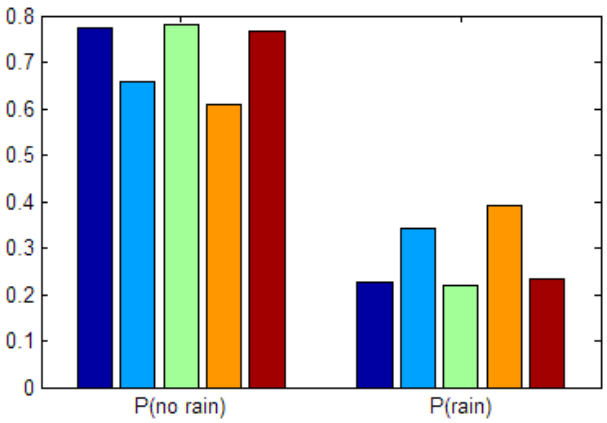

Sep

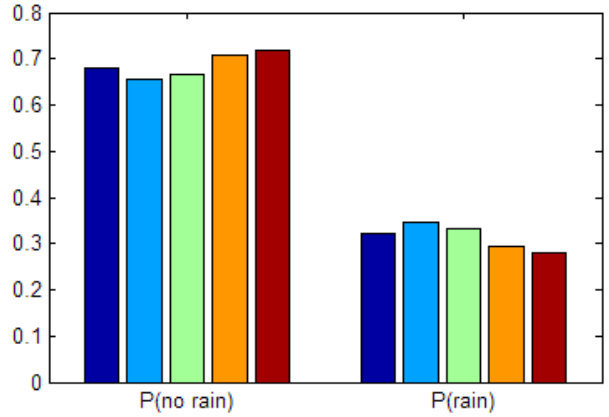
0.8
0.7
0.6
0.5
0.4
0.3
0.2
0.1
0
P(no rain)
P(rain)

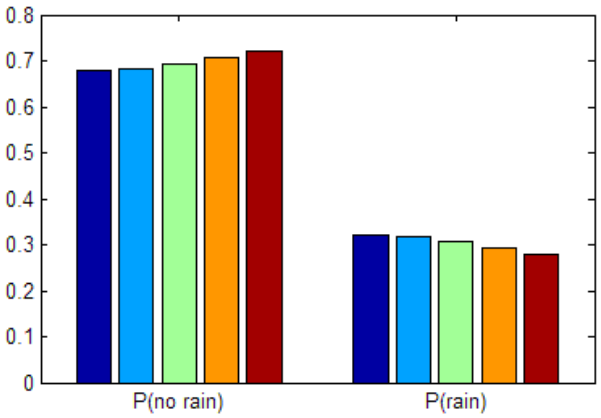
0.8
0.7
0.6
0.5
0.4
0.3
0.2
0.1
0
P(no rain)
P(rain)

Oct

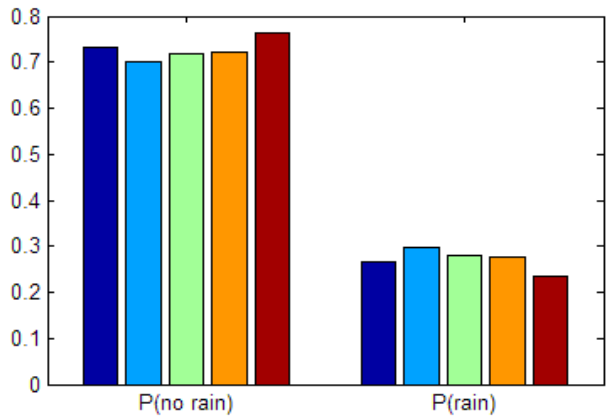
0.8
0.7
0.6
0.5
0.4
0.3
0.2
0.1
0
P(no rain)
P(rain)

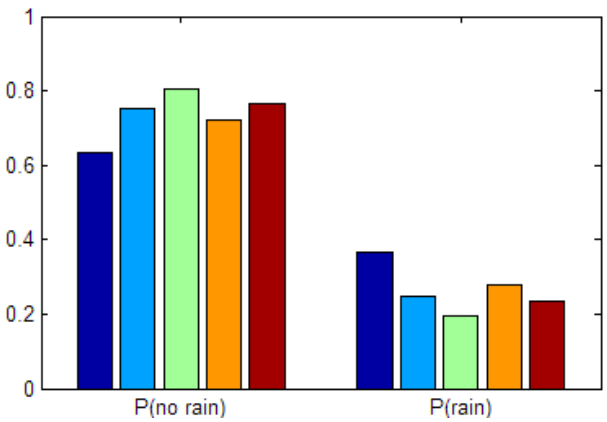
1
0.8
0.6
0.4
0.2
0
P(no rain)
P(rain)

Nov

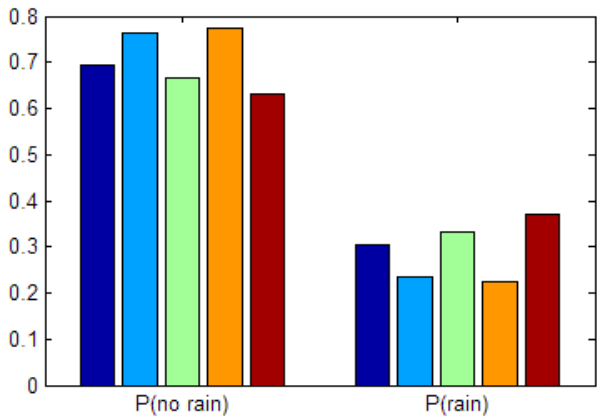
0.8
0.7
0.6
0.5
0.4
0.3
0.2
0.1
0
P(no rain)
P(rain)

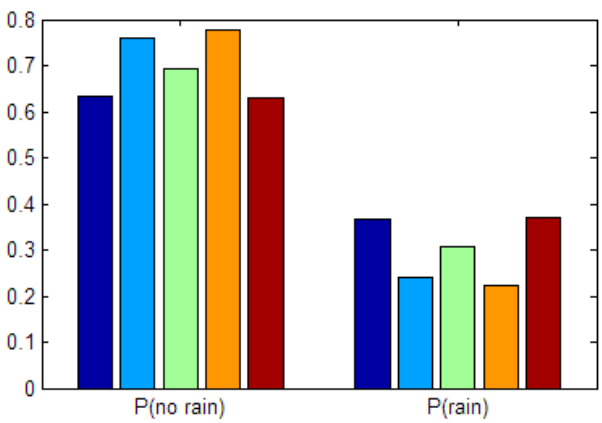
0.8
0.7
0.6
0.5
0.4
0.3
0.2
0.1
0
P(no rain)
P(rain)

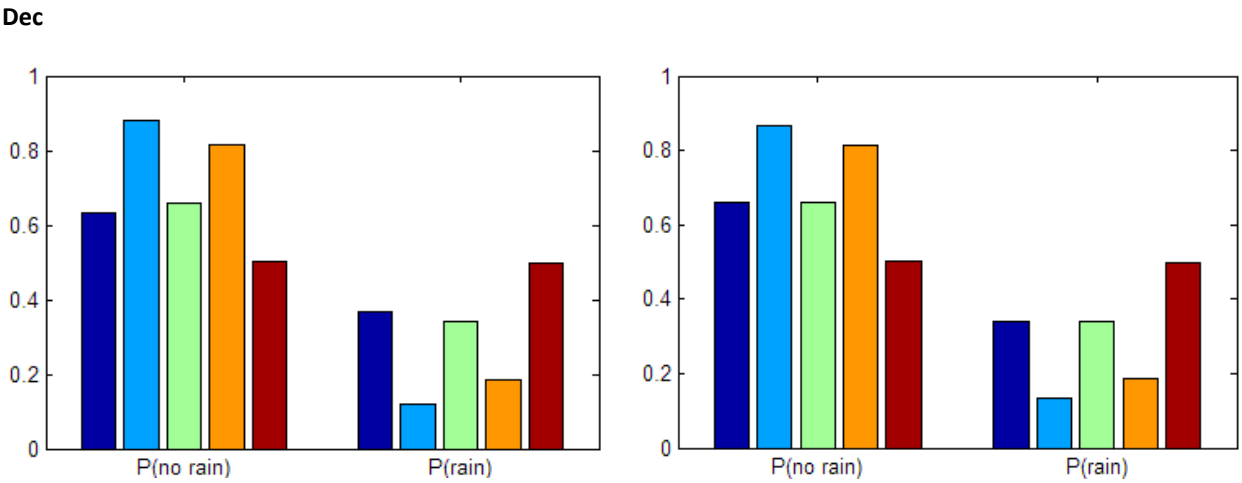

Figure 5.4 Probability of precipitation over 1 mm in observed data, raw and corrected ARPEGE precipitation occurrence over two periods: (a) calibration (left side) and (b) validation (right side) of Ottawa Airport station.

5.3 Precipitation projections

The projected warmer climate is expected to alter other climate system variables, such as precipitation and evaporation, which in turn will affect stream flow. This could lead to more frequent occurrences of severe hydrologic anomalies, including both floods and droughts.

5.3.1 Changes in precipitation occurrence

Wet day refers to the annual number of days with at least 1 millimeter of precipitation. As presented in Table 5.2, after correction CRCM is faultlessly consistent with observed wet days, whereas wet days are still underestimated in the corrected ARPEGE outputs. A slightly higher percentage of wet days is projected for the future, compared to the last four decades of

the 20th century. It is important to emphasize that the rising in number of wet days associated with higher temperatures implies a tendency toward more convective weather systems, which in turn will lead to more localized thunderstorms as found by Mailhot *et al*. (2007).

Table 5.2 Mean annual wet days for observed, corrected, and projected ARPEGE and CRCM, and projected change.

Station	OBS	1961-2001		2041-2081		Change (%)	
		ARPEGE	CRCM	ARPEGE	CRCM	ARPEGE	CRCM
Airport	117.1	104.41	118.24	119.32	123.59	2%	6%
Avonmore	131.12	119.27	127.66	127.98	134.76	-2%	3%
Brockville	124.33	117.51	124.9	128.37	132.85	3%	7%
Pointe au Chene	110.41	101.71	112.49	110.17	117.8	0%	7%
Russell	129.79	114.85	126.27	122.76	131.85	-5%	2%
South Mountain	125.32	121.37	124.22	125.34	131.07	0%	5%
St. Albert	134.31	125.22	135.98	138.24	140.73	3%	5%
Average	124.63	114.91	124.25	124.6	130.38	0%	5%

5.3.2 CRCM Simulations

According to the corrected CRCM simulations, a wetter climate is expected when the number of rainy days is projected to increase from 30% to 40% during the winter months, and the intensity of precipitation is also projected to increase. In addition, the corrected CRCM slightly overestimates annual total precipitation (PRCTOT) under the current climate, as shown in Table 5.3. For PRCTOT, any year with more than one month of missing data was

excluded. For example, Pointe au Chene station has missing data from numerous months, which affects its results (i.e. data from 15 years have been excluded, thus the final number of included years is 26). The results of annual total precipitation (PRCPTOT) suggest considerable change, as it is projected to rise to an average of 1100 mm in all stations, as presented in Table 5.3. This is an average increase of approximately 16%, compared to the mean annual total precipitation over the last four decades of 947 to 1122 mm per year. At the Ottawa Airport station, projected precipitation amounts show an increase of 20%. The lowest increase between the current period and future period (2041 to 2081) is 10% (from 923 to 1024), at the Pointe au Chene station.

Table 5.3 Mean annual total precipitation of all stations for observed, corrected and projected ARPEGE and CRCM, and projected changes.

Station	OBS	1961-2001		2041-2081		Change (%)	
		ARPEGE	CRCM	ARPEGE	CRCM	ARPEGE	CRCM
Airport	900	894	945	1140	1114	27%	24%
Avonmore	987	956	979	1103	1114	12%	13%
Brockville	970	942	990	1101	1141	14%	18%
Pointe au Chene	923	855	882	976	1024	6%	11%
Russell	914	926	946	1082	1102	18%	21%
South Mountain	894	936	950	1067	1090	19%	22%
St. Albert	1043	1044	1100	1255	1270	20%	22%
Average	947	936	970	1103	1122	16%	18%

5.3.3 ARPEGE Simulations

The ARPEGE model projects more wet days, with an average increase in total annual precipitation of 14.2%. The highest increase of 21% (240 mm/year) is expected at the Airport station, compared to the average (from 900 to 1140 mm per year) of the last four decades of the 21st century.

In summary, the CRCM and ARPEGE models project an increase in total precipitation of 5.4 to 21.1% annually. These results are somewhat consistent with the study of Dibike *et al*. (2012), who downscaled three RCMs under the conditions of SRES's A2 emission scenario in the Lake Winnipeg watershed. They found that total annual precipitation will increase by 5.5 to 7.7% in the 2050s (2041–2070) compared to the 1980s (1971–2000).

5.4 Maximum Temperature Projections

5.4.1 CRCM Simulations

Russell Station is projected to have the hottest climate, with an increase in mean annual maximum temperature to 14.79 °C, 3.08 °C above the historical mean of 11.71 °C. The anticipated warming in all locations is from 2.63 to 3.34 °C, as shown in Table 5.3.

Table 5.4 Mean annual maximum temperature in °C at all stations for current (observed, corrected ARPEGE and corrected CRCM), future (corrected ARPEGE and corrected CRCM), and projected change.

Station	OBS	1961-2001		2041-2081		Change in °C	
		ARPEGE	CRCM	ARPEGE	CRCM	ARPEGE	CRCM
Airport	11.07	11.17	10.93	14.47	14.22	3.4	3.15
Avonmore	11.42	11.25	11.08	13.64	14.13	2.22	2.71
Brockville	11.66	11.67	11.58	14.15	14.54	2.49	2.88
Pointe au Chene	10.88	10.99	10.75	12.83	13.77	1.95	2.89
Russell	11.71	11.51	11.3	14.79	14.56	3.08	2.85
South Mountain	11.25	11.49	11.34	13.96	14.59	2.71	3.34
St. Albert	11.38	10.85	10.8	14.14	14.02	2.76	2.64
Average	11.34	11.28	11.11	14	14.26	2.66	2.92

5.4.2 ARPEGE Simulations

The mean annual maximum temperature produced by the corrected ARPEGE showed significant projected changes, with increases ranging from 1.95 to 3.39°C. These results were slightly less in certain locations, such as the Pointe au Chene station temperature increase that was 9% lower than the corrected CRCM. As shown in Table 5.4, the Airport station is expected to experience the most significant rise in temperature, with an increase of 3.4 °C.

Both CRCM and ARPEGE indicated a net increase in maximum temperature of 1.95 to 3.4 °C in the region. These results are consistent with Dibike *et al*. (2012), who downscaled three RCMs under the conditions of SRES's A2 emission scenario in the Lake Winnipeg watershed, and projected that the maximum temperature will increase by 2.0 to 2.8 °C from 2041 to 2070, compared to the 1971 to 2000 period. One of the important implications of climate change in Canada, as shown by a study conducted on the Chaudière River, Québec by Quilbé *et al*. (2008), is the projected winter increase in stream flow due to higher temperatures associated with earlier snowmelt, particularly from 2010 to 2039.

5.5 Minimum Temperature Projections

5.5.1 CRCM Simulations

After correction, the CRCM model projected an increase of 3.3 °C in minimum temperatures across the watershed for the 2041 to 2081 period, compared to the current climate (see Table 5.5). However, it is worth noting that corrected CRCM slightly underestimates T_{MIN} for the current climate (e.g. 1.25 °C is the observed average minimum temperature, whereas the corrected CRCM outputs suggest 0.93 for the same period).

Table 5.5 Mean annual minimum temperature of all stations in °C for current (observed, corrected ARPEGE and corrected CRCM), future (corrected ARPEGE and corrected CRCM), and projected change.

Station	OBS	1961-2001		2041-2081		Change in °C	
		ARPEGE	CRCM	ARPEGE	CRCM	ARPEGE	CRCM
Airport	1.15	1.29	0.95	4.55	4.25	3.4	3.1
Avonmore	0.75	0.68	0.43	3.41	4.16	2.66	3.41
Brockville	2.94	2.85	2.71	5.4	6.07	2.46	3.13
Pointe au Chene	0.99	0.73	0.46	2.98	3.99	1.99	3
Russell	1.23	1.08	0.75	4.6	4.5	3.37	3.27
South Mountain	0.93	1.21	0.91	4.01	4.72	3.08	3.79
St. Albert	0.79	0.48	0.28	4.16	4.06	3.37	3.27
Average	1.25	1.19	0.93	4.16	4.54	2.91	3.29

5.5.2 ARPEGE Simulations

As seen in Table 5.5, ARPEGE projects a future increase in mean minimum temperature from 0.79 to 2.94 °C, to 2.98 to 5.4 °C. Compared to CRCM, ARPEGE simulations represent historical records more accurately. ARPEGE is also slightly more conservative in terms of anticipated changes. These significant shifts will undoubtedly affect the hydrological regime of the South Nation watershed.

The CRCM and ARPEGE models project a continuous regional increment in minimum temperature increase from 2041 to 2081 of 1.99 to 3.79 °C. This finding is

consistent with a previous study by the U.S. EPA (2008), which projected a warmer climate in the Great Lakes basin (which comprises the South Nation watershed) of 2 to 4 °C by the middle of the 21st century, when the carbon dioxide level will be twice its pre-industrial level. Similarly, Dibike *et al*. (2012) downscaled three RCMs under the conditions of SRES's A2 emission scenario in the Lake Winnipeg watershed, and found that the minimum temperature will increase by 2.2 to 2.9 °C from 2041 to 2070, compared to 1971 to 2000. In turn, thise anticipated augmentation in air temperature would accelerate evaporation and evapotranspiration from the lake, river and land surfaces of the watershed, accompanied by a shortage in the percentage of precipitation that drains into the river (Abdel-Fattah & Krantzberg, 2014). As stated by the U.S. EPA (2008), several studies have demonstrated that the changing climate will reduce the net watershed supply to the overall hydrologic system of the Great Lakes basin by 23 to 50 %, which will significantly impact future hydrological regimes.

5.6 Trend Detection

Non-parametric classical and seasonal Mann-Kendall tests were applied to identify trends in precipitation, maximum temperature and minimum temperature time series, and the Sen's Slope Estimator was used to calculate the magnitude of slopes. Trend analysis of these climate variables was performed using the data of both corrected RCMs, from 1961 to 2001 and 2041 to 2081, as well as observed data. It is very interesting that no significant decreasing trends of the three variables for all times, stations and models were detected. Table 5.5 presents the results of trend detection applied to all variables, and the results for each variable are discussed in further detail below.

Table 5.6 Number of stations (out of seven) with an upward trend for the five data sets, based on original and seasonal Mann-Kendall trend tests. Note that no stations had a downward trend in any variable, meaning that the five stations that do not have an upward trend have no trend. T_{MAX}, T_{MIN}, PRCP and PRCTOT refer to maximum temperature, minimum temperature, annual maximum precipitation, and annual accumulated precipitation, respectively.

Test	**Classical Mann-Kendall trend**				**Seasonal Mann-Kendall trend**	
Model	T_{MAX}	T_{MIN}	PRCP	PRCTOT	T_{MAX}	T_{MIN}
Observations	6	7	2	2	5	7
ARPEGE 1961-2001	1	7	3	0	7	7
CRCM 1961-2001	7	7	0	0	7	7
ARPEGE 2041-2081	7	7	0	0	7	7
CRCM 2041-2081	7	7	0	6	7	7

5.6.1 Trends in annual precipitation amounts

This study investigated whether the past forty-year increasing trends in annual maximum and annual accumulated precipitation detected at some stations will continue over the coming decades, by examining two time series: annual maximum precipitation (PRCP) and annual total precipitation (PRCTOT). Table 5.7 presents a sample of the analysis for the Airport station, which shows an upward historical trend for both variables at this particular station. However, no variation trends were detected in the current and future time periods of the outputs of both RCMs. The only exception is CRCM's future annual accumulated

precipitation Sen's slope of 0.0557 (mm /year), which is steeper than the historical Sen's slope of 0.02887; this upward trend was also detected at five other stations. Although the slope magnitude is high in some cases, the Mann-Kendall test does not consider this a trend, which is likely due to the relatively short length of data sets used, combined with high variability. Five of the stations under study did not show any significant trends in maximum annual and accumulated annual precipitation. In a similar study, Dibike *et al*. (2012) used the Mann–Kendall test to examine observed data (1961-2003) in the Lake Winnipeg watershed, and no significant trend in annual precipitation was detected.

Table 5.7 Trend analysis and estimated Sen's Slope of annual maximum (PRCP) and annual accumulated (PRCTOT) precipitation for the Airport station (where α is the significance level)

Model	Variable	Min	Max	Mean	α	Sen's slope (mm /year)	Trend
Obs 1961-2001	PRCP	26.9	135.4	67.22	0.05	0.0333	Upward
ARPEGE 1961-2001	PRCP	25	57.6	44.44	0.05	0	No trend
CRCM 1961-2001	PRCP	27.05	135.4	60.54	0.0	0	No trend
ARPEGE 2041-2081	PRCP	34.9	57.6	46.52	0.05	0	o trend
CRCM 2041-2081	PRCP	27.05	135.4	65.09	0.05	0	No trend
Obs 1961-2001	PRCTOT	621.4	1166.1	916.28	0.05	0.0288	Upward
ARPEGE 1961-2001	PRCTOT	510.47	1400.15	910.88	0.05	0.0396	No trend
CRCM 1961-2001	PRCTOT	742.87	1178.02	963.86	0.05	0.0148	No trend
ARPEGE 2041-2081	PRCTOT	690.22	1683.61	1155.21	0.05	0.0375	No trend
CRCM 2041-2081	PRCTOT	850.19	1436.29	1133.39	0.05	0.0557	Upward

5.6.2 Trends in maximum temperature using the classical and seasonal tests

Both the seasonal and classical Mann-Kendall test results using daily data showed a general positive (upward) trend in terms of maximum temperature in the area, with the magnitude varying according to the station. In some cases, the seasonal test can overcome the issue of seasonality and the classical test cannot, as in the ARPEGE model for the period of 1961 to 2001 (see Table 5.8). Although both corrected RCMs displayed a positive trend in the historical period (from 1961 to 2001), the observed trend slope (0.66 °C decade^{-1}) was overestimated by CRCM (0.84) and underestimated by ARPEGE (0.47). The average estimated slope of daily maximum temperature is projected to be 1.02 °C per decade in both RCMs, suggesting a steeper upward trend of maximum temperatures in the future.

Table 5.8 Trend analysis of daily maximum temperature (T_{MAX}) for the Airport station (**α** is significance level)

Model	Period	Min	Max	Mean	Sen's slope (°C decade^{-1})	α	Trend (classical test)	Trend (seasonal test)
Obs	1961-2001	-28.10	36.90	10.95	0.657	0.05	Upward	Upward
ARPEGE	1961-2001	-25.90	35.80	11.03	0.4745	0.05	No Trend	Upward
CRCM	1961-2001	-25.65	36.30	10.85	0.8395	0.05	Upward	Upward
ARPEGE	2041-2081	-25.65	35.80	14.33	1.022	0.05	Upward	Upward
CRCM	2041-2081	-25.65	36.30	14.10	1.022	0.05	Upward	Upward

5.6.3 Minimum Temperature Trend

The results indicate that, with regard to all stations and models in all periods, minimum temperatures have been increasing, and will continue to increase with almost the same acceleration as maximum temperatures, as shown by the Sen's slope (Table 5.9). The average trend of daily minimum temperatures in the historical period of 1961 to 2001 is lower for ARPEGE (0.55 °C per decade) than for CRCM (0.99), and the magnitude of the detected trend is higher for CRCM (1.10) for the future (2041-2081) compared to ARPEGE (0.99). It is worth noting that that CRCM presents a trend magnitude that is comparable to observations in the historical period (an average of 0.54 °C per decade), which means more confidence can be placed on the projections of CRCM in this respect. In a similar study, Dibike et al. (2012) used the Mann–Kendall trend to examine observed data from 1961 to 2003 in the Lake Winnipeg watershed and found an increasing trend in the mean annual air temperature, though no significant trend in annual precipitation was detected.

Table 5.9 Trend analysis of daily minimum temperature (T_{MIN}) for Airport station

Model	Variable	Min	Max	Mean	Sen's slope (°C decade^{-1})	α	Trend (classical test)	Trend (seasonal test)
Obs	1961-2001	-35.20	23.90	1.04	0.657	0.05	Upward	Upward
ARPEGE	1961-2001	-33.10	23.10	1.26	0.5475	0.05	Upward	Upward
CRCM	1961-2001	-32.80	23.40	0.91	0.9855	0.05	Upward	Upward
ARPEGE	2041-2081	-32.80	23.10	4.50	0.9855	0.05	Upward	Upward
CRCM	2041-2081	-30.95	24.50	4.19	1.095	0.05	Upward	Upward

5.7 Extreme Events Analysis

Frequency analysis was applied to annual maximum precipitation and presented in this section as well as certain indices of extremes. The results are compared for the current period (1961-2001) and future period (2041-2081).

5.7.1 Frequency Analysis Results for Precipitation

The following probability distributions were tested on current and future maximum precipitation time series: Normal (NOR), Lognormal (LN2), the Generalized Extreme Value (GEV), Lognormal (LN3) and Log Pearson Type III (LP3). Thirty-five datasets were used (i.e. five datasets multiplied by seven stations), the distributions were ranked based on their test statistic, and the ranks were then summed to select the best distribution. Based on the KS, AD and Chi-Squared tests (see Table 5.10), the two-parameter distributions (NOR and LN2) showed less skills compared to the three-parameter distributions (GEV, LN3, and LP3). In addition, the normal distribution ranked at the bottom of the distribution list in all tests. The GEV distribution was the best fitting overall, followed by Log-Pearson Type 3. Thus, the GEV distribution was selected for modeling annual maximum precipitation series for all seven stations, with parameters derived by the maximum likelihood (ML) method. Several other studies selected GEV distribution for Canadian precipitation data. Mailhot *et al*. (2007) found that only the GEV distribution was suitable to be fitted to observed data in Southern Quebec. More recently, Millington and Simonovic (2013) compared the GEV distribution with the Gumbel (EV1) and the Log-Pearson type 3 distributions, which are broadly used in

North America. They concluded that the GEV provided the best fit for use in climate change impact studies for London, Ontario.

Table 5.10 Ranking distributions of annual maximum precipitation based on KS, AD and Chi-Squared tests

Distribution	Kolmogorov Smirnov (KS)		Anderson Darling (AD)		Chi-Squared		Overall Rank
	Statistic test	Rank	Statistic test	Rank	Statistic test	Rank	
Gen. Extreme Value	0.078494643	1	0.2284814	1	1.362238571	2	**1**
Log-Pearson 3	0.081428214	2	0.2436204	2	1.411098214	4	**2**
Lognormal (3P)	0.083278571	3	0.2747646	3	1.402143214	3	**3**
Lognormal (2P)	0.088948929	4	0.3296571	4	1.298990714	1	**4**
Normal	0.092726786	5	0.3509807	5	2.019830357	5	**5**

Figure 5.5 shows the estimated precipitation magnitude for a 24hr storm at different return periods (i.e. 2-, 5-, 10-, 25-, 50-, and 100-year), calculated using five data sets: observation, corrected ARPEGE for 1961 to 2001, corrected CRCM for 1961-2001, corrected ARPEGE for 2041-2081, and corrected CRCM for 2041-2081. Due to the limit on setting predictor values that exceed the historical range of the observed values, unreliable RCM frequency analysis results were detected. However, these results indicate the necessity for a modification on calculating IDF curves to adopt the likely future increase in the intensity and frequency of extreme precipitation events. For example, based on the comparison made with

historic perturbed data, Millington and Simonovic (2013) recommended that the IDF curves established from the recorded historical data should be increased by approximately 30% to reflect the impact of future changes. Also, the City of London decided to take this in consideration and to increase the current IDF measurements by 21% based on a work of Peck *et al.* (2013).

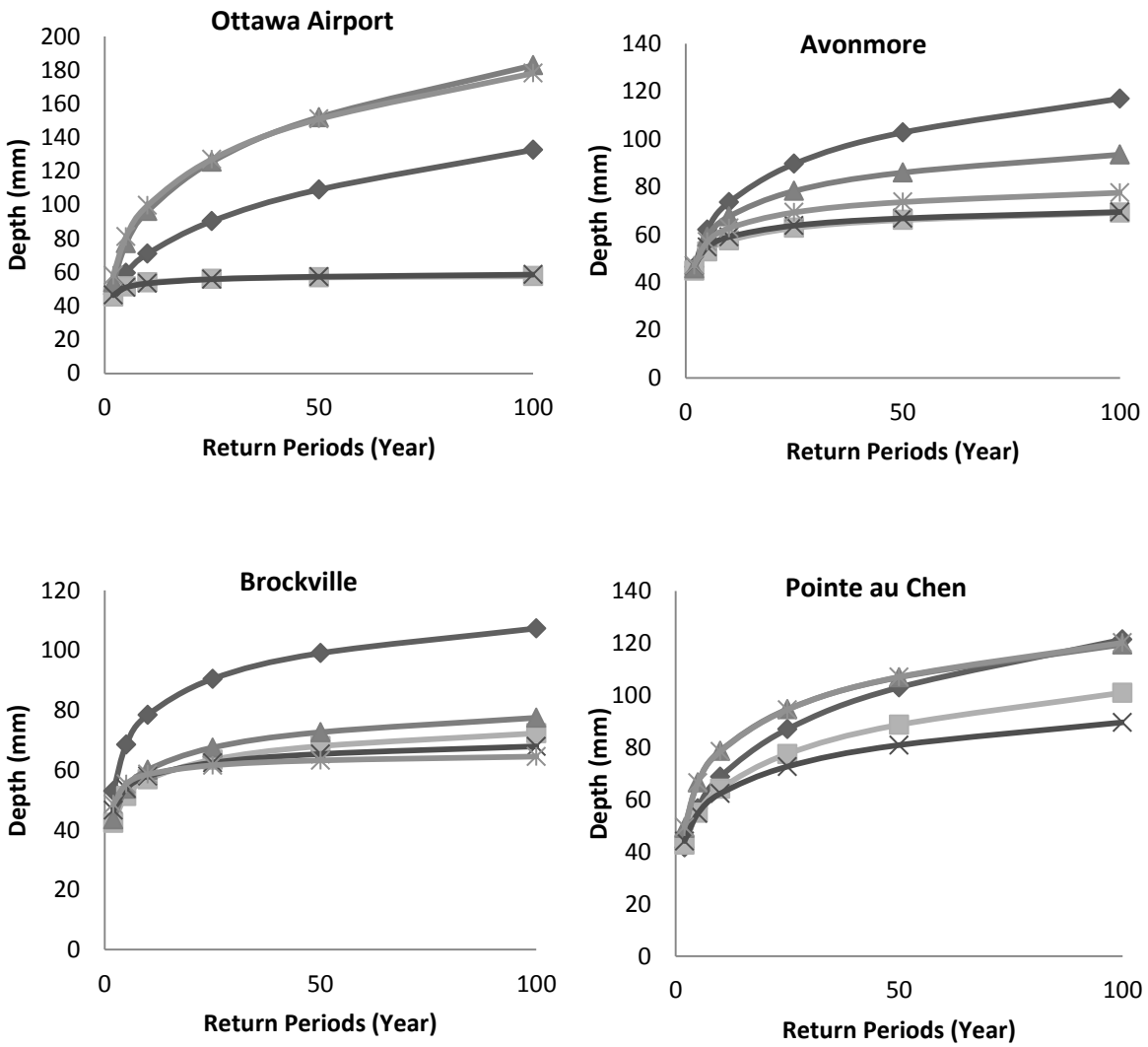

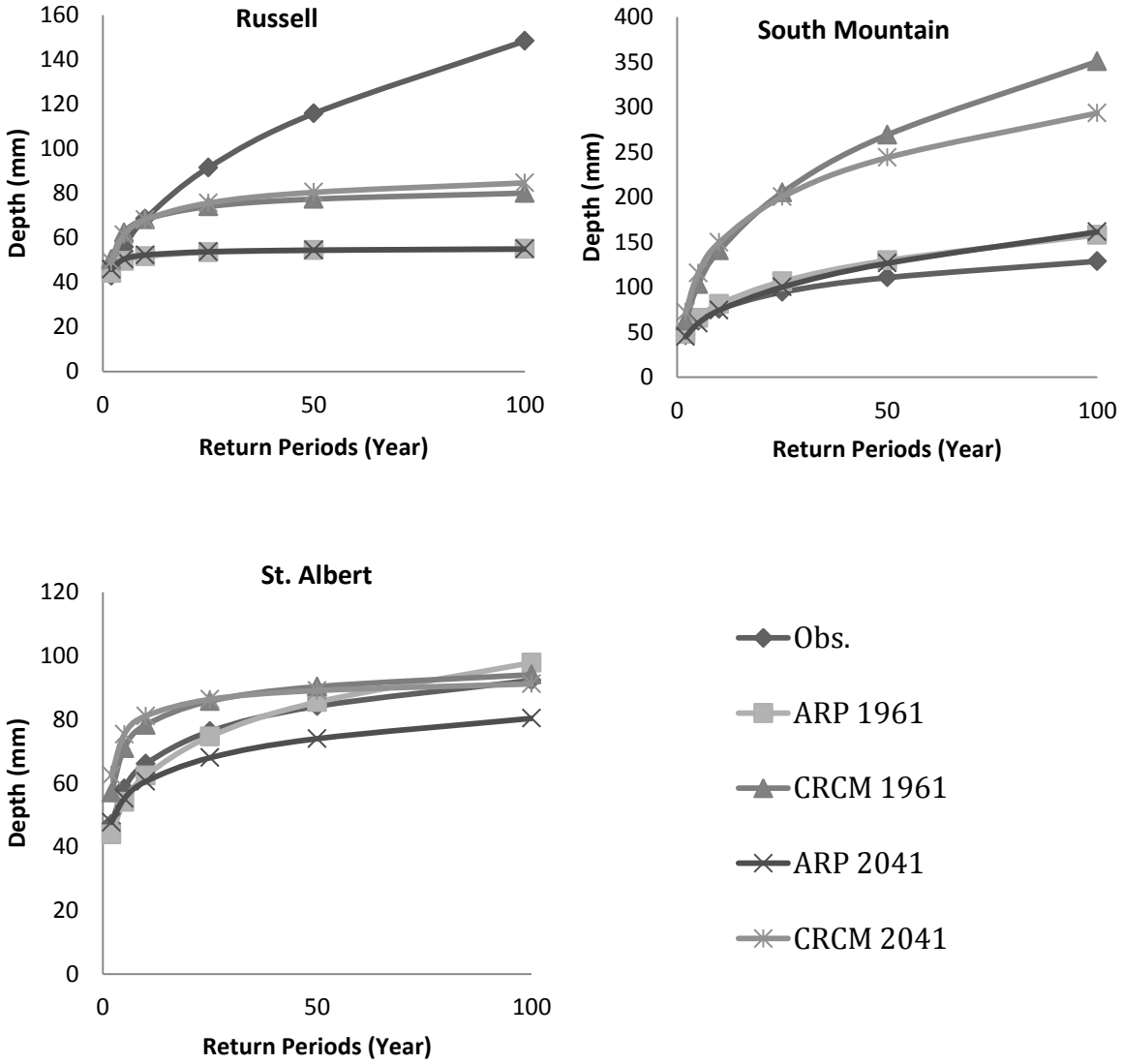

Figure 5.5 Return precipitation levels for each station, based on observations (Obs.), corrected ARPEGE 1961-2001, corrected CRCM 1961-2001, corrected ARPEGE 2041-2081, and corrected CRCM 2041-2081).

Therefore, the analysis of historical data could provide more reliable estimations. The distributions were re-ranked again based solely on historical data, and GEV was the best

fitting distribution. Figure 5.6 shows boxplot of the returned annual maximum precipitation values of all stations for various return periods. The minimum and the maximum values for 24-hour storm (i.e. the annual maximum precipitation) in Figure 5.6 are 92.3 mm and 148.4 mm respectively, for a return period of 100 years. However, these observations do not appear to agree with the findings of Millington and Simonovic (2013), as their minimum and maximum estimated values for the same storm duration and return period for London, Ontario were 140 mm and 290 mm respectively. These results might be due to variations in spatial and temporal patterns.

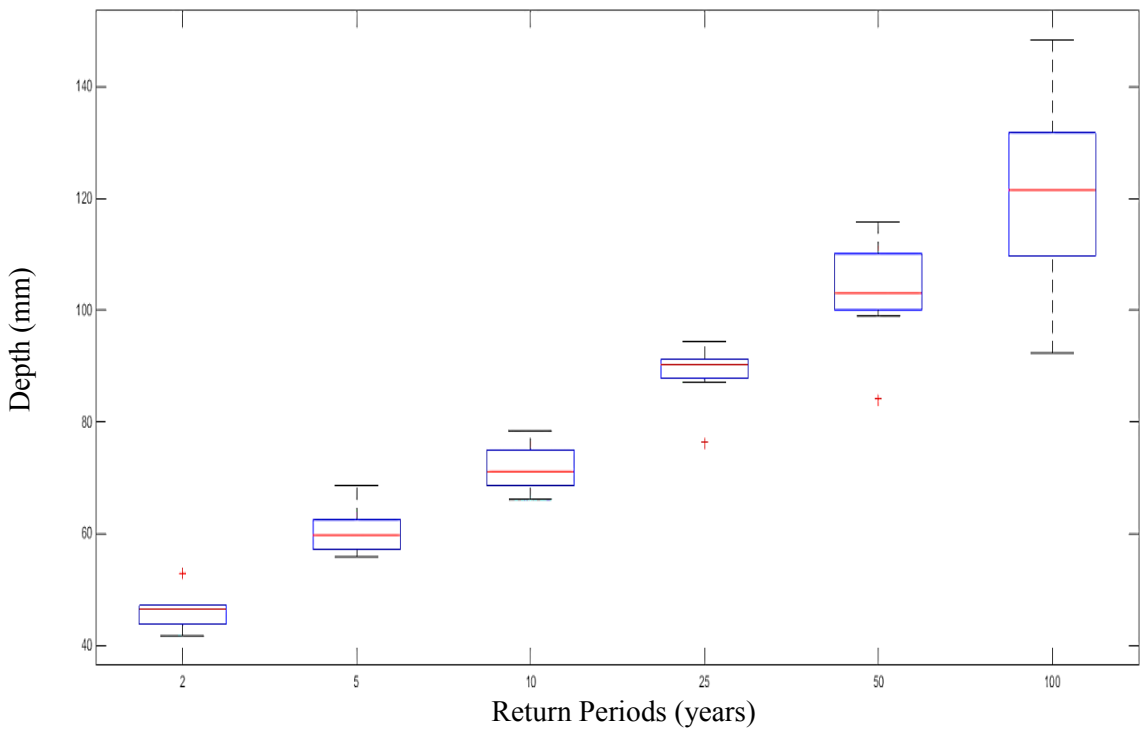

Figure 5.6 Boxplot of returned annual maximum precipitation values of all stations for various return periods.

5.7.2 Indices of extremes

Seven indices were used to investigate extreme events, and describe the climate categories of precipitation and maximum and minimum temperature. The latest IPCC report proved that some climate extremes, such as hot days and heavy precipitation events, had increased in the last century (Stocker *et al*., 2014), and our findings project more unpleasant climates over the coming decades, as detailed in Figure 5.7.

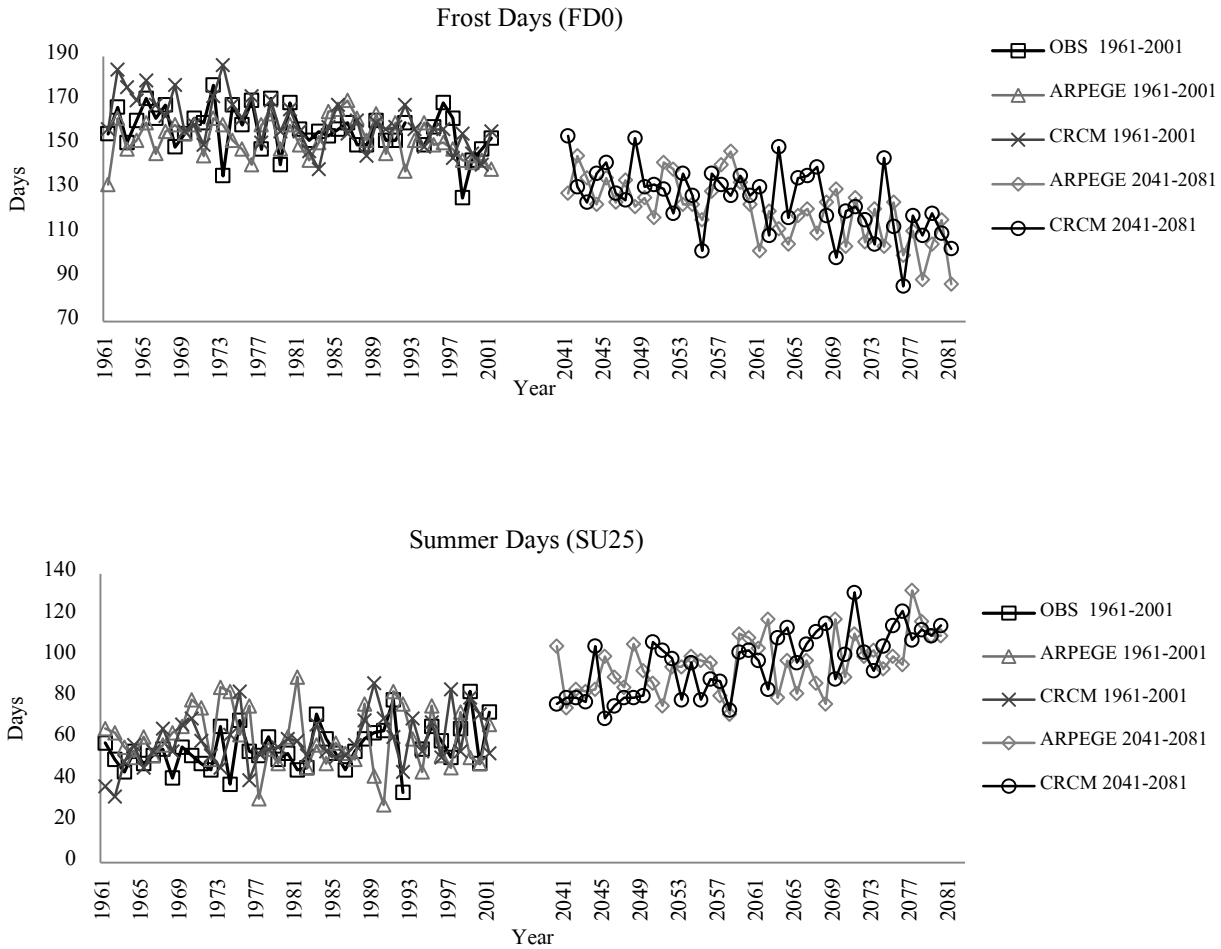

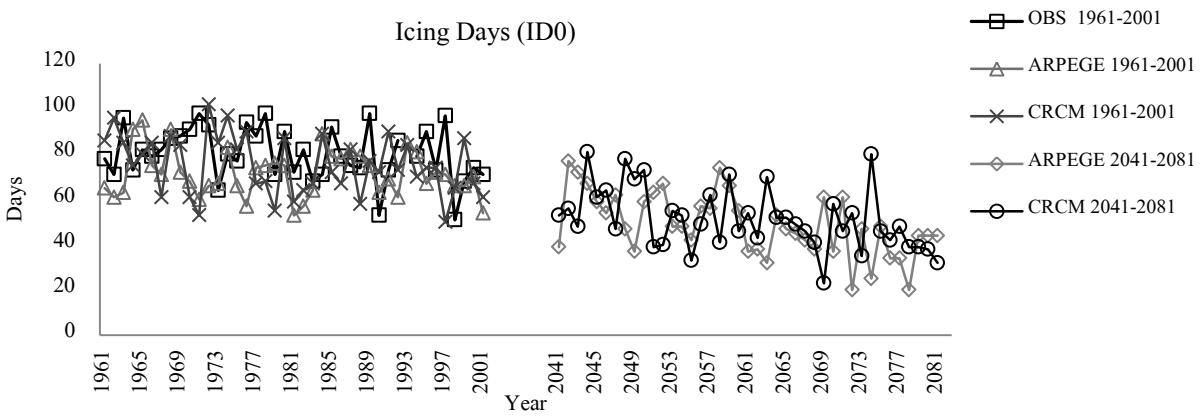
Icing Days (ID0)
Days
Year
OBS 1961-2001
ARPEGE 1961-2001
CRCM 1961-2001
ARPEGE 2041-2081
CRCM 2041-2081

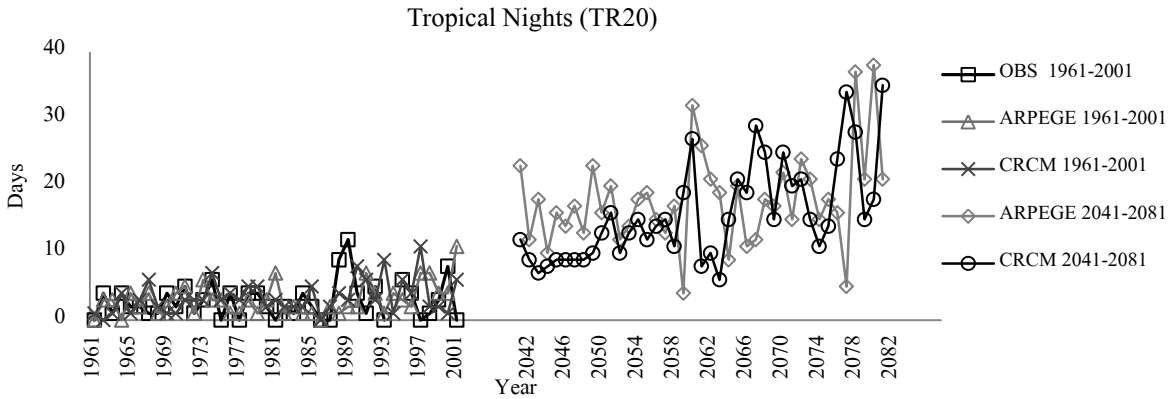
Tropical Nights (TR20)
Days
Year
OBS 1961-2001
ARPEGE 1961-2001
CRCM 1961-2001
ARPEGE 2041-2081
CRCM 2041-2081

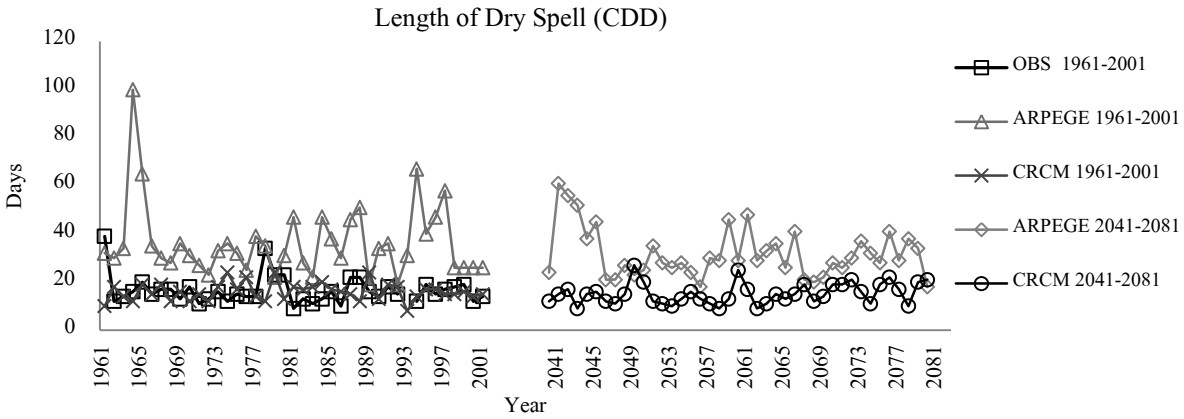
Length of Dry Spell (CDD)
Days
Year
OBS 1961-2001
ARPEGE 1961-2001
CRCM 1961-2001
ARPEGE 2041-2081
CRCM 2041-2081

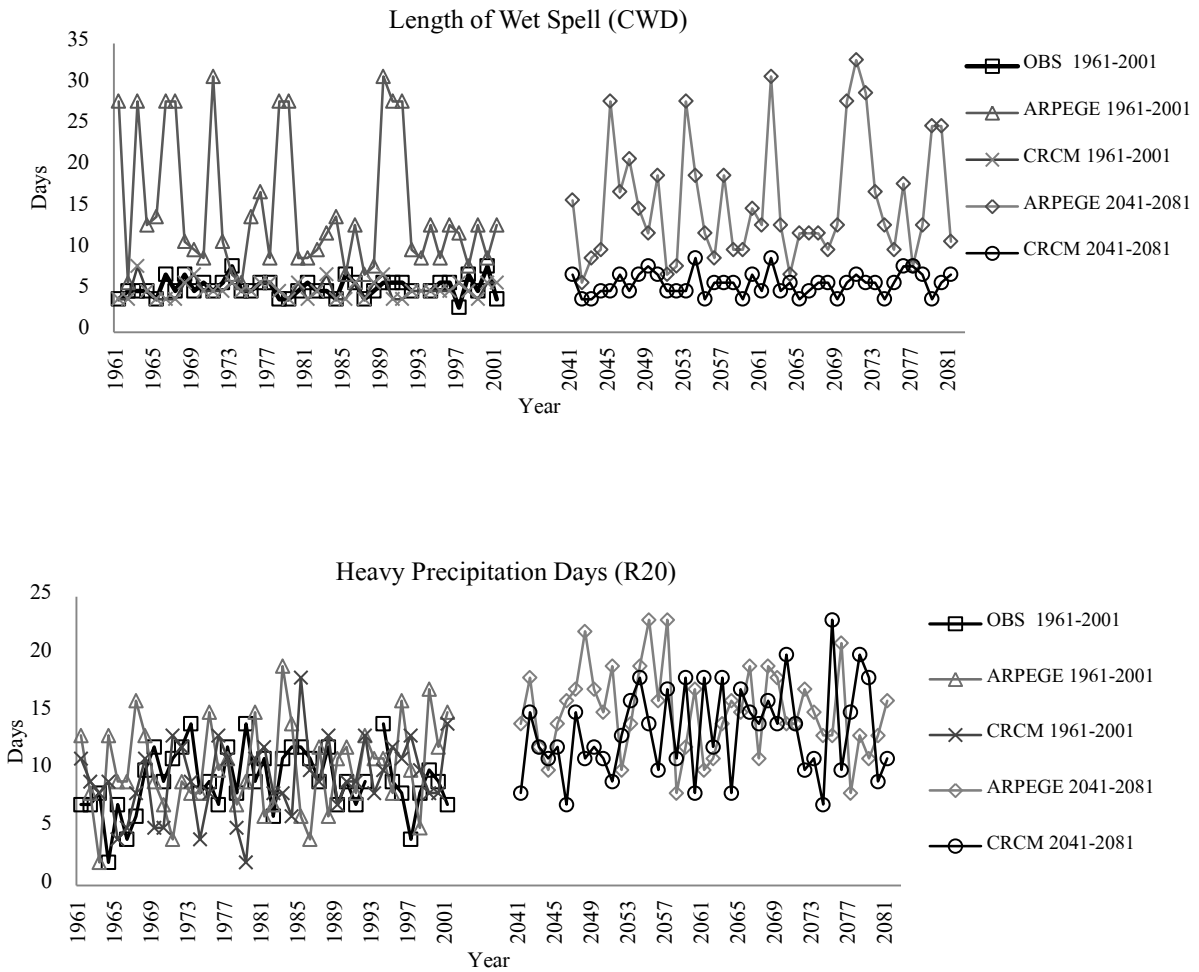

Figure 5.7 Comparison between occurrences of observed, corrected and projected climate extreme indices for the Ottawa Airport station.

5.7.2.1 Indices of Extreme Precipitation

Three indices were used to determine how annual precipitation extremes might change in the future. CDD and CWD describe the dry and wet spells respectively, and R20 represents the annual percentage of daily precipitation that exceeds 20 mm. As shown in Table 5.11,

ARPEGE simulated current dry and wet spells poorly compared to observations, and thus was not included in the discussion. CRCM, however, produced results that were very close to observed consecutive dry and wet days, and no significant future changes were projected. On the other hand, both models projected a 50% increase of future heavy precipitation events (R20). Average of 14 annual heavy precipitation events are expected in the future; while only nine were received.

Table 5.11 Occurrence of extreme precipitation events in days: (a) consecutive dry days; (b) consecutive wet days and (c) daily amounts of precipitation exceeding 20 mm

Station	AIRPORT	Avonmore	Brockville	Pointe au Chen	Russell	South Mountai	St. Albert	Mean
(a) CDD								
OBS	16.53	14.57	14.95	15.23	15.32	15.09	15.2	15.27
ARP 61-01	36.29	34.07	33.78	38.15	35.95	33.56	36.29	35.44
CRCM 61-01	16	15.39	15.68	16.76	15.34	16.39	14.49	15.72
ARP 41-81	31.78	29.93	30.24	35.83	31.49	31.02	29.34	31.38
CRCM 41-81	15.17	16.07	15.66	16.76	14.76	15.83	13.78	15.43
ARPEGE	92.20%	105.40%	102.27%	135.24%	105.50%	105.57%	93.03%	105.47%
CRCM	-8.20%	10.30%	4.75%	10.01%	-3.66%	4.90%	-9.34%	1.06%
(b) CWD								
OBS	5.4	6.43	6.23	5.81	6.32	6.34	7.15	6.24
ARP 61-02	14.9	15.8	16.07	11	16.93	23.02	15.9	16.23
CRCM 61-02	5.15	5.59	5.17	5.22	5.54	5.71	6.12	5.5
ARP 41-82	15.68	17.29	17.02	13.07	17.07	18.34	17.54	16.57
CRCM 41-82	5.88	6.24	6.24	5.46	6.12	6.34	6.51	6.11
ARPEGE	190%	168.90%	173.19%	125.05%	170%	189.27%	145.31%	165.60%
CRCM	8.89%	-2.95%	0.16%	-5.99%	-3.16%	0.00%	-8.95%	-2.03%
(c) R20								
OBS	9.03	9.71	9.95	9.19	9.21	8.53	10.15	9.4
ARP 61-03	10.2	10.46	10.88	10.37	11.2	10.27	12.32	10.81
CRCM 61-03	9.24	10.54	10.54	9.34	10.32	9.2	11.29	10.07
ARP 41-83	15.05	13.59	14.41	12.9	14.9	13.29	16.63	14.4
CRCM 41-83	13.37	13.71	14.51	12.85	14.17	12.24	15.24	13.73
ARPEGE	66.60%	39.90%	44.82%	40.33%	61.78%	55.80%	63.84%	53.21%
CRCM	48.10%	41.10%	45.83%	39.79%	53.85%	43.49%	50.15%	46.09%

5.7.2.2 Extreme Maximum temperature Indices

To estimate changes in future maximum temperatures, ID0 and SU25 were calculated to track the annual number of days with maximum temperatures below 0 °C (icing days) and above 25 °C (summer days), respectively. Observed records show that icing days were in the range of 68.22 to 80.15) days per year, and summer days were from 48.63 to 60.15 days per year. However, the Brockville station stood out, as it appeared to have more observed summer days and less icing days over the past four decades. Comparable results were reported by Mohsin (2009), who studied temperature extremes of rural areas in the vicinity of Toronto for the period of 1970 to 2000, and found ID0 and SU25 values of 51.8 to 71.4 and 47.2 to 61.4 days per year, respectively. As shown in Table 5.12, both ARPEGE and CRCM effectively represented observed data, and each projected an important change in the climate regime: a decrease in the annual number of icing days and an increase in the annual number of summer days. Icing days are projected to decrease from the current average of 72 days to 46 days (~55%), and summer days are projected to increase from the current average of 54 days to 90 days (~65%).

Table 5.12 Occurrence of maximum temperature events in days: (a) icing days (T_{MAX} < 0 ºC) and (b) summer days (T_{MAX} > 25 ºC)

Station	AIRPORT	Avonmore	Brockville	Pointe au Chene	Russell	South Mountain	St. Albert	Mean
(a) ID0								
OBS	80.15	70.63	62.77	75.66	68.22	73.84	72.55	71.97
ARP 61-01	71.51	66.59	57.93	70.44	65.76	65.27	68.59	66.58
CRCM 61-01	75.34	69.32	58.59	72.39	68.39	67.78	70.9	68.95
ARP 41-81	48.78	50.54	40.29	56.24	44.34	48.93	45.71	47.83
CRCM 41-81	51.37	45.95	36	48.73	43.51	45.02	46.59	45.31
ARPEGE	-39.14%	-28.44%	-35.81%	-25.67%	-35.00%	-33.74%	-37.00%	-33.54%
CRCM	-35.91%	-34.94%	-42.65%	-35.59%	-36.22%	-39.03%	-35.78%	-37.05%
(b) SU25								
OBS	51.73	56.85	46.18	48.63	60.15	57.19	56.25	53.85
ARP 61-02	60.12	57.98	51.07	59.05	62.66	63.44	55.85	58.59
CRCM 61-02	58.68	58.24	50.49	57.61	61.68	60.76	58.22	57.95
ARP 41-82	96.37	83.12	78.9	81.15	98.1	88.66	91.39	88.24
CRCM 41-82	96.76	91.34	83.85	93.32	99.12	94.44	94.9	93.39
ARPEGE	86.29%	46.21%	70.85%	66.87%	63.09%	55.03%	62.47%	63.85%
CRCM	87.05%	60.67%	81.57%	91.90%	64.79%	65.13%	68.71%	73.41%

5.7.2.3 Extreme minimum temperature indices

The indices selected to represent extremes in minimum temperatures are the number of Frost Days (FD0) and Tropical Nights (TR20), used to track minimum temperatures of less than 0 ºC and maximum temperatures of more than 20ºC, respectively. Observation records at six stations show that frost days were in the range of 150.44 to 156.57, and tropical nights from 2.5 to 4.41 (at the Brockville station frost days occurred less frequently, and tropical nights more frequently). Comparable results were reported by Mohsin (2009), who studied

temperature extremes of rural areas in the vicinity of Toronto for the period of 1970 to 2000, and found that FD0 and TR20 were 137.8 to 157.5 days and 42.9 to 3.6 nights, respectively. As shown in Table 5.12, converging the results of both models projected a decline of 20% in FD0 for all stations. A net increase in TR20 was detected, with an average rate four times what the area experienced over the last four decades of the twentieth century.

Table 5.13 Occurrence of minimum temperature events in days: (a) frost days (T_{MIN} < 0 ºC); and (b) tropical nights (T_{MIN} > 20 ºC)

Station	AIRPORT	Avonmore	Brockville	Pointe au Chene	Russell	South Mountain	St. Albert	Mean
(a) FD0								
OBS	156.75	152.89	132.89	150.23	150.44	153.09	153.55	149.97
ARP 61-01	152.71	152.34	130.51	151.39	150.41	146.32	156.24	148.56
CRCM 61-01	160.39	155.44	130.66	156	155.59	150.1	160.12	152.61
ARP 41-81	120.49	124.73	103.85	128.83	116.15	119.68	117.37	118.72
CRCM 41-81	125.12	113.27	92.8	116.98	113.49	108.39	116.49	112.36
ARPEGE	-23.13%	-18.42%	-21.85%	-14.24%	-22.79%	-21.82%	-23.56%	-20.84%
CRCM	-20.18%	-25.91%	-30.17%	-22.13%	-24.56%	-29.20%	-24.14%	-25.08%
(b) TN25								
OBS	2.8	3.37	5.92	2.5	4.41	3.75	3.95	3.81
ARP 61-02	3	3.56	6.29	4.02	5.76	7.83	3.8	4.89
CRCM 61-02	3.41	4.88	7.02	4.17	5.46	5.78	4.63	5.05
ARP 41-82	17.85	14.44	18.29	13.9	23.61	23.37	19.44	18.7
CRCM 41-82	15.98	19.9	24.85	17.63	21.15	20.71	19.41	19.94
ARPEGE	537.50%	328.49%	208.95%	456.00%	435.37%	523.20%	392.15%	390.26%
CRCM	470.71%	490.50%	319.76%	605.20%	379.59%	452.27%	391.39%	422.96%

Chapter 6. CONCLUSION

6.1 Thesis Contribution

This study has led to a better understanding of how precipitation and temperature in the South Nation watershed could change over the coming decades, in response to increases in atmospheric GHG concentrations. The outputs of the two RCMs used in this study (ARPEGE and CRCM) under A1B scenario were utilized. Comparisons of observations and raw outputs provided by ARPEGE and CRCM demonstrated the need for an effective correction method to realistically simulate climate variables in the area. To address this, the Quantile-Quantile transformation approach (Amadou *et al*., 2014) was applied to correct the Probability Distribution Functions (PDFs) of three simulated climate variables (minimum and maximum temperature and 24-hour precipitation accumulation), in order to match observations by remapping their cumulative distribution function (CDF). Visual inspection and the Kolmogorov-Smirnov (KS) test proved the ability of this approach to reproduce a valid agreement between the corrected and observed PDFs of maximum and minimum temperature. However, in terms of precipitation the performance was limited compared to the temperature analyses, due to the highly skewed shape of the PDF, and the extra caution required when applying and interpreting the outputs of the QQ-transformation. The results show that the recent 40-year increase of maximum and minimum temperatures will likely continue over the coming decades. Annual precipitation is also projected to rise by

approximately 15% over the period, with a higher percentage of wet days. The warmer and moister climate is anticipated to alter the frequency of severe hydrologic anomalies in the region, such as floods and droughts.

This study also outlined how the frequency and intensity of some extreme weather events will change from 2041 to 2081. Trends in four extreme temperature indices and three precipitation indices were investigated, and it was determined that under the current climate change scenario hot events are expected to occur more frequently and intensely, while cold events will be less frequent and weaker. Curiously, no discernible difference was detected between observed and projected dry/wet spells. Among the five tested distributions, GEV was chosen as the best distribution based on three best fit tests, and fitted to maximum annual precipitation time series. Frequency analysis was applied and compared in both periods. However, the study of the annual maxima was limited, because the QQ-transformation as implemented is unable to reproduce maxima beyond the historical values. Analyses of trends for both periods based on the Mann-Kendall test and Sen's slope estimator showed a discernible and often significant increase of maximum and minimum temperatures. There was relatively poor evidence of change in the time series of maximum and accumulated annual precipitation. Future projections of both temperature variables also exhibited stronger positive slopes.

6.2 Publication

A proceeding based on findings of this thesis was submitted to the 36th IAHR World Congress, as follows:

Alodah, A. S., Seidou, O. (2015). Development of climate change scenarios for the South Nation watershed using Quantile-Quantile transformation. The 36th IAHR World Congress, The Hague, the Netherlands (submitted)

6.3 Future Work and Recommendations

This study improved the accuracy of climate change projections for the area of interest (versus raw RCM outputs), and we recommend the following for further research:

1. Extending the work with more regional climate models and/or climate change scenarios, particularly new IPCC pathways (RCPs), will minimize associated uncertainty in climate change studies.
2. Exploring the projected changes based on seasons and/or months would facilitate better understanding of future climates; for example, considering the four different seasons in analysis.
3. Due to the limitations of the QQ transformation as implemented, frequency analysis of temperatures was unfeasible in this study when using the annual maximum (AM) precipitation data, since the maximum annual values were repeated. The Peaks over Threshold (POT) series method (also known as the partial duration series) would be more powerful when all values exceeding a defined threshold are considered. Also, The QQ transformation could be improved by extrapolation beyond observed values.
4. Studying the impact of climate change on the hydrology of the watershed by feeding a hydrological model with the results, would thereby lead to better decisions regarding effective mitigation and adaptation measures.

References

Abdel-Fattah, S., Krantzberg, G. (2014) Commentary: Climate change adaptive management in the Great Lakes, Journal of Great Lakes Research, http://dx.doi.org/10.1016/j.jglr.2014.05.007

Al-Ansari, N., Abdellatif, M., Ali, S.S., Knutsson, S. (2014) Long Term Effect of Climate Change on Rainfall in Northwest Iraq. Central European Journal of Engineering, 1-14.

Amadou, A., Gado, D. A., Seidou, O., Seidou, S. I., and Ketvara, S. (2014) Changes to flow regime on the Niger River at Koulikoro under a changing climate, Hydrological Sciences Journal.

Boe, J., Terray, L., Habets, F. and Martin, E. (2007) Statistical and dynamical downscaling of the Seine basin climate for hydro-meteorological studies. Int. J. Climatol. 27: 1643–1655

Bosetti, V. and Lubowski, R.N. (eds) (2010) Deforestation and Climate Change: Reducing Carbon Emmissions from Deforestation and Forest Degradation. Massachussetts: Edward Elgar Publishing

Boyer, C., Chaumont, D., Chartier, I., Roy, A. G. (2010) Impact of climate change on the hydrology of St. Lawrence tributaries. Journal of Hydrology 384 65–83

Bürger, G., & Chen, Y. (2005). Regression-based downscaling of spatial variability for hydrologic applications. Journal of Hydrology, 311(1-4), 299-317.

Brissette, F.P., Khalili, M., Leconte, R. (2007) Efficient stochastic generation of multi-site synthetic precipitation data. Journal of Hydrology ; 345, 121– 133

Brissette, J. C. F., and Leconte, R. (2012) Coupling statistical and dynamical methods for spatial downscaling of precipitation. Climatic Change 114:509–526 DOI 10.1007/s10584-012-0452-2

Burger, G. (2002) Selected precipitation scenarios across Europe. Journal of Hydrology, 262, 99–110.

Campbell-Lendrum, D.& Corvalan, C. (2007). Climate change and developing country cities: implications for environmental health and equity. Journal of Urban Health, 84(3) 109–117.

Canadell, J.G.; Le Quere, C.; Raupach, M.R.; Field, C.B.; Buitenhuis, E.T.; Ciais, P.; Conway, T.J.; Gillett, N.P.; Houghton, R.A.; Marland, G. (2007). "Contributions to accelerating atmospheric CO2 growth from economic activity, carbon intensity, and efficiency of natural sinks". Proceedings of the National Academy of Sciences, U.S.A. 104 (47)

Chakravarti, R., Laha, R.G. and Mohan, I. (1967). Handbook of Methods of Applied Statistics, Volume I, John Wiley and Sons, pp. 392-394.

Chen, C., Haerter, J.O., Hagemann, S., Piani, C. (2011) On the contribution of statistical bias correction to the uncertainty in the projected hydrological cycle. Geophys Res Lett 38: L20403, doi: 10.1029/2011GL049318

Christensen, J. H., Boberg, F., Christensen, O. B., and Lucas-Picher, P. (2008) On the need for bias correction of regional climate change projections of temperature and precipitation, Geophysical Research Letters, 35, L20709, doi:10.1029/2008GL035694.

Christensen, J.H., Hewitson, B., Busuioc, A. et al. (2007) Regional climate projections. In: Solomon, S., Quin, D., Manning, M. et al.. (eds), Climate Change 2007: The Physical Science Basis. Contribution of Working Group I to the Fourth Assessment Report of the Intergovernmental Panel on Climate Change. Cambridge University Press, UK.

Clarke, L., Edmonds, J., Jacoby, H., Pitcher, H., Reilly, J., Richels, R. (2007) CCSP synthesis and assessment product 2.1, Part A: scenarios of greenhouse gas emissions and atmospheric concentrations. U.S. Government Printing Office, Washington, DC

Coyne, P. (2001) Reflections of the South Nation Watershed: A Pictorial History of Its People and Natural Resources. General Store Publishing House, Burnstown, ON.

Cummings, D. I., Russell, H. A. J. (2007) The Vars–Winchester esker aquifer, South Nation River watershed, Ontario.

Cunderlik J. M., Simonovic S.P. (2005) Hydrological extremes in a southwestern Ontario river basin under future climate conditions. Journal of Hydrological Sciences 50(4).

Das, S., Millington, N., and Simonovic, S. P. (2013) Distribution Choice for the

Assessment of Design Rainfall for the City of London (Ontario, Canada) under Climate Change. Canadian Journal of Civil Engineering, 40(2):121-129.

Déqué, M., Dreveton, C., Braun, A., Cariolle, D. (1994) The ARPEGE/IFS atmosphere model: a contribution to the French community climate modelling. Climate Dynamics, Volume 10, Issue 4-5, pp 249-266

Dibike, Y.B., Prowse, T., Shrestha, R. and Ahmed, R. (2012) Observed trends and future projections of precipitation and air temperature in the Lake Winnipeg watershedd, Journal of Great Lakes Research, special issue on Lake Winnipeg – the Forgotten Great Lake, Vol.38, pp.72-82

El Khoury, A. (2012). Modeling Land-Use Changes in the South Nation Watershed using Dyna-CLUE. M.A.Sc. Thesis, Department of Civil Engineering, The University of Ottawa

Fowler, H. J., Blenkinsop, S. and Tebaldi, C. (2007) Linking climate change modelling to impacts studies: recent advances in downscaling techniques for hydrological modelling. International Journal of Climatology, 27: 1547–1578

Frei, C., Scholl, R., Fukutome, S., Schmidli, J. and Vidale, P.L. (2006) Future change of precipitation extremes in Europe: An intercomparison of scenarios from regional climate models. Journal of Geophysical Research-Atmospheres, 111, D06105, doi: 10.1029/2005JD005965.

Frich, P., Alexander, L. V., Della-Marta, P., Gleason, B., Haylock, M., Tank, A. K., and Peterson, T. (2002) Global changes in climatic extremes during the 2nd half of the 20th century, Clim. Res., 19, 193–212, 2002.

Giorgi F., Hewitson, B., Christensen, J., Hulme, M., von Storch, H., Whetton, P., Jones, R., Mearns, L. and Fu, C. (2001), Regional climate information - evaluation and projections. In: Climate Change 2001: The Scientific Basis. Contribution of Working Group I to the Third Assessment Report of the Intergovernmental Panel on Climate Change (Eds., Houghton, J.T., Ding, Y., Griggs, D.J., Noguer, M., van der Linden, P.J., Dai, X., Maskell, K. and Johnson, C.A.), Cambridge University Press, Cambridge and New York, pp. 583-638.

Goosse, H., Barriat, P.Y., Lefebvre, W., Loutre, M.F. and Zunz, V. (2010) Introduction to climate dynamics and climate modeling. Online textbook available at http://www.climate.be/textbook. Data Accessed: 2013-2014.

Hayhoe, K. A. (2010) A Standardized Framework for Evaluating the Skill ff Regional

Climate Downscaling Techniques. PhD Dissertation, University of Illinois at Urbana-Champaign.

Helsel, D.R. and Hirsch, R. M. (2002) Statistical Methods in Water Resources Techniques of Water Resources Investigations, Book 4, chapter A3. U.S. Geological Survey. 522 pages

Hessami, M., Gachon, P., Ouarda, T. & St-Hilaire, A. (2008). Automated regression-based Statistical Downscaling Tool, Environmental Modelling and Software, vol. 23, pp. 813-834

Hewitson, B. C. and Crane, R. G. (1996) Climate downscaling techniques and applications. Climate Research, 7: 85-95

Hirsch, R.M., Slack, J.R & Smith R.A. (1982). Techniques of trend analysis for monthly water quality data. Water Resour. Res, 18, 107-121.

Intergovernmental Panel on Climate Change: IPCC (2000) SPECIAL REPORT 2000; Emissions Scenario

Intergovernmental Panel on Climate Change: IPCC (2007) Climate Change 2007, Synthesis Report (AR4).

Kingsley, J. (2005) Using Electrical Conductivity and Temperature Mapping to Locate Zones of Groundwater Discharge in the South Nation River, Eastern Ontario. M.Sc. Thesis, University of Ottawa.

Kistler, R., Kalnay, E., Collins, W., Saha, S., White, G., Woollen, J., Chelliah, M., Ebisuzaki, W., Kanamitsu, M., Kousky, V., Dool, H., Jenne, R., Fiorino, M. (2001) The NCEP/NCAR 50-Year Reanalysis. Bulletin of the American Meteorological Society 82(2): 247–267.

Kotz, S. and Nadarajah, S. (2000). Extreme Value Distributions: Theory and Applications. London: Imperial College Press.

Leider, J. (2012) A Quantile Regression Study of Climate Change in Chicago, 1960-2010. http://dx.doi.org/10.1137/12S01174X Data Accessed: 2013-2014.

Lemmen, D. S. and Warren, F. J. (2004) Climate Change Impacts and Adaptation: A Canadian Perspective. Natural Resources Canada; http://cfs.nrcan.gc.ca/pubwarehouse/pdfs/27428.pdf k. Data Accessed: 2013-2014

Mailhot, A., Duchesne, S., Caya, D., and Talbot, G. (2007). Assessment of future change in

intensity-duration-frequency (IDF) curves for Southern Quebec using the Canadian Regional Climate Model (CRCM). Journal of Hydrology, 347: 197–210.

Maraun, D., Wetterhall, F., Ireson, A. M., Chandler, R. E., Kendon, E. J., Widmann, M., Brienen, S., Rust, H. W., Sauter, T., Themeßl, M., Venema, V. K. C., Chun, K. P., Goodess, C. M., Jones, R. G., Onof, C., Vrac, M., and Thiele-Eich, I. (2010) Precipitation downscaling under climate change: Recent developments to bridge the gap between dynamical models and the end user, Rev. Geophys., 48, RG3003, doi:10.1029/2009RG000314.

Meals, D. W., Spooner, J., Dressing, S. A., and Harcum, J. B. (2011) Statistical analysis for monotonic trends, Tech Notes 6, November 2011. Developed for U.S. Environmental Protection Agency by Tetra Tech, Inc., Fairfax, VA, 23 p. Available online at www.bae.ncsu.edu/programs/extension/wqg/319monitoring/tech_notes.htm [Accessed 9-2014].

Mehrotra, R. (2005). Multisite rainfall stochastic downscaling for climate change impact assessment (PhD thesis). The University of New South Wales, Sydney, Australia.

Mikael Hook, Anders Sivertsson, Kjell Aleklett, (2010). Validity of the fossil fuel production outlooks in the IPCC Emission Scenarios. Natural Resources Research Volume 19, Issue 2, June 2010, Pages 63-81 doi:10.1007/s11053-010-9113-1

Mizuta, R., Oouchi, K., Yoshimura, H. et al. (2006) 20-km-Mesh global climate simulations using JMAGSM model – Mean climate states. Journal of the Meteorological Society of Japan, 84, 165–185.

Mohsin, Tanzina. (2009) Greater Toronto Area Urban Heat Island: Analysis of Temperature and Extremes. Ph.D. Thesis. University of Toronto: Canada.

Moss, R., Babiker, M., Brinkman, S., Calvo, E., Carter, T., Edmonds, J., Elgizouli, I., Emori, S., Erda, L., Hibbard, K., Jones, R., Kainuma, M., Kelleher, J., Lamarque, J.F., Manning, M., Matthews, B., Meehl, G., Meyer, L., Mitchell, J., Nakicenovic, N., O'Neill, B., Pichs, T., Riahi, K., Rose, S., Runci, P., Stouffer, R., van Vuuren, D., Weyant, J.W.T, van Ypersele, J.P., Zurek, M., (2008) Towards New Scenarios for Analysis of Emissions, Climate Change, Impacts, and Response Strategies. Intergovernmental Panel on Climate Change, Geneva.

Moss, R.H., Edmonds, J.A., Hibbard, K.A., Manning, M.R., Rose, S.K., van Vuuren, D.P., Carter, T.R., Emori, S., Kainuma, M., Kram, T., Meehl, G.A., Mitchell, J.F.B.,

Nakicenovic, N., Riahi, K., Smith, S.J., Stouffer, R.J., Thomson, A.M., Weyant, J.P., Wilbanks, T.J., (2010) . The next generation of scenarios for climate change research and assessment. Nature 463, 747–756.

Murphy J.M. (2000) Predictions of climate change over Europe using statistical and dynamical downscaling techniques. Int. J. Climatol.. 20,489- 501

New, M., Liverman, D. and Anderson, K. (2009) Mind the gap. Nature Reports Climate Change (0912), 143–144.

Peck, A., Prodanovic, P. and Simonovic, S. (2012) Rainfall Intensity Duration Frequency Curves Under Climate Change: City of London, Ontario, Canada , Canadian Water Resources Journal / Revue canadienne des ressources hydriques, 37:3, 177-189, DOI: 10.4296/cwrj2011-935

Quilbe, R., Rousseau, A. N., Moquet, J.-S., Trinh, N. B., Dibike, Y. B., Gachon, P., and Chaumont, D. (2008) Assessing the effect of climate change on river flow using general circulation models and hydrological modelling. Application to the Chaudiere River (Quebec, Canada), Can. Water Resour. J. Vol 33(1)

Sachindra, D. A., Huang, F., Barton, A. F. and Perera, B. J. C. (2013) Multi-model ensemble approach for statistically downscaling general circulation model outputs to precipitation. Quarterly Journal of the Royal Meteorological Society, DOI:10.1002/qj.2205

Salathe, EP. (2003). Comparison of various precipitation downscaling methods for the simulation of streamflow in a rainshadow river basin. International Journal of Climatology 23: 887–901.

Samuel J., Coulibaly P., Metcalfe R.A., (2011). Evaluation of future flow variability inungauged basins: validation of combined methods. Advances in Water Resources35. 121-140.

Sarr M.A., Zoromé, M., Seidou, O., Bryant, C. R., and Gachon, P. (2013) Recent trends in selected extreme precipitation indices in Senegal-A change point approach, Journal of Hydrology, 505, 326-334.

Seidou, O., Ramsay, A., Nistor, I. (2012) Climate change impacts on extreme floods II: improving flood future peaks simulation using non-stationary frequency analysis. Nat Hazards 60:715–726

Sharma, M., Coulibaly, P., Dibike, Y. B. (2011). Assessing the need for downscaling RCM

data for hydrologic impact study. ASCE Journal of Hydrologic Engineering 16(6): 534-539.

Sillmann, J. and Roeckner, E. (2008) Indices for extreme events in projections of anthropogenic climate change, Climatic Change, 86, 83-104

SNC (South Nation Conservation) (2012a) Annual Report. Available on: http://www.nation.on.ca. Data Accessed 2013-2014

SNC (South Nation Conservation) (2012b) Assessment Report, South Nation Source Protection Area.

Solaiman, T.A., (2011). Uncertainty Estimation of Extreme Precipitations under Climatic Change: A Non-Parametric Approach. PhD Thesis, Department of Civil and Environmental Engineering, The University of Western Ontario

Stocker, T. F., and Coauthors, Eds., (2014). Climate change 2013: The physical science basis. Cambridge University Press.

Sulis M., Paniconi C., Huard D., Chaumont D., (2011). Hydrological responses to downscaled climate model outputs using an integrated, physically-based model of groundwater/surface water interactions. http://www.geohydro2011.ca/gh2011_user/cle_usb/pdf/doc-2282.pdf. Data Accessed: 2013-2014

U.S. Environmental Protection Agency (EPA), 2008. The Great Lakes: An Environmental Atlas and Resource Book. Last access 2014 from http://www.epa.gov/glnpo/atlas/glat-ch2.html

UNFCCC. (1992). United Nations Framework Convention on Climate Change, Retrieved November 21, 2008 http://unfccc.int/resource/docs/convkp/conveng.pdf.

United States Environmental Protection Agency (2006). Data Quality Assessment: Statistical Methods for Practitioners. EPA/240/B-06/003. Office of Environmental Information Washington, DC 20460.

Van Vuuren, D.P., Riahi, K., Moss R., Edmond, J., Thomson, A., Nakicenovic, N., Kram, T., Berkhout, F., Swart, R., Janetos, A., et al. (2012) A proposal for a new scenario framework to support research and assessment in different climate research communities. Glob. Environ. Chang. 22:21–35. doi: 10.1016/j.gloenvcha.2011.08.002

Wheater, H. S. (2002) Progress in and prospects for fluvial flood modelling. Philosophical Transactions: Mathematical Physical and Engineering Sciences, 360 (1796), 1409-1431.

Wilby, R. L. and Fowler, H. J. (2011). Regional Climate Downscaling: Modelling the Impact of Climate Change on Water Resources. Edited by Fai Fung, Ana Lopez and Mark New, Blackwell Publishing Ltd. ISBN: 978-1-405-19671-0

Wilby, R.L. and Wigley, T. (1997). Downscaling general circulation model output: a review of methods and limitations. Progress in Physical Geography, 21: 530

Wilby, R.L., Charles, S., Mearns, L.O., Whetton, P., Zorito, E. and Timbal, B. (2004). Guidelines for Use of Climate Scenarios Developed from Statistical Downscaling Methods. IPCC Task Group on Scenarios for Climate Impact Assessment (TGCIA) (http://www.ipcc-data.org/guidelines/dgm_no2_v1_09_2004.pdf). Data Accessed: 2013-2014

Wilby, R.L., Wigley, T. (2000). Precipitation predictors for downscaling: Observed and general circulation model relationships. Int. J. Climatol. 20: 641–661, DOI: 10.1002/(SICI)1097-0088(200005).

Xu C.Y., (1999). Review Paper, Climate change and hydrologic models: A review of existing gaps and recent research developments. Water Resources Management 13: 369–382, 1999.

Zhang, X., Alexander, L., Gabriele, C., Jones, P., Tank, A. K., Peterson, T. C., Trewin, B. and Zwiers, F.W. (2011) Indices for monitoring changes in extremes based on daily temperature and precipitation data, WIREs Clim Change doi: 10.1002/wcc.147

Appendix A: KS-Test Results

Table A.1 KS test results of T_{MIN} of ARPEGE model in calibration and validation periods for all stations (S.D: Similar Distribution and N.S.D: Non-Similar Distribution)

Airport	CALIBRATION PERIOD		VALIDATION PERIOD	
Month	RCM (UNC.)	RCM (CORR.)	RCM (UNC.)	RCM (CORR.)
1	N.S.D.(p=1.2015e-036)	S.D.(p=1)	N.S.D.(p=1.6105e-037)	S.D.(p=0.8386)
2	N.S.D.(p=1.8849e-018)	S.D.(p=1)	N.S.D.(p=6.6976e-018)	S.D.(p=0.24977)
3	N.S.D.(p=2.3983e-007)	S.D.(p=1)	N.S.D.(p=0.00032646)	S.D.(p=0.13552)
4	N.S.D.(p=4.4416e-022)	S.D.(p=0.9792)	N.S.D.(p=8.6685e-012)	N.S.D.(p=0.0038232)
5	N.S.D.(p=3.3598e-040)	S.D.(p=0.99356)	N.S.D.(p=7.5619e-033)	S.D.(p=0.35519)
6	N.S.D.(p=2.6707e-011)	S.D.(p=0.99997)	N.S.D.(p=9.3057e-020)	S.D.(p=0.069025)
7	N.S.D.(p=3.6994e-009)	S.D.(p=0.98245)	N.S.D.(p=0.00023565)	S.D.(p=0.19161)
8	S.D.(p=0.3074)	S.D.(p=0.99998)	S.D.(p=0.093551)	S.D.(p=0.46424)
9	N.S.D.(p=0.0011958)	S.D.(p=1)	S.D.(p=0.8776)	N.S.D.(p=0.00033876)
10	S.D.(p=0.3074)	S.D.(p=1)	S.D.(p=0.71783)	S.D.(p=0.19161)
11	S.D.(p=0.24698)	S.D.(p=0.99782)	N.S.D.(p=0.00012328)	N.S.D.(p=0.00017374)
12	N.S.D.(p=3.3298e-014)	S.D.(p=0.99973)	N.S.D.(p=1.7839e-016)	S.D.(p=0.52275)
S.D.	3	12	3	9

Avonmore	CALIBRATION PERIOD		VALIDATION PERIOD	
Month	RCM (UNC.)	RCM (CORR.)	RCM (UNC.)	RCM (CORR.)
1	N.S.D.(p=1.6634e-042)	S.D.(p=0.98245)	N.S.D.(p=4.867e-042)	S.D.(p=0.26427)
2	N.S.D.(p=4.1731e-030)	S.D.(p=0.97339)	N.S.D.(p=7.5121e-022)	S.D.(p=0.65621)
3	N.S.D.(p=1.2049e-012)	S.D.(p=0.88957)	N.S.D.(p=2.5081e-008)	S.D.(p=0.093551)
4	N.S.D.(p=8.0271e-011)	S.D.(p=0.38691)	N.S.D.(p=1.8813e-006)	N.S.D.(p=0.029048)
5	N.S.D.(p=1.3707e-009)	S.D.(p=0.46424)	N.S.D.(p=9.7482e-009)	N.S.D.(p=0.026645)
6	N.S.D.(p=0.023037)	S.D.(p=0.63226)	S.D.(p=0.069025)	S.D.(p=0.12378)
7	N.S.D.(p=0.0079362)	S.D.(p=0.35519)	N.S.D.(p=8.5503e-005)	N.S.D.(p=0.00083741)
8	N.S.D.(p=0.00023565)	S.D.(p=0.40756)	N.S.D.(p=1.7514e-010)	N.S.D.(p=2.9398e-005)
9	N.S.D.(p=3.11e-009)	S.D.(p=0.69845)	N.S.D.(p=5.2806e-007)	N.S.D.(p=0.00046866)
10	N.S.D.(p=0.0061181)	S.D.(p=0.3074)	N.S.D.(p=0.0011327)	S.D.(p=0.11294)
11	N.S.D.(p=0.023037)	S.D.(p=0.24698)	N.S.D.(p=0.0028858)	N.S.D.(p=0.00024336)
12	N.S.D.(p=5.1061e-015)	S.D.(p=0.8386)	N.S.D.(p=8.1799e-020)	N.S.D.(p=0.026305)
S.D.	0	12	1	5

Brockville	CALIBRATION PERIOD		VALIDATION PERIOD	
Month	RCM (UNC.)	RCM (CORR.)	RCM (UNC.)	RCM (CORR.)
1	N.S.D.(p=9.5584e-024)	S.D.(p=0.93123)	N.S.D.(p=2.1439e-020)	S.D.(p=0.40756)
2	N.S.D.(p=1.0436e-013)	S.D.(p=0.73547)	N.S.D.(p=7.9572e-011)	S.D.(p=0.52124)
3	N.S.D.(p=3.7002e-007)	S.D.(p=0.52468)	N.S.D.(p=0.0061181)	N.S.D.(p=0.0061181)
4	N.S.D.(p=1.5659e-024)	S.D.(p=0.14852)	N.S.D.(p=2.2416e-016)	N.S.D.(p=0.011073)
5	N.S.D.(p=7.0018e-026)	S.D.(p=0.35519)	N.S.D.(p=2.7006e-015)	N.S.D.(p=0.0061181)
6	N.S.D.(p=6.0925e-005)	S.D.(p=0.14852)	N.S.D.(p=4.8931e-012)	N.S.D.(p=0.0028858)
7	N.S.D.(p=2.9571e-006)	S.D.(p=0.05129)	N.S.D.(p=0.00023565)	S.D.(p=0.05129)
8	N.S.D.(p=0.0011327)	S.D.(p=0.3074)	S.D.(p=0.11294)	N.S.D.(p=1.4003e-005)
9	S.D.(p=0.28882)	S.D.(p=0.44294)	N.S.D.(p=6.0925e-005)	N.S.D.(p=0.00017374)
10	N.S.D.(p=0.0035714)	S.D.(p=0.46424)	N.S.D.(p=0.00016908)	N.S.D.(p=0.021164)
11	N.S.D.(p=0.036402)	S.D.(p=0.12378)	N.S.D.(p=8.3631e-009)	N.S.D.(p=2.9374e-005)
12	N.S.D.(p=2.9571e-006)	S.D.(p=0.78052)	N.S.D.(p=5.682e-009)	N.S.D.(p=0.0019943)
S.D.	1	12	1	3

Pointe au Chene	CALIBRATION PERIOD		VALIDATION PERIOD	
Month	RCM (UNC.)	RCM (CORR.)	RCM (UNC.)	RCM (CORR.)
1	N.S.D.(p=1.889e-047)	S.D.(p=0.5861)	N.S.D.(p=2.6343e-049)	S.D.(p=0.11294)
2	N.S.D.(p=9.9301e-025)	S.D.(p=0.59829)	N.S.D.(p=3.7365e-021)	S.D.(p=0.34457)
3	N.S.D.(p=3.5152e-011)	S.D.(p=0.26427)	N.S.D.(p=1.5452e-007)	S.D.(p=0.093551)
4	N.S.D.(p=1.5157e-018)	S.D.(p=0.12273)	N.S.D.(p=2.7449e-012)	N.S.D.(p=0.00033876)
5	N.S.D.(p=3.8712e-033)	S.D.(p=0.18763)	N.S.D.(p=9.5584e-024)	N.S.D.(p=6.0259e-005)
6	N.S.D.(p=2.1949e-007)	S.D.(p=0.24698)	N.S.D.(p=2.3537e-010)	S.D.(p=0.10252)
7	N.S.D.(p=0.016711)	N.S.D.(p=0.041479)	S.D.(p=0.16164)	N.S.D.(p=0.016711)
8	S.D.(p=0.19161)	S.D.(p=0.13552)	N.S.D.(p=0.016009)	N.S.D.(p=0.00015544)
9	N.S.D.(p=4.2435e-005)	S.D.(p=0.24698)	S.D.(p=0.17447)	N.S.D.(p=0.00023021)
10	S.D.(p=0.19161)	S.D.(p=0.40756)	S.D.(p=0.15923)	N.S.D.(p=0.040531)
11	S.D.(p=0.38312)	S.D.(p=0.17447)	N.S.D.(p=8.6933e-005)	N.S.D.(p=0.0021647)
12	N.S.D.(p=1.6287e-014)	S.D.(p=0.65111)	N.S.D.(p=4.6431e-010)	S.D.(p=0.5861)
S.D.	3	11	3	5

Russell	CALIBRATION PERIOD		VALIDATION PERIOD	
Month	RCM (UNC.)	RCM (CORR.)	RCM (UNC.)	RCM (CORR.)
1	N.S.D.(p=2.6931e-039)	S.D.(p=0.9622)	N.S.D.(p=2.3411e-035)	S.D.(p=0.52468)
2	N.S.D.(p=4.2917e-021)	S.D.(p=0.94642)	N.S.D.(p=1.5795e-017)	S.D.(p=0.21253)
3	N.S.D.(p=1.5683e-008)	S.D.(p=0.71783)	N.S.D.(p=1.4003e-005)	N.S.D.(p=0.026645)
4	N.S.D.(p=9.3057e-020)	S.D.(p=0.24698)	N.S.D.(p=4.8931e-012)	N.S.D.(p=0.0038232)
5	N.S.D.(p=4.2758e-024)	S.D.(p=0.65295)	N.S.D.(p=4.6917e-023)	N.S.D.(p=0.041479)
6	N.S.D.(p=2.194e-008)	S.D.(p=0.82367)	N.S.D.(p=1.5263e-011)	S.D.(p=0.17709)
7	N.S.D.(p=2.035e-005)	S.D.(p=0.35519)	S.D.(p=0.063044)	N.S.D.(p=0.00032646)
8	S.D.(p=0.3074)	S.D.(p=0.58801)	N.S.D.(p=0.0061181)	N.S.D.(p=0.0061181)
9	N.S.D.(p=0.0008805)	S.D.(p=0.63226)	N.S.D.(p=0.0028858)	N.S.D.(p=0.00064437)
10	S.D.(p=0.71783)	S.D.(p=0.71783)	S.D.(p=0.16164)	S.D.(p=0.13552)
11	S.D.(p=0.24698)	S.D.(p=0.63226)	N.S.D.(p=1.8813e-006)	N.S.D.(p=0.00012328)
12	N.S.D.(p=1.2049e-012)	S.D.(p=0.9622)	N.S.D.(p=6.6763e-016)	S.D.(p=0.0624)
S.D.	2	12	2	5

South Mountain	CALIBRATION PERIOD		VALIDATION PERIOD	
Month	RCM (UNC.)	RCM (CORR.)	RCM (UNC.)	RCM (CORR.)
1	N.S.D.(p=7.0286e-029)	S.D.(p=0.92765)	N.S.D.(p=8.3295e-026)	S.D.(p=0.58992)
2	N.S.D.(p=8.6826e-019)	S.D.(p=0.99332)	N.S.D.(p=8.2146e-016)	N.S.D.(p=0.010097)
3	N.S.D.(p=8.8889e-011)	S.D.(p=0.98603)	N.S.D.(p=0.00014847)	N.S.D.(p=0.00046954)
4	N.S.D.(p=1.3962e-012)	S.D.(p=0.4941)	N.S.D.(p=4.9685e-010)	S.D.(p=0.11181)
5	N.S.D.(p=1.3527e-015)	S.D.(p=0.81342)	N.S.D.(p=6.7681e-012)	S.D.(p=0.062189)
6	N.S.D.(p=0.0079402)	S.D.(p=0.72322)	N.S.D.(p=0.0001077)	S.D.(p=0.25316)
7	S.D.(p=0.3811)	S.D.(p=0.51571)	S.D.(p=0.098721)	N.S.D.(p=0.005164)
8	S.D.(p=0.15159)	S.D.(p=0.58992)	N.S.D.(p=0.0070373)	N.S.D.(p=0.0095113)
9	N.S.D.(p=3.0336e-005)	S.D.(p=0.72322)	N.S.D.(p=0.010749)	N.S.D.(p=0.0010783)
10	S.D.(p=0.098721)	S.D.(p=0.92765)	N.S.D.(p=0.037901)	N.S.D.(p=0.022348)
11	S.D.(p=0.56848)	S.D.(p=0.64576)	N.S.D.(p=0.0058154)	N.S.D.(p=0.00035412)
12	N.S.D.(p=1.0317e-008)	S.D.(p=0.92765)	N.S.D.(p=1.2718e-014)	N.S.D.(p=0.0013787)
S.D.	4	12	1	4

ST.ALBERT	CALIBRATION PERIOD		VALIDATION PERIOD	
Month	RCM (UNC.)	RCM (CORR.)	RCM (UNC.)	RCM (CORR.)
1	N.S.D.(p=3.6536e-026)	S.D.(p=0.9374)	N.S.D.(p=1.5282e-024)	S.D.(p=0.2707)
2	N.S.D.(p=3.7589e-016)	S.D.(p=0.9596)	N.S.D.(p=6.4696e-022)	S.D.(p=0.055374)
3	N.S.D.(p=1.484e-005)	S.D.(p=0.74349)	N.S.D.(p=1.1878e-005)	N.S.D.(p=0.04875)
4	N.S.D.(p=2.183e-009)	S.D.(p=0.40737)	N.S.D.(p=1.5099e-007)	N.S.D.(p=0.043006)
5	N.S.D.(p=4.2854e-009)	S.D.(p=0.58089)	N.S.D.(p=5.4317e-018)	N.S.D.(p=0.00032253)
6	N.S.D.(p=7.1041e-007)	S.D.(p=0.4941)	N.S.D.(p=1.5099e-007)	N.S.D.(p=0.033152)
7	N.S.D.(p=0.0037582)	S.D.(p=0.098721)	S.D.(p=0.2707)	N.S.D.(p=0.00067793)
8	N.S.D.(p=0.0095113)	S.D.(p=0.3811)	N.S.D.(p=0.00021973)	N.S.D.(p=0.0095113)
9	N.S.D.(p=0.0010783)	S.D.(p=0.56848)	N.S.D.(p=7.9128e-006)	N.S.D.(p=0.025339)
10	N.S.D.(p=0.037901)	S.D.(p=0.51571)	S.D.(p=0.078679)	S.D.(p=0.062189)
11	S.D.(p=0.17122)	S.D.(p=0.4941)	N.S.D.(p=0.0015364)	N.S.D.(p=0.0001077)
12	N.S.D.(p=5.3539e-008)	S.D.(p=0.96415)	N.S.D.(p=2.5024e-015)	N.S.D.(p=0.00065609)
S.D.	1	12	2	3

Table A.2 KS test results of T_{MIN} of CRCM model in calibration and validation periods for all stations (S.D: Similar Distribution and N.S.D: Non-Similar Distribution)

Airport	CALIBRATION PERIOD		VALIDATION PERIOD	
Month	RCM (UNC.)	RCM (CORR.)	RCM (UNC.)	RCM (CORR.)
1	S.D.(p=0.27847)	S.D.(p=1)	N.S.D.(p=2.6831e-005)	N.S.D.(p=5.5971e-006)
2	N.S.D.(p=6.3683e-014)	S.D.(p=1)	N.S.D.(p=1.6611e-010)	N.S.D.(p=0.029775)
3	N.S.D.(p=5.5431e-021)	S.D.(p=1)	N.S.D.(p=1.582e-021)	S.D.(p=0.39804)
4	N.S.D.(p=1.8758e-039)	S.D.(p=0.98559)	N.S.D.(p=2.8961e-024)	N.S.D.(p=0.0052195)
5	N.S.D.(p=1.5368e-031)	S.D.(p=0.99516)	N.S.D.(p=1.0312e-020)	N.S.D.(p=0.0078539)
6	N.S.D.(p=6.4983e-029)	S.D.(p=0.99954)	N.S.D.(p=9.86e-044)	N.S.D.(p=0.0041612)
7	N.S.D.(p=1.1313e-044)	S.D.(p=0.988)	N.S.D.(p=2.3031e-027)	N.S.D.(p=0.037882)
8	N.S.D.(p=1.582e-021)	S.D.(p=1)	N.S.D.(p=1.5145e-032)	N.S.D.(p=0.011929)
9	N.S.D.(p=1.4951e-008)	S.D.(p=1)	N.S.D.(p=1.4951e-008)	S.D.(p=0.17282)
10	N.S.D.(p=0.021653)	S.D.(p=0.99995)	N.S.D.(p=0.014611)	S.D.(p=0.14052)
11	S.D.(p=0.067533)	S.D.(p=0.99954)	N.S.D.(p=0.027458)	N.S.D.(p=0.018597)
12	N.S.D.(p=0.045273)	S.D.(p=0.99995)	N.S.D.(p=1.2615e-008)	N.S.D.(p=4.8804e-005)
S.D.	2	5	0	3

Avonmore	CALIBRATION PERIOD		VALIDATION PERIOD	
Month	RCM (UNC.)	RCM (CORR.)	RCM (UNC.)	RCM (CORR.)
1	S.D.(p=0.15565)	S.D.(p=0.88717)	S.D.(p=0.090572)	N.S.D.(p=0.0021596)
2	N.S.D.(p=0.00012674)	S.D.(p=0.98061)	N.S.D.(p=0.0007684)	S.D.(p=0.34579)
3	N.S.D.(p=4.417e-012)	S.D.(p=0.6218)	N.S.D.(p=3.4557e-014)	S.D.(p=0.15044)
4	N.S.D.(p=3.0203e-022)	S.D.(p=0.19469)	N.S.D.(p=1.0839e-012)	N.S.D.(p=0.03768)
5	N.S.D.(p=2.3155e-014)	S.D.(p=0.50933)	N.S.D.(p=1.2857e-011)	N.S.D.(p=0.01503)
6	N.S.D.(p=2.2525e-011)	S.D.(p=0.54323)	N.S.D.(p=3.2383e-016)	N.S.D.(p=0.0048769)
7	N.S.D.(p=2.972e-019)	S.D.(p=0.17635)	N.S.D.(p=1.9026e-007)	N.S.D.(p=0.00030331)
8	N.S.D.(p=1.0348e-009)	S.D.(p=0.31585)	N.S.D.(p=2.3671e-008)	S.D.(p=0.10781)
9	N.S.D.(p=0.0009865)	S.D.(p=0.5524)	N.S.D.(p=0.0048769)	N.S.D.(p=0.00625)
10	N.S.D.(p=0.0016564)	S.D.(p=0.36039)	S.D.(p=0.062956)	S.D.(p=0.31585)
11	N.S.D.(p=0.0029233)	S.D.(p=0.22217)	N.S.D.(p=0.00625)	S.D.(p=0.79138)
12	S.D.(p=0.05209)	S.D.(p=0.80773)	N.S.D.(p=4.0794e-009)	N.S.D.(p=4.1065e-006)
S.D.	2	12	2	5

Brockville	CALIBRATION PERIOD		VALIDATION PERIOD	
Month	RCM (UNC.)	RCM (CORR.)	RCM (UNC.)	RCM (CORR.)
1	N.S.D.(p=9.5584e-024)	S.D.(p=0.93123)	N.S.D.(p=2.1439e-020)	S.D.(p=0.40756)
2	N.S.D.(p=1.0436e-013)	S.D.(p=0.73547)	N.S.D.(p=7.9572e-011)	S.D.(p=0.52124)
3	N.S.D.(p=3.7002e-007)	S.D.(p=0.52468)	N.S.D.(p=0.0061181)	N.S.D.(p=0.0061181)
4	N.S.D.(p=1.5659e-024)	S.D.(p=0.14852)	N.S.D.(p=2.2416e-016)	N.S.D.(p=0.011073)
5	N.S.D.(p=7.0018e-026)	S.D.(p=0.35519)	N.S.D.(p=2.7006e-015)	N.S.D.(p=0.0061181)
6	N.S.D.(p=6.0925e-005)	S.D.(p=0.14852)	N.S.D.(p=4.8931e-012)	N.S.D.(p=0.0028858)
7	N.S.D.(p=2.9571e-006)	S.D.(p=0.05129)	N.S.D.(p=0.00023565)	S.D.(p=0.05129)
8	N.S.D.(p=0.0011327)	S.D.(p=0.3074)	S.D.(p=0.11294)	N.S.D.(p=1.4003e-005)
9	S.D.(p=0.28882)	S.D.(p=0.44294)	N.S.D.(p=6.0925e-005)	N.S.D.(p=0.00017374)
10	N.S.D.(p=0.0035714)	S.D.(p=0.46424)	N.S.D.(p=0.00016908)	N.S.D.(p=0.021164)
11	N.S.D.(p=0.036402)	S.D.(p=0.12378)	N.S.D.(p=8.3631e-009)	N.S.D.(p=2.9374e-005)
12	N.S.D.(p=2.9571e-006)	S.D.(p=0.78052)	N.S.D.(p=5.682e-009)	N.S.D.(p=0.0019943)
S.D.	1	12	1	3

.

Pointe au Chene	CALIBRATION PERIOD		VALIDATION PERIOD	
Month	RCM (UNC.)	RCM (CORR.)	RCM (UNC.)	RCM (CORR.)
1	S.D.(p=0.15473)	S.D.(p=0.56322)	N.S.D.(p=0.028625)	N.S.D.(p=0.028625)
2	N.S.D.(p=4.6548e-005)	S.D.(p=0.61401)	N.S.D.(p=1.4584e-005)	S.D.(p=0.094815)
3	N.S.D.(p=7.9183e-016)	S.D.(p=0.20997)	N.S.D.(p=5.04e-017)	S.D.(p=0.062956)
4	N.S.D.(p=3.2316e-024)	S.D.(p=0.071355)	N.S.D.(p=3.8131e-018)	N.S.D.(p=0.0029233)
5	N.S.D.(p=9.7019e-025)	S.D.(p=0.078972)	N.S.D.(p=6.1856e-015)	N.S.D.(p=4.6304e-005)
6	N.S.D.(p=7.8337e-016)	S.D.(p=0.16718)	N.S.D.(p=1.2578e-026)	N.S.D.(p=0.0029233)
7	N.S.D.(p=1.0028e-022)	N.S.D.(p=0.047001)	N.S.D.(p=2.7005e-017)	N.S.D.(p=0.0075414)
8	N.S.D.(p=2.9565e-019)	S.D.(p=0.080772)	N.S.D.(p=7.6163e-024)	S.D.(p=0.12244)
9	N.S.D.(p=7.0111e-006)	S.D.(p=0.19469)	N.S.D.(p=2.4629e-006)	S.D.(p=0.066622)
10	S.D.(p=0.080772)	S.D.(p=0.20997)	S.D.(p=0.17421)	S.D.(p=0.23603)
11	N.S.D.(p=0.003554)	S.D.(p=0.1652)	N.S.D.(p=0.0013045)	N.S.D.(p=0.03768)
12	S.D.(p=0.18021)	S.D.(p=0.45491)	N.S.D.(p=0.0075414)	N.S.D.(p=0.042882)
S.D.	3	11	1	5

Russell	CALIBRATION PERIOD		VALIDATION PERIOD	
Month	RCM (UNC.)	RCM (CORR.)	RCM (UNC.)	RCM (CORR.)
1	N.S.D.(p=0.017355)	S.D.(p=0.97785)	N.S.D.(p=0.00022456)	N.S.D.(p=4.7394e-006)
2	N.S.D.(p=1.4113e-008)	S.D.(p=0.88603)	N.S.D.(p=6.6304e-007)	S.D.(p=0.28175)
3	N.S.D.(p=2.9565e-019)	S.D.(p=0.48506)	N.S.D.(p=1.0195e-020)	N.S.D.(p=0.048346)
4	N.S.D.(p=1.0562e-027)	S.D.(p=0.31433)	N.S.D.(p=4.9796e-017)	N.S.D.(p=0.041072)
5	N.S.D.(p=5.9243e-021)	S.D.(p=0.54836)	N.S.D.(p=3.4557e-014)	N.S.D.(p=0.0012899)
6	N.S.D.(p=4.4513e-015)	S.D.(p=0.66106)	N.S.D.(p=1.037e-021)	N.S.D.(p=0.018694)
7	N.S.D.(p=8.1584e-027)	S.D.(p=0.20647)	N.S.D.(p=2.7189e-012)	N.S.D.(p=0.002809)
8	N.S.D.(p=1.4062e-015)	S.D.(p=0.51738)	N.S.D.(p=2.972e-019)	S.D.(p=0.089632)
9	N.S.D.(p=2.4083e-006)	S.D.(p=0.43453)	N.S.D.(p=0.00012055)	N.S.D.(p=0.01478)
10	S.D.(p=0.08017)	S.D.(p=0.51868)	S.D.(p=0.23856)	S.D.(p=0.21847)
11	N.S.D.(p=0.041429)	S.D.(p=0.58132)	N.S.D.(p=0.0048769)	S.D.(p=0.46516)
12	N.S.D.(p=0.0035332)	S.D.(p=0.88717)	N.S.D.(p=0.00030331)	N.S.D.(p=0.00095982)
S.D.	1	12	1	4

South Mountain	CALIBRATION PERIOD		VALIDATION PERIOD	
Month	RCM (UNC.)	RCM (CORR.)	RCM (UNC.)	RCM (CORR.)
1	N.S.D.(p=0.04875)	S.D.(p=0.92765)	N.S.D.(p=4.3583e-005)	N.S.D.(p=9.1174e-008)
2	N.S.D.(p=0.00062541)	S.D.(p=0.99253)	N.S.D.(p=0.00042391)	N.S.D.(p=0.032571)
3	N.S.D.(p=9.1174e-008)	S.D.(p=0.98603)	N.S.D.(p=2.6403e-014)	N.S.D.(p=0.0013787)
4	N.S.D.(p=4.4147e-020)	S.D.(p=0.4941)	N.S.D.(p=1.6898e-013)	S.D.(p=0.055314)
5	N.S.D.(p=4.5158e-013)	S.D.(p=0.81342)	N.S.D.(p=1.023e-009)	S.D.(p=0.22506)
6	N.S.D.(p=7.9128e-006)	S.D.(p=0.72322)	N.S.D.(p=3.4454e-013)	N.S.D.(p=0.0079402)
7	N.S.D.(p=1.7773e-012)	S.D.(p=0.51571)	N.S.D.(p=5.3539e-008)	S.D.(p=0.22506)
8	N.S.D.(p=1.8457e-009)	S.D.(p=0.58992)	N.S.D.(p=3.118e-008)	N.S.D.(p=0.04875)
9	S.D.(p=0.08919)	S.D.(p=0.72322)	N.S.D.(p=0.0015364)	N.S.D.(p=0.033152)
10	S.D.(p=0.062189)	S.D.(p=0.92765)	S.D.(p=0.18549)	S.D.(p=0.2707)
11	S.D.(p=0.13896)	S.D.(p=0.64576)	S.D.(p=0.17122)	S.D.(p=0.64576)
12	S.D.(p=0.15159)	S.D.(p=0.92765)	N.S.D.(p=1.5399e-007)	N.S.D.(p=4.2852e-007)
S.D.	4	12	2	5

ST.ALBERT	CALIBRATION PERIOD		VALIDATION PERIOD	
Month	RCM (UNC.)	RCM (CORR.)	RCM (UNC.)	RCM (CORR.)
1	N.S.D.(p=0.010301)	S.D.(p=0.98852)	N.S.D.(p=0.044446)	N.S.D.(p=0.02803)
2	N.S.D.(p=0.0031978)	S.D.(p=0.95528)	N.S.D.(p=0.0043293)	N.S.D.(p=0.037568)
3	N.S.D.(p=9.4026e-012)	S.D.(p=0.59204)	N.S.D.(p=5.1598e-015)	N.S.D.(p=0.035413)
4	N.S.D.(p=1.0316e-021)	S.D.(p=0.28075)	N.S.D.(p=1.1884e-009)	N.S.D.(p=0.0027482)
5	N.S.D.(p=9.3024e-011)	S.D.(p=0.59204)	N.S.D.(p=2.3758e-009)	N.S.D.(p=0.003407)
6	N.S.D.(p=4.6444e-011)	S.D.(p=0.20981)	N.S.D.(p=1.663e-015)	N.S.D.(p=0.039094)
7	N.S.D.(p=1.9904e-016)	N.S.D.(p=0.021164)	N.S.D.(p=1.1791e-006)	N.S.D.(p=9.4405e-005)
8	N.S.D.(p=5.6748e-007)	S.D.(p=0.3074)	N.S.D.(p=2.9501e-008)	S.D.(p=0.21564)
9	N.S.D.(p=0.029048)	S.D.(p=0.28882)	S.D.(p=0.16715)	N.S.D.(p=0.0014892)
10	N.S.D.(p=0.00016908)	S.D.(p=0.40756)	S.D.(p=0.10325)	S.D.(p=0.055418)
11	S.D.(p=0.056114)	S.D.(p=0.38691)	N.S.D.(p=0.0020299)	N.S.D.(p=0.049108)
12	S.D.(p=0.05129)	S.D.(p=0.93123)	N.S.D.(p=7.7165e-008)	N.S.D.(p=6.5502e-005)
S.D.	2	11	2	2

Table A.3 KS test results of T_{MAX} of ARPEGE model in calibration and validation periods (S.D: Similar Distribution and N.S.D: Non-Similar Distribution)

Airport	CALIBRATION PERIOD		VALIDATION PERIOD	
Month	RCM (UNC.)	RCM (CORR.)	RCM (UNC.)	RCM (CORR.)
1	N.S.D.(p=2.2484e-022)	S.D.(p=1)	N.S.D.(p=1.9311e-019)	N.S.D.(p=0.00016908)
2	N.S.D.(p=1.3763e-016)	S.D.(p=1)	N.S.D.(p=6.4556e-013)	S.D.(p=0.29361)
3	N.S.D.(p=0.0001206)	S.D.(p=1)	N.S.D.(p=0.0020355)	N.S.D.(p=0.041479)
4	N.S.D.(p=0.00012328)	S.D.(p=1)	N.S.D.(p=0.0028858)	N.S.D.(p=0.023037)
5	N.S.D.(p=2.1439e-020)	S.D.(p=1)	N.S.D.(p=3.9701e-019)	N.S.D.(p=0.026645)
6	N.S.D.(p=2.0844e-020)	S.D.(p=1)	N.S.D.(p=8.1091e-024)	N.S.D.(p=0.0065874)
7	N.S.D.(p=2.644e-017)	S.D.(p=0.99973)	N.S.D.(p=5.5279e-027)	S.D.(p=0.05129)
8	N.S.D.(p=6.0398e-011)	S.D.(p=0.99973)	N.S.D.(p=1.5683e-008)	S.D.(p=0.88957)
9	S.D.(p=0.10252)	S.D.(p=1)	N.S.D.(p=2.194e-008)	N.S.D.(p=1.3588e-008)
10	N.S.D.(p=0.033344)	S.D.(p=0.99998)	N.S.D.(p=6.5124e-006)	N.S.D.(p=0.033344)
11	S.D.(p=0.69845)	S.D.(p=0.99997)	N.S.D.(p=9.3879e-006)	N.S.D.(p=2.9374e-005)
12	N.S.D.(p=9.5782e-006)	S.D.(p=1)	N.S.D.(p=3.4848e-009)	S.D.(p=0.050735)
S.D.	2	8	0	4

Avonmore	CALIBRATION PERIOD		VALIDATION PERIOD	
Month	RCM (UNC.)	RCM (CORR.)	RCM (UNC.)	RCM (CORR.)
1	N.S.D.(p=1.0521e-021)	S.D.(p=0.93123)	N.S.D.(p=8.1134e-019)	N.S.D.(p=0.0035714)
2	N.S.D.(p=1.8849e-018)	S.D.(p=0.90763)	N.S.D.(p=7.9229e-012)	N.S.D.(p=0.043349)
3	N.S.D.(p=6.5124e-006)	S.D.(p=0.52468)	N.S.D.(p=2.035e-005)	N.S.D.(p=0.021164)
4	N.S.D.(p=0.0065874)	S.D.(p=0.76307)	S.D.(p=0.24698)	N.S.D.(p=0.0065874)
5	N.S.D.(p=3.3298e-014)	S.D.(p=0.8386)	N.S.D.(p=3.3298e-014)	N.S.D.(p=0.0027043)
6	N.S.D.(p=3.1605e-015)	S.D.(p=0.5031)	N.S.D.(p=4.0531e-019)	N.S.D.(p=0.0028858)
7	N.S.D.(p=3.5152e-011)	S.D.(p=0.13552)	N.S.D.(p=3.8544e-016)	S.D.(p=0.063044)
8	N.S.D.(p=8.6512e-007)	S.D.(p=0.35519)	N.S.D.(p=2.9398e-005)	N.S.D.(p=0.010233)
9	S.D.(p=0.20981)	S.D.(p=0.38691)	N.S.D.(p=4.2549e-006)	N.S.D.(p=1.8813e-006)
10	S.D.(p=0.11294)	S.D.(p=0.71783)	N.S.D.(p=8.5503e-005)	N.S.D.(p=0.016711)
11	N.S.D.(p=0.029048)	S.D.(p=0.69845)	N.S.D.(p=0.00033876)	N.S.D.(p=0.00024336)
12	N.S.D.(p=2.035e-005)	S.D.(p=0.71783)	N.S.D.(p=1.6349e-010)	N.S.D.(p=0.0035049)
S.D.	2	12	1	1

Brockville	CALIBRATION PERIOD		VALIDATION PERIOD	
Month	RCM (UNC.)	RCM (CORR.)	RCM (UNC.)	RCM (CORR.)
1	N.S.D.(p=1.128e-013)	S.D.(p=0.93123)	N.S.D.(p=4.9586e-010)	N.S.D.(p=0.001523)
2	N.S.D.(p=3.636e-013)	S.D.(p=0.79966)	N.S.D.(p=1.7683e-007)	S.D.(p=0.054128)
3	N.S.D.(p=4.2215e-005)	S.D.(p=0.52468)	N.S.D.(p=0.0027043)	N.S.D.(p=0.026645)
4	N.S.D.(p=0.029048)	S.D.(p=0.5031)	S.D.(p=0.38691)	N.S.D.(p=0.0028858)
5	N.S.D.(p=4.9586e-010)	S.D.(p=0.40756)	N.S.D.(p=6.0232e-009)	N.S.D.(p=4.2215e-005)
6	N.S.D.(p=1.402e-007)	S.D.(p=0.20981)	N.S.D.(p=7.5134e-014)	N.S.D.(p=8.6933e-005)
7	N.S.D.(p=1.311e-006)	N.S.D.(p=0.021164)	N.S.D.(p=3.799e-012)	N.S.D.(p=0.00061541)
8	N.S.D.(p=0.026645)	S.D.(p=0.13552)	N.S.D.(p=0.0027043)	S.D.(p=0.22574)
9	S.D.(p=0.44294)	S.D.(p=0.44294)	N.S.D.(p=0.00012328)	N.S.D.(p=0.00012328)
10	S.D.(p=0.11294)	S.D.(p=0.71783)	N.S.D.(p=2.9398e-005)	N.S.D.(p=0.026645)
11	S.D.(p=0.38691)	S.D.(p=0.44294)	N.S.D.(p=2.838e-006)	N.S.D.(p=0.00024336)
12	N.S.D.(p=2.5081e-008)	S.D.(p=0.71783)	N.S.D.(p=5.4262e-007)	N.S.D.(p=0.0014908)
S.D.	3	11	1	2

Pointe au Chene	CALIBRATION PERIOD		VALIDATION PERIOD	
Month	RCM (UNC.)	RCM (CORR.)	RCM (UNC.)	RCM (CORR.)
1	N.S.D.(p=1.8701e-020)	S.D.(p=0.65111)	N.S.D.(p=4.6917e-023)	N.S.D.(p=0.001523)
2	N.S.D.(p=9.6159e-016)	S.D.(p=0.53184)	N.S.D.(p=5.7139e-014)	S.D.(p=0.45791)
3	N.S.D.(p=8.9037e-006)	S.D.(p=0.26113)	N.S.D.(p=0.00061541)	N.S.D.(p=0.0035714)
4	N.S.D.(p=1.9506e-005)	S.D.(p=0.38502)	S.D.(p=0.056114)	N.S.D.(p=0.00024336)
5	N.S.D.(p=5.6179e-028)	S.D.(p=0.45849)	N.S.D.(p=5.213e-017)	N.S.D.(p=6.5124e-006)
6	N.S.D.(p=9.1236e-023)	S.D.(p=0.10252)	N.S.D.(p=1.7001e-027)	N.S.D.(p=0.0011958)
7	N.S.D.(p=1.128e-013)	S.D.(p=0.077028)	N.S.D.(p=1.9694e-030)	N.S.D.(p=6.3002e-008)
8	N.S.D.(p=1.128e-013)	N.S.D.(p=0.021164)	N.S.D.(p=4.6503e-014)	S.D.(p=0.18763)
9	S.D.(p=0.12378)	S.D.(p=0.24698)	N.S.D.(p=1.1862e-006)	N.S.D.(p=4.8141e-009)
10	S.D.(p=0.52468)	S.D.(p=0.46424)	N.S.D.(p=0.00011381)	N.S.D.(p=0.03254)
11	S.D.(p=0.38502)	S.D.(p=0.38502)	N.S.D.(p=0.00017374)	N.S.D.(p=8.6933e-005)
12	N.S.D.(p=4.0886e-005)	S.D.(p=0.2627)	N.S.D.(p=0.0002294)	N.S.D.(p=0.010074)
S.D.	3	11	1	2

Russell	CALIBRATION PERIOD		VALIDATION PERIOD	
Month	RCM (UNC.)	RCM (CORR.)	RCM (UNC.)	RCM (CORR.)
1	N.S.D.(p=1.0521e-021)	S.D.(p=0.93123)	N.S.D.(p=2.0576e-013)	N.S.D.(p=0.00032646)
2	N.S.D.(p=1.0436e-013)	S.D.(p=0.90763)	N.S.D.(p=5.8389e-009)	S.D.(p=0.39882)
3	N.S.D.(p=0.001523)	S.D.(p=0.8386)	N.S.D.(p=0.016711)	S.D.(p=0.063044)
4	N.S.D.(p=8.1151e-007)	S.D.(p=0.76307)	N.S.D.(p=0.00012328)	N.S.D.(p=0.0085669)
5	N.S.D.(p=8.404e-025)	S.D.(p=0.8386)	N.S.D.(p=4.8782e-022)	N.S.D.(p=0.0020355)
6	N.S.D.(p=5.4211e-026)	S.D.(p=0.5031)	N.S.D.(p=4.8293e-029)	N.S.D.(p=0.0038232)
7	N.S.D.(p=1.0181e-020)	S.D.(p=0.3074)	N.S.D.(p=7.1262e-029)	S.D.(p=0.05129)
8	N.S.D.(p=6.147e-014)	S.D.(p=0.40756)	N.S.D.(p=3.5152e-011)	N.S.D.(p=0.010233)
9	N.S.D.(p=0.036402)	S.D.(p=0.44294)	N.S.D.(p=1.1283e-009)	N.S.D.(p=2.0208e-005)
10	N.S.D.(p=0.001523)	S.D.(p=0.78052)	N.S.D.(p=2.9558e-010)	N.S.D.(p=0.021164)
11	S.D.(p=0.10252)	S.D.(p=0.76307)	N.S.D.(p=2.1949e-007)	N.S.D.(p=0.00033876)
12	N.S.D.(p=2.9398e-005)	S.D.(p=0.71783)	N.S.D.(p=3.7823e-008)	N.S.D.(p=0.0035049)
S.D.	1	12	0	3

South Mountain	CALIBRATION PERIOD		VALIDATION PERIOD	
Month	RCM (UNC.)	RCM (CORR.)	RCM (UNC.)	RCM (CORR.)
1	N.S.D.(p=1.2718e-014)	S.D.(p=0.74197)	N.S.D.(p=8.9959e-013)	N.S.D.(p=0.037901)
2	N.S.D.(p=8.6826e-019)	S.D.(p=0.84212)	N.S.D.(p=8.0619e-009)	S.D.(p=0.17769)
3	N.S.D.(p=4.7913e-006)	S.D.(p=0.92765)	N.S.D.(p=0.00046954)	S.D.(p=0.062189)
4	N.S.D.(p=0.010749)	S.D.(p=0.79727)	S.D.(p=0.17122)	N.S.D.(p=0.033152)
5	N.S.D.(p=4.5158e-013)	S.D.(p=0.32269)	N.S.D.(p=1.023e-009)	N.S.D.(p=0.00032253)
6	N.S.D.(p=1.8939e-014)	S.D.(p=0.64576)	N.S.D.(p=3.7993e-017)	N.S.D.(p=0.025339)
7	N.S.D.(p=3.0657e-010)	S.D.(p=0.44568)	N.S.D.(p=1.1101e-013)	S.D.(p=0.3811)
8	N.S.D.(p=1.5399e-007)	S.D.(p=0.3811)	N.S.D.(p=4.7913e-006)	S.D.(p=0.098721)
9	S.D.(p=0.25316)	S.D.(p=0.79727)	N.S.D.(p=0.0015364)	N.S.D.(p=3.0336e-005)
10	S.D.(p=0.078679)	S.D.(p=0.74197)	N.S.D.(p=3.0056e-006)	N.S.D.(p=0.022348)
11	S.D.(p=0.08919)	S.D.(p=0.72322)	N.S.D.(p=0.0058154)	N.S.D.(p=0.0058154)
12	N.S.D.(p=0.0027126)	S.D.(p=0.74197)	N.S.D.(p=6.7681e-012)	N.S.D.(p=0.012749)
S.D.	3	12	1	4

ST.ALBERT	CALIBRATION PERIOD		VALIDATION PERIOD	
Month	RCM (UNC.)	RCM (CORR.)	RCM (UNC.)	RCM (CORR.)
1	N.S.D.(p=6.5709e-013)	S.D.(p=0.97218)	N.S.D.(p=3.4827e-012)	N.S.D.(p=0.012749)
2	N.S.D.(p=5.417e-009)	S.D.(p=0.9154)	N.S.D.(p=1.8411e-013)	S.D.(p=0.090752)
3	N.S.D.(p=0.00048037)	S.D.(p=0.81953)	N.S.D.(p=0.00097076)	N.S.D.(p=0.04875)
4	S.D.(p=0.11999)	S.D.(p=0.80364)	N.S.D.(p=0.010749)	S.D.(p=0.055314)
5	N.S.D.(p=2.3268e-011)	S.D.(p=0.88567)	N.S.D.(p=1.4555e-020)	N.S.D.(p=0.029224)
6	N.S.D.(p=7.3831e-018)	S.D.(p=0.56848)	N.S.D.(p=7.628e-023)	N.S.D.(p=0.0079402)
7	N.S.D.(p=8.8889e-011)	S.D.(p=0.12284)	N.S.D.(p=1.0424e-018)	N.S.D.(p=0.00046954)
8	N.S.D.(p=4.7913e-006)	S.D.(p=0.18549)	N.S.D.(p=7.0606e-007)	S.D.(p=0.098721)
9	S.D.(p=0.08919)	S.D.(p=0.4941)	N.S.D.(p=1.5099e-007)	N.S.D.(p=0.00075031)
10	S.D.(p=0.18549)	S.D.(p=0.58992)	N.S.D.(p=7.0606e-007)	N.S.D.(p=0.00097076)
11	S.D.(p=0.30368)	S.D.(p=0.36084)	N.S.D.(p=1.249e-005)	N.S.D.(p=4.6675e-005)
12	N.S.D.(p=0.00032253)	S.D.(p=0.74197)	N.S.D.(p=2.8448e-006)	N.S.D.(p=0.012488)
S.D.	4	12	0	3

Table A.4 KS test results of T_{MAX} of CRCM model in calibration and validation periods (S.D: Similar Distribution and N.S.D: Non-Similar Distribution)

Airport	CALIBRATION PERIOD		VALIDATION PERIOD	
Month	RCM (UNC.)	RCM (CORR.)	RCM (UNC.)	RCM (CORR.)
1	N.S.D.(p=6.5417e-005)	S.D.(p=1)	N.S.D.(p=0.00075989)	N.S.D.(p=2.5742e-007)
2	S.D.(p=0.10547)	S.D.(p=1)	N.S.D.(p=0.0053792)	S.D.(p=0.074825)
3	N.S.D.(p=0.037882)	S.D.(p=1)	N.S.D.(p=0.037882)	S.D.(p=0.10379)
4	N.S.D.(p=2.2215e-008)	S.D.(p=1)	N.S.D.(p=8.3637e-005)	N.S.D.(p=0.00058311)
5	N.S.D.(p=5.2846e-015)	S.D.(p=1)	N.S.D.(p=2.6831e-005)	N.S.D.(p=1.0607e-005)
6	N.S.D.(p=0.010042)	S.D.(p=1)	N.S.D.(p=3.1552e-007)	N.S.D.(p=0.0016114)
7	N.S.D.(p=0.0005882)	S.D.(p=0.99848)	N.S.D.(p=8.7327e-005)	N.S.D.(p=0.045273)
8	N.S.D.(p=0.0020316)	S.D.(p=0.99848)	N.S.D.(p=1.8657e-008)	N.S.D.(p=1.8657e-008)
9	N.S.D.(p=0.039859)	S.D.(p=1)	N.S.D.(p=0.012384)	N.S.D.(p=0.039859)
10	N.S.D.(p=0.00045345)	S.D.(p=0.99995)	N.S.D.(p=3.6843e-007)	S.D.(p=0.063872)
11	N.S.D.(p=0.0004475)	S.D.(p=0.99993)	N.S.D.(p=0.0052195)	S.D.(p=0.067533)
12	N.S.D.(p=0.021653)	S.D.(p=1)	N.S.D.(p=8.163e-013)	N.S.D.(p=3.6843e-007)
S.D.	1	12	0	4

Avonmore	CALIBRATION PERIOD		VALIDATION PERIOD	
Month	RCM (UNC.)	RCM (CORR.)	RCM (UNC.)	RCM (CORR.)
1	N.S.D.(p=1.2796e-006)	S.D.(p=0.92503)	N.S.D.(p=0.00016542)	N.S.D.(p=4.2271e-007)
2	N.S.D.(p=0.00023642)	S.D.(p=0.84705)	N.S.D.(p=0.0003076)	N.S.D.(p=0.043298)
3	N.S.D.(p=5.9071e-008)	S.D.(p=0.56473)	N.S.D.(p=8.8408e-005)	S.D.(p=0.090572)
4	N.S.D.(p=0.034047)	S.D.(p=0.82733)	S.D.(p=0.13791)	N.S.D.(p=0.03768)
5	N.S.D.(p=2.6342e-006)	S.D.(p=0.7365)	N.S.D.(p=0.0059323)	N.S.D.(p=0.01503)
6	N.S.D.(p=0.041429)	S.D.(p=0.54323)	N.S.D.(p=0.00041348)	N.S.D.(p=0.0013045)
7	N.S.D.(p=0.00054504)	S.D.(p=0.12768)	N.S.D.(p=2.3671e-008)	N.S.D.(p=0.0021596)
8	N.S.D.(p=0.00030331)	S.D.(p=0.20565)	N.S.D.(p=2.8431e-007)	N.S.D.(p=0.0036156)
9	S.D.(p=0.081615)	S.D.(p=0.34058)	N.S.D.(p=0.024812)	S.D.(p=0.1164)
10	N.S.D.(p=1.3478e-006)	S.D.(p=0.51606)	N.S.D.(p=1.3478e-006)	S.D.(p=0.31585)
11	N.S.D.(p=3.1785e-012)	S.D.(p=0.61236)	N.S.D.(p=1.1041e-007)	S.D.(p=0.16254)
12	N.S.D.(p=5.8933e-006)	S.D.(p=0.51606)	N.S.D.(p=1.6036e-012)	N.S.D.(p=2.8431e-007)
S.D.	1	12	1	4

Brockville	CALIBRATION PERIOD		VALIDATION PERIOD	
Month	RCM (UNC.)	RCM (CORR.)	RCM (UNC.)	RCM (CORR.)
1	N.S.D.(p=5.3816e-005)	S.D.(p=0.7365)	N.S.D.(p=0.01503)	N.S.D.(p=2.847e-006)
2	N.S.D.(p=0.0013547)	S.D.(p=0.73642)	S.D.(p=0.053116)	N.S.D.(p=0.0041222)
3	N.S.D.(p=8.8199e-008)	S.D.(p=0.50933)	N.S.D.(p=0.0059323)	N.S.D.(p=0.0036156)
4	N.S.D.(p=0.034047)	S.D.(p=0.54323)	N.S.D.(p=0.0048769)	S.D.(p=0.067806)
5	N.S.D.(p=0.0035332)	S.D.(p=0.35997)	S.D.(p=0.51606)	N.S.D.(p=0.0012641)
6	N.S.D.(p=2.4931e-007)	S.D.(p=0.19469)	N.S.D.(p=0.0048769)	N.S.D.(p=0.00030622)
7	N.S.D.(p=4.417e-012)	N.S.D.(p=0.0140)	N.S.D.(p=5.8138e-016)	S.D.(p=0.090572)
8	N.S.D.(p=7.4196e-009)	S.D.(p=0.095843)	N.S.D.(p=2.847e-006)	N.S.D.(p=4.6304e-005)
9	N.S.D.(p=0.0059484)	S.D.(p=0.26005)	N.S.D.(p=0.001716)	S.D.(p=0.25763)
10	N.S.D.(p=1.4755e-005)	S.D.(p=0.4564)	N.S.D.(p=5.8933e-006)	S.D.(p=0.10781)
11	N.S.D.(p=0.00024285)	S.D.(p=0.34018)	N.S.D.(p=6.3086e-005)	N.S.D.(p=0.0048769)
12	N.S.D.(p=0.047001)	S.D.(p=0.4564)	N.S.D.(p=6.4846e-010)	N.S.D.(p=4.0431e-010)
S.D.	0	11	2	3

Pointe au Chene	CALIBRATION PERIOD		VALIDATION PERIOD	
Month	RCM (UNC.)	RCM (CORR.)	RCM (UNC.)	RCM (CORR.)
1	N.S.D.(p=0.00023903)	S.D.(p=0.62032)	N.S.D.(p=8.8408e-005)	N.S.D.(p=0.00072511)
2	S.D.(p=0.068401)	S.D.(p=0.49619)	S.D.(p=0.053116)	N.S.D.(p=0.0069)
3	N.S.D.(p=0.00095031)	S.D.(p=0.1792)	S.D.(p=0.27525)	N.S.D.(p=0.042882)
4	N.S.D.(p=9.3466e-006)	S.D.(p=0.19252)	N.S.D.(p=1.1406e-005)	N.S.D.(p=0.016001)
5	N.S.D.(p=9.4894e-014)	S.D.(p=0.35575)	N.S.D.(p=1.3478e-006)	N.S.D.(p=0.0016564)
6	N.S.D.(p=0.0017079)	S.D.(p=0.060459)	N.S.D.(p=1.1041e-007)	N.S.D.(p=0.0005554)
7	N.S.D.(p=1.0552e-005)	S.D.(p=0.056563)	N.S.D.(p=1.3478e-006)	S.D.(p=0.17635)
8	N.S.D.(p=5.322e-006)	N.S.D.(p=0.0173)	N.S.D.(p=1.0484e-012)	N.S.D.(p=4.8526e-006)
9	S.D.(p=0.072507)	S.D.(p=0.26005)	N.S.D.(p=0.0048014)	N.S.D.(p=0.030326)
10	N.S.D.(p=7.3504e-005)	S.D.(p=0.35997)	N.S.D.(p=0.00015777)	S.D.(p=0.35736)
11	N.S.D.(p=5.0824e-005)	S.D.(p=0.33876)	N.S.D.(p=0.0048769)	S.D.(p=0.38813)
12	N.S.D.(p=0.008911)	S.D.(p=0.24092)	N.S.D.(p=2.8431e-007)	N.S.D.(p=0.00030331)
S.D.	2	11	2	3

Russell	CALIBRATION PERIOD		VALIDATION PERIOD	
Month	RCM (UNC.)	RCM (CORR.)	RCM (UNC.)	RCM (CORR.)
1	N.S.D.(p=0.00057164)	S.D.(p=0.85464)	S.D.(p=0.12768)	N.S.D.(p=4.3884e-008)
2	N.S.D.(p=0.038459)	S.D.(p=0.79432)	N.S.D.(p=0.011294)	N.S.D.(p=0.0092437)
3	S.D.(p=0.18122)	S.D.(p=0.84099)	N.S.D.(p=0.042882)	S.D.(p=0.18512)
4	N.S.D.(p=3.2965e-008)	S.D.(p=0.69804)	N.S.D.(p=1.991e-008)	N.S.D.(p=0.029106)
5	N.S.D.(p=7.9183e-016)	S.D.(p=0.81173)	N.S.D.(p=1.643e-009)	N.S.D.(p=0.0017485)
6	N.S.D.(p=0.0046797)	S.D.(p=0.5533)	N.S.D.(p=1.8097e-006)	N.S.D.(p=0.0018396)
7	N.S.D.(p=2.8444e-005)	S.D.(p=0.21174)	N.S.D.(p=1.9638e-006)	N.S.D.(p=0.027798)
8	N.S.D.(p=7.3504e-005)	S.D.(p=0.2206)	N.S.D.(p=5.8092e-011)	N.S.D.(p=7.798e-005)
9	N.S.D.(p=0.0022134)	S.D.(p=0.44448)	N.S.D.(p=0.00625)	N.S.D.(p=0.027389)
10	N.S.D.(p=0.031693)	S.D.(p=0.55422)	N.S.D.(p=0.0095386)	S.D.(p=0.15733)
11	S.D.(p=0.060459)	S.D.(p=0.61305)	N.S.D.(p=0.012749)	S.D.(p=0.062231)
12	S.D.(p=0.56473)	S.D.(p=0.6218)	N.S.D.(p=1.1955e-005)	N.S.D.(p=5.5316e-008)
S.D.	3	12	1	3

South Mountain	CALIBRATION PERIOD		VALIDATION PERIOD	
Month	RCM (UNC.)	RCM (CORR.)	RCM (UNC.)	RCM (CORR.)
1	N.S.D.(p=1.1538e-006)	S.D.(p=0.74197)	S.D.(p=0.18549)	N.S.D.(p=4.7275e-011)
2	N.S.D.(p=0.00028472)	S.D.(p=0.83423)	S.D.(p=0.17769)	N.S.D.(p=0.0073637)
3	N.S.D.(p=9.9489e-005)	S.D.(p=0.92765)	N.S.D.(p=0.04875)	N.S.D.(p=0.0070373)
4	N.S.D.(p=0.004223)	S.D.(p=0.79727)	N.S.D.(p=0.014428)	S.D.(p=0.13896)
5	N.S.D.(p=4.7913e-006)	S.D.(p=0.32269)	N.S.D.(p=0.00046954)	N.S.D.(p=0.0019418)
6	N.S.D.(p=0.025339)	S.D.(p=0.64576)	N.S.D.(p=0.019202)	N.S.D.(p=0.00016153)
7	N.S.D.(p=0.012749)	S.D.(p=0.44568)	N.S.D.(p=0.00046954)	S.D.(p=0.078679)
8	N.S.D.(p=0.0095113)	S.D.(p=0.3811)	N.S.D.(p=6.6121e-005)	N.S.D.(p=0.029224)
9	S.D.(p=0.4245)	S.D.(p=0.79727)	S.D.(p=0.07054)	S.D.(p=0.30368)
10	S.D.(p=0.12284)	S.D.(p=0.74197)	N.S.D.(p=0.022348)	S.D.(p=0.3811)
11	N.S.D.(p=0.00016153)	S.D.(p=0.72322)	N.S.D.(p=0.0001077)	S.D.(p=0.07054)
12	S.D.(p=0.74197)	S.D.(p=0.74197)	N.S.D.(p=5.3539e-008)	N.S.D.(p=1.6576e-010)
S.D.	3	12	1	5

ST.ALBERT	CALIBRATION PERIOD		VALIDATION PERIOD	
Month	RCM (UNC.)	RCM (CORR.)	RCM (UNC.)	RCM (CORR.)
1	S.D.(p=0.12538)	S.D.(p=0.72814)	S.D.(p=0.29911)	N.S.D.(p=0.00013517)
2	S.D.(p=0.16952)	S.D.(p=0.59538)	N.S.D.(p=0.047626)	S.D.(p=0.059938)
3	N.S.D.(p=0.00019226)	S.D.(p=0.66025)	S.D.(p=0.25487)	N.S.D.(p=0.00027168)
4	N.S.D.(p=0.0020299)	S.D.(p=0.63966)	N.S.D.(p=0.0010851)	N.S.D.(p=0.018934)
5	N.S.D.(p=7.7165e-008)	S.D.(p=0.59204)	N.S.D.(p=2.1031e-005)	N.S.D.(p=0.02803)
6	N.S.D.(p=0.00046866)	S.D.(p=0.38691)	N.S.D.(p=2.9199e-007)	N.S.D.(p=1.1356e-006)
7	N.S.D.(p=0.001523)	S.D.(p=0.093551)	N.S.D.(p=6.3642e-006)	S.D.(p=0.40291)
8	N.S.D.(p=0.0011327)	S.D.(p=0.19161)	N.S.D.(p=3.0917e-005)	N.S.D.(p=6.5502e-005)
9	N.S.D.(p=0.0016139)	S.D.(p=0.33547)	S.D.(p=0.28075)	N.S.D.(p=0.039094)
10	N.S.D.(p=0.0011327)	S.D.(p=0.46424)	N.S.D.(p=0.010301)	N.S.D.(p=0.013362)
11	N.S.D.(p=0.029048)	S.D.(p=0.24698)	N.S.D.(p=0.0036953)	N.S.D.(p=0.0065465)
12	N.S.D.(p=0.0046884)	S.D.(p=0.71783)	N.S.D.(p=4.2168e-006)	N.S.D.(p=0.0060026)
S.D.	2	12	3	2

Appendix B: CRCM MODEL CALIBRATION AND VALIDATION RESULTS

(c) Calibration **(d) Validation**

Jan

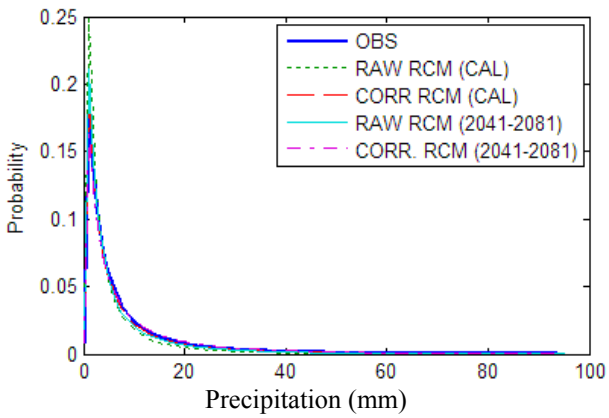

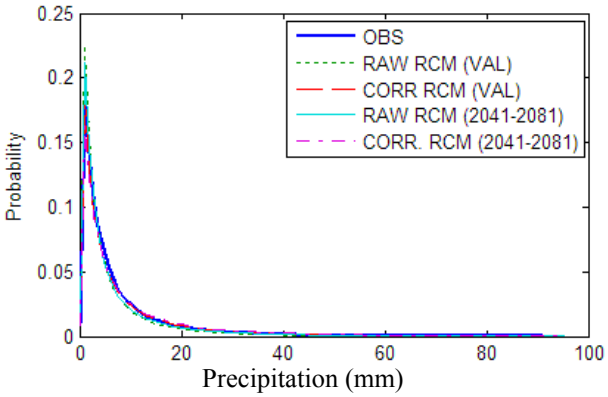

Feb

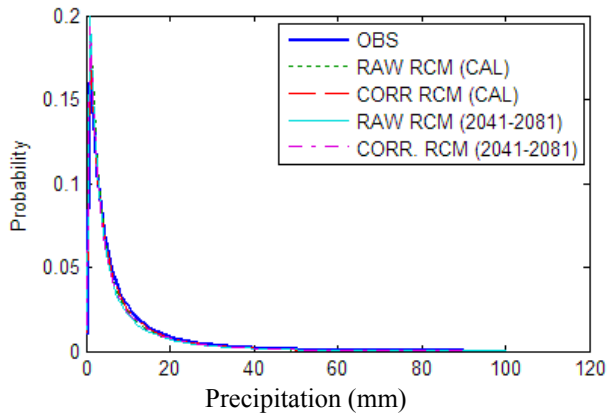

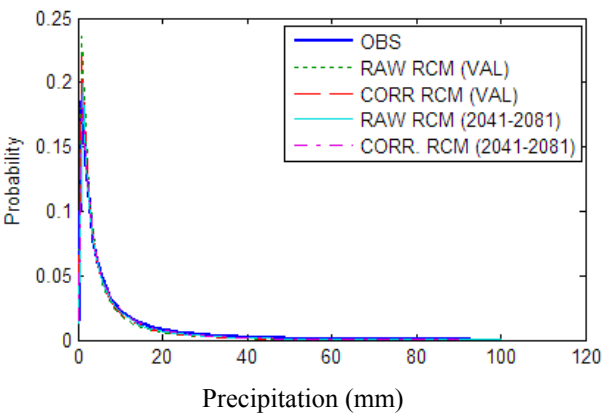

March

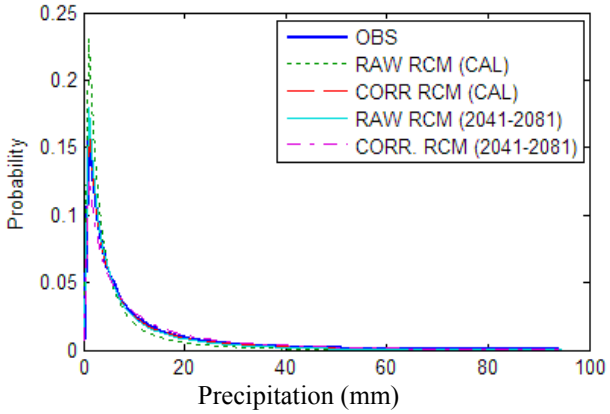

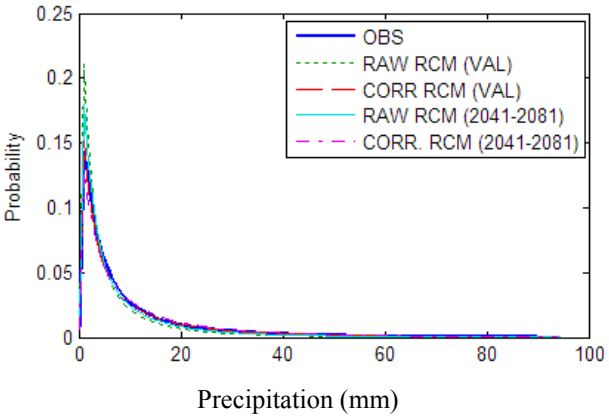

April

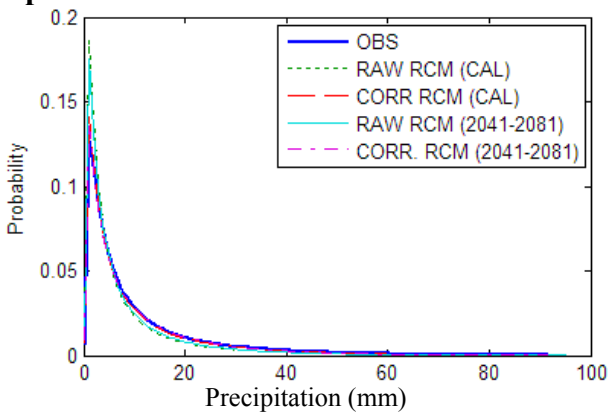

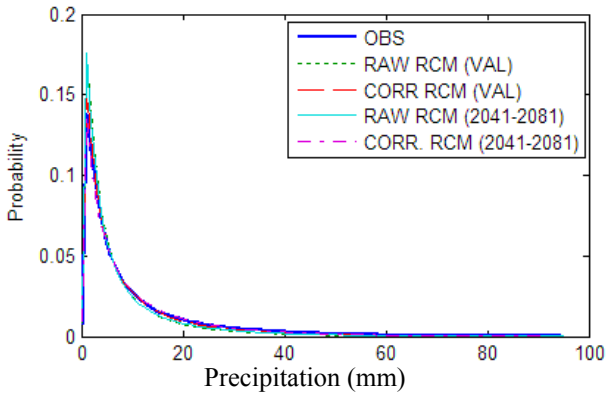

May

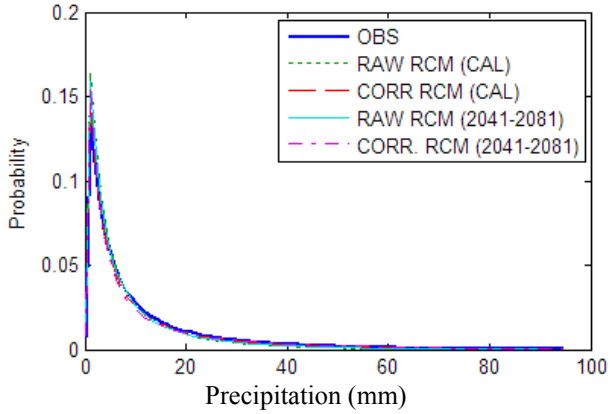

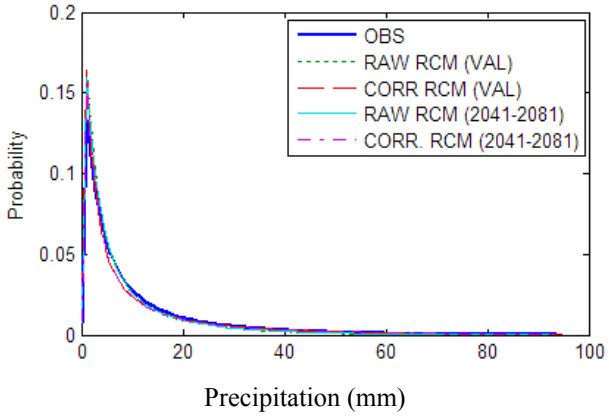

June

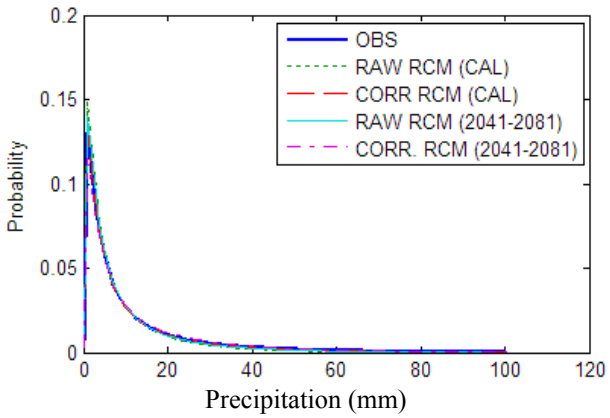

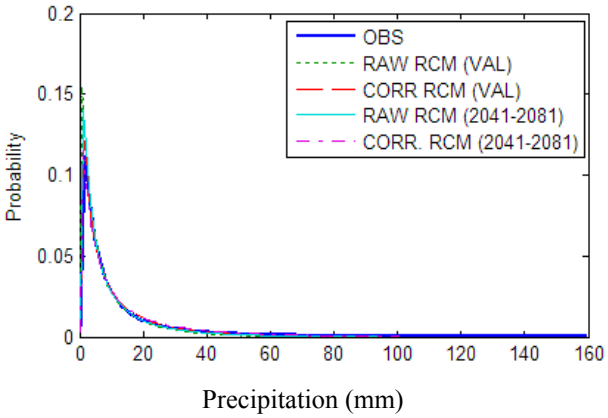

July

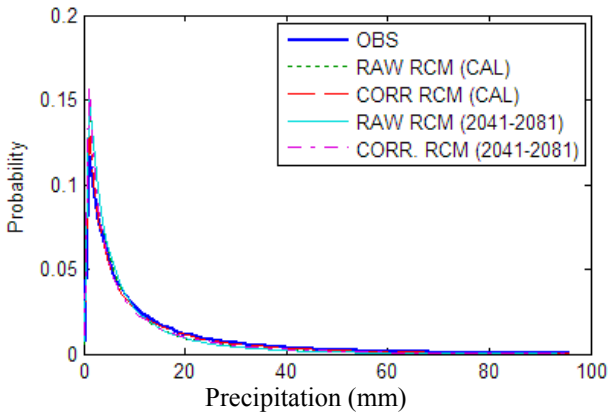

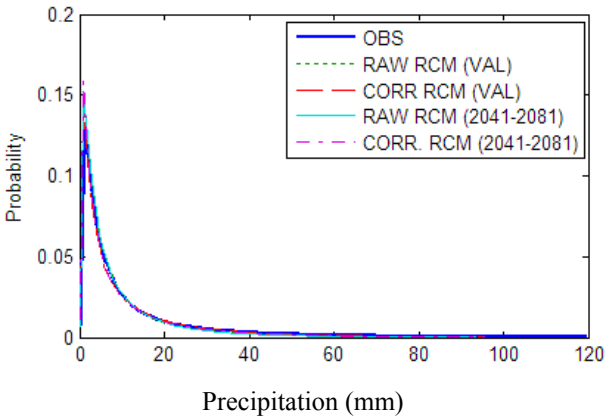

Aug

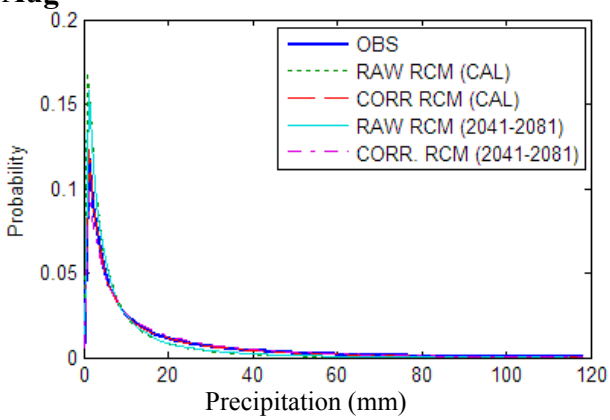

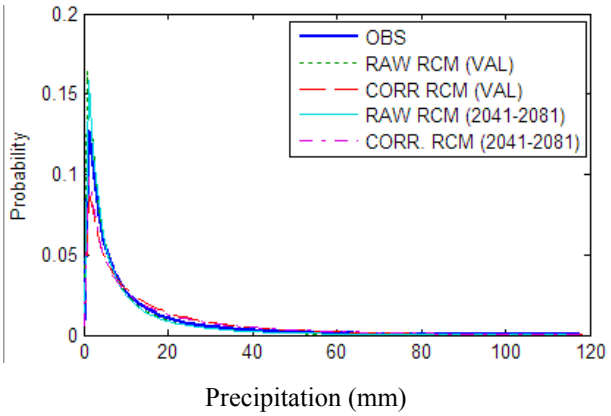

Sep

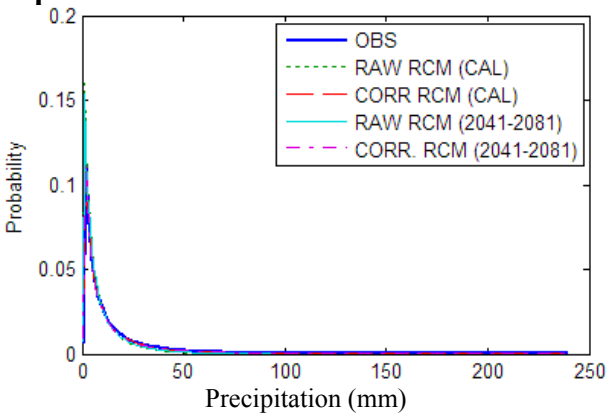
OBS
RAW RCM (CAL)
CORR RCM (CAL)
RAW RCM (2041-2081)
CORR. RCM (2041-2081)
Probability
Precipitation (mm)

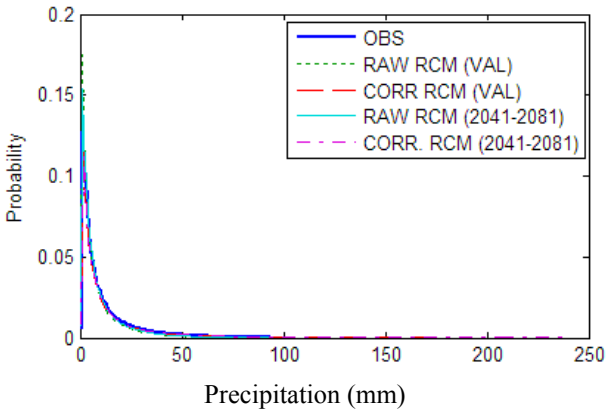
OBS
RAW RCM (VAL)
CORR RCM (VAL)
RAW RCM (2041-2081)
CORR. RCM (2041-2081)
Probability
Precipitation (mm)

Oct

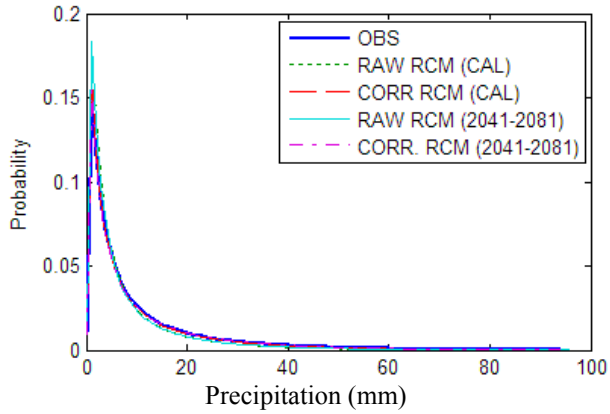
OBS
RAW RCM (CAL)
CORR RCM (CAL)
RAW RCM (2041-2081)
CORR. RCM (2041-2081)
Probability
Precipitation (mm)

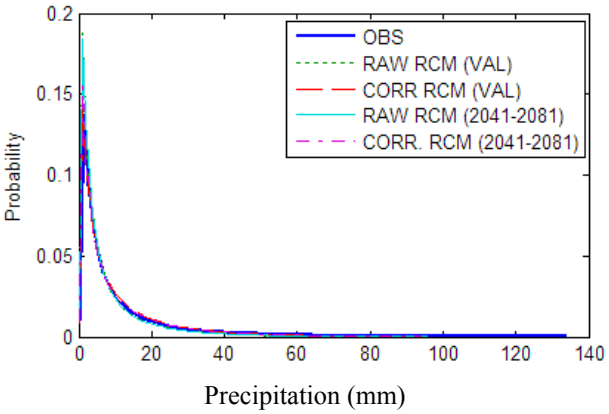
OBS
RAW RCM (VAL)
CORR RCM (VAL)
RAW RCM (2041-2081)
CORR. RCM (2041-2081)
Probability
Precipitation (mm)

Nov

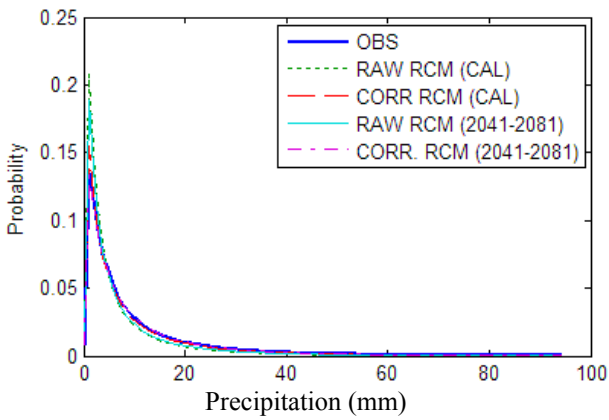
OBS
RAW RCM (CAL)
CORR RCM (CAL)
RAW RCM (2041-2081)
CORR. RCM (2041-2081)
Probability
Precipitation (mm)

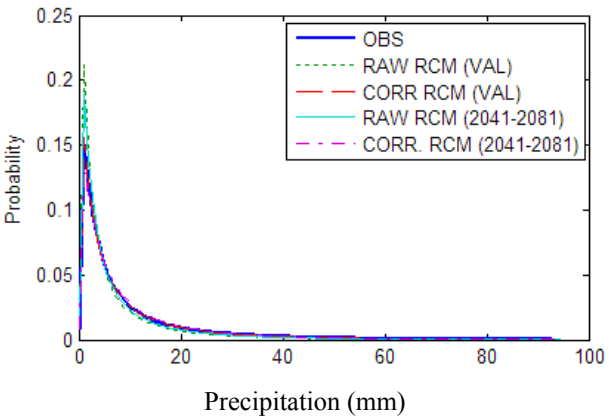
OBS
RAW RCM (VAL)
CORR RCM (VAL)
RAW RCM (2041-2081)
CORR. RCM (2041-2081)
Probability
Precipitation (mm)

Dec

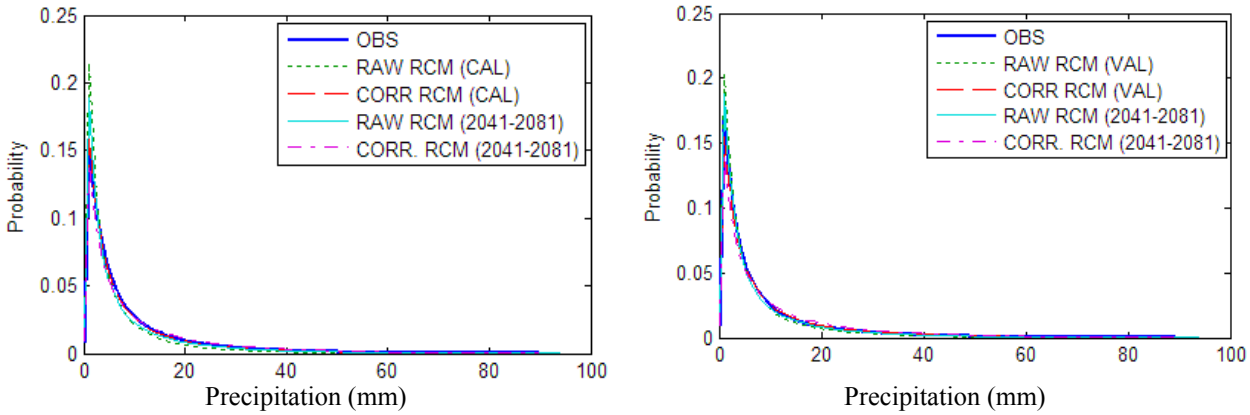

Figure B.1 Empirical monthly PDF of observed, raw, and corrected CRCM precipitation (mm d^{-1}) in the historical period (1961-2001) as well as future raw and corrected CRCM precipitation (2041-2081) over two periods: (a) calibration (left side) and (b) validation (right side) of Ottawa Airport station.

(c) Calibration **(d) Validation**

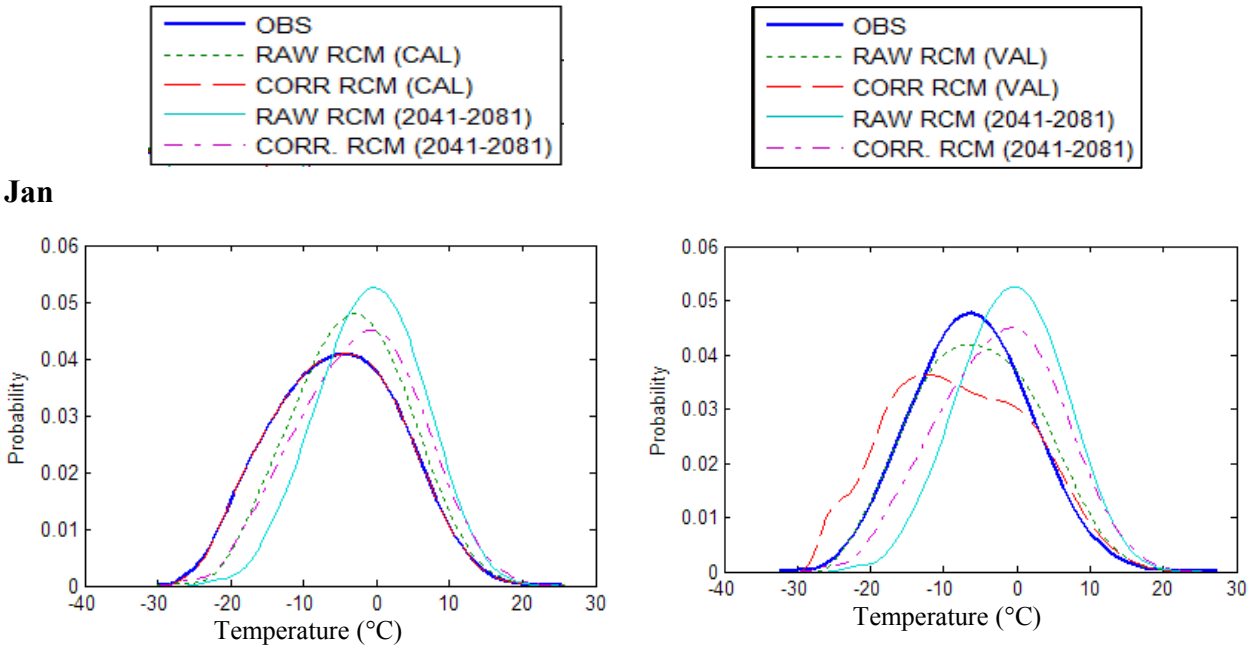

March

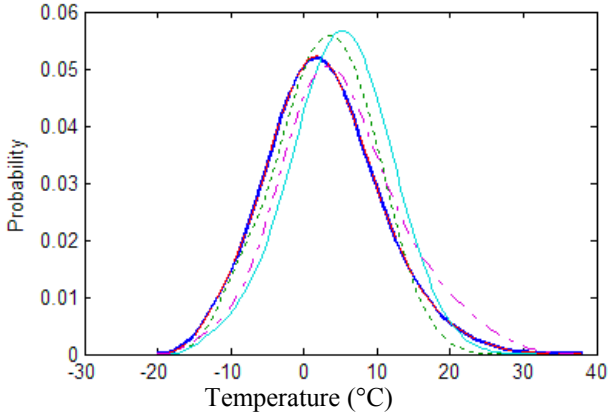

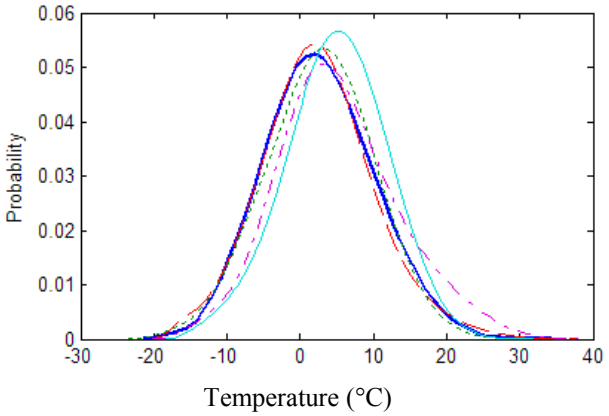

April

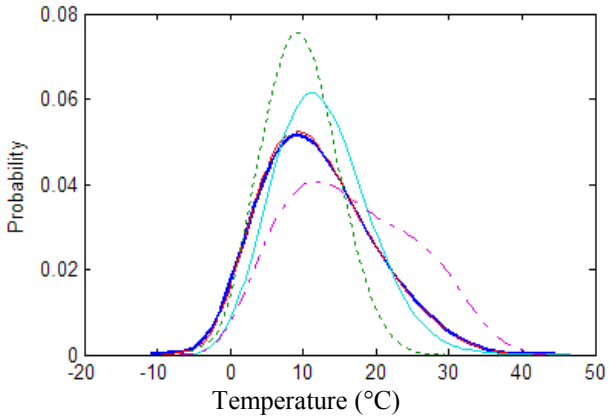

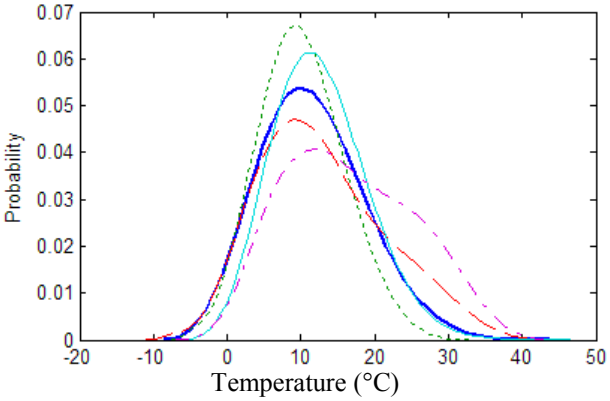

May

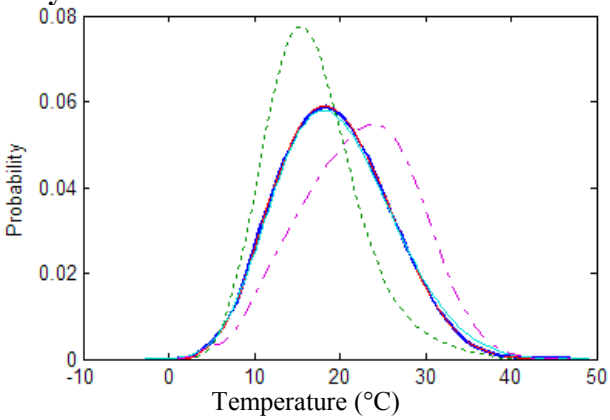

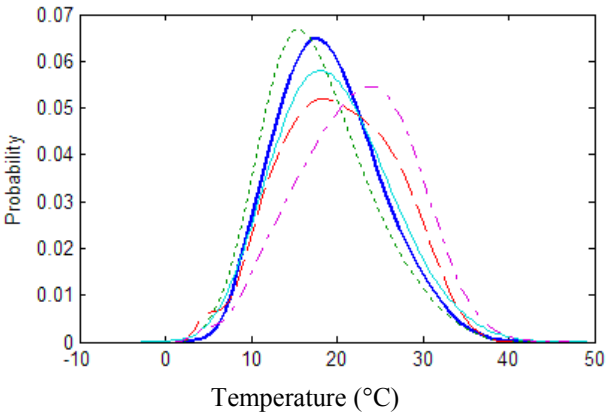

June

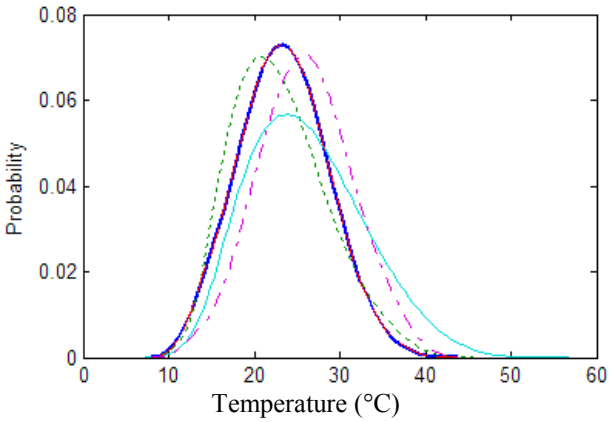

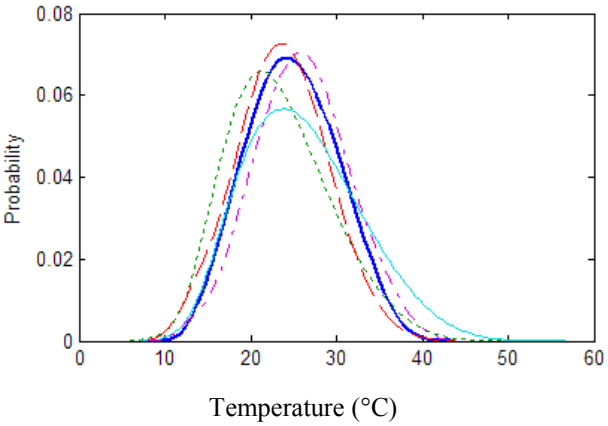

July

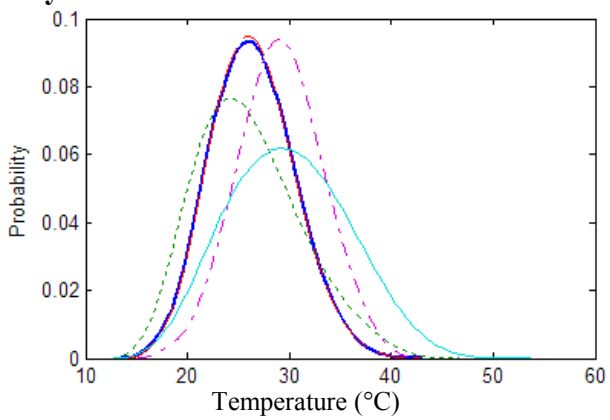

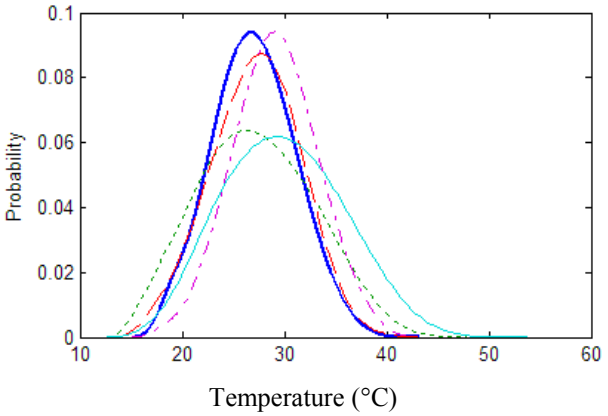

Aug

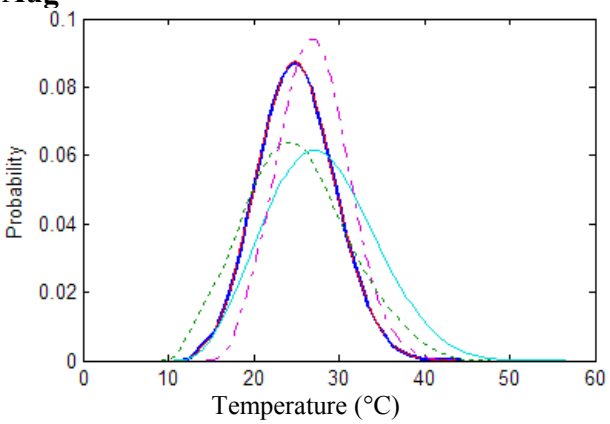

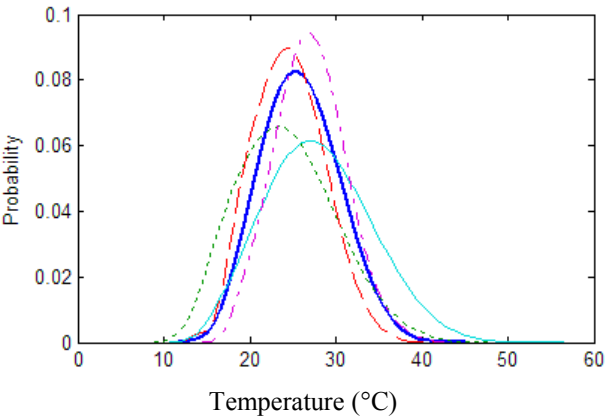

Sep

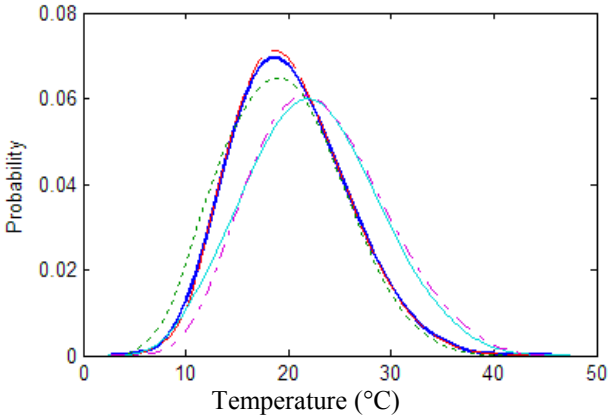
Probability
Temperature (°C)

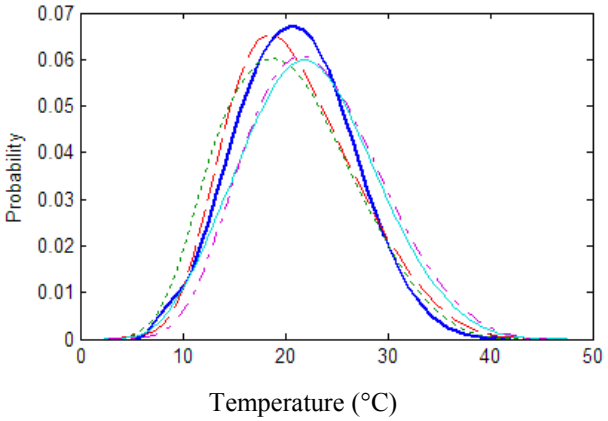
Probability
Temperature (°C)

Oct

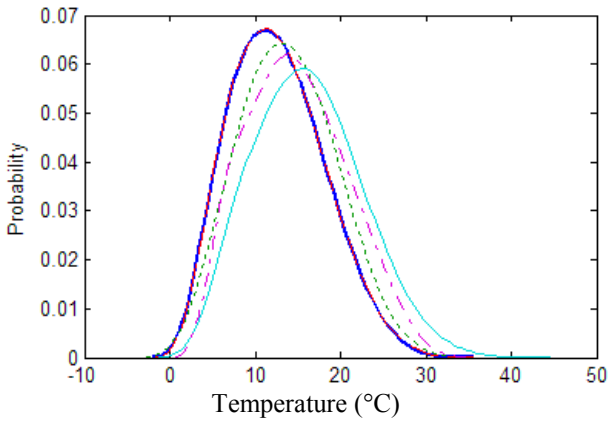
Probability
Temperature (°C)

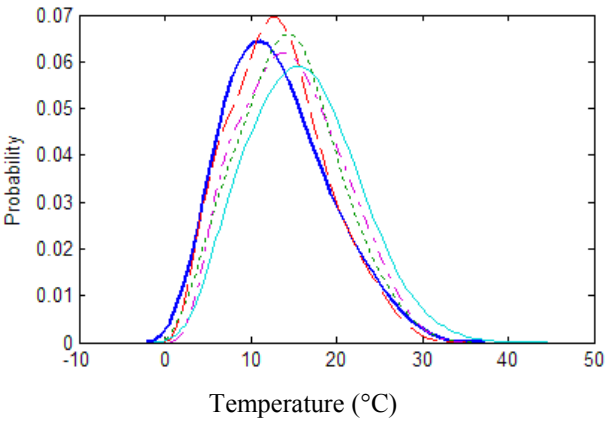
Probability
Temperature (°C)

Nov

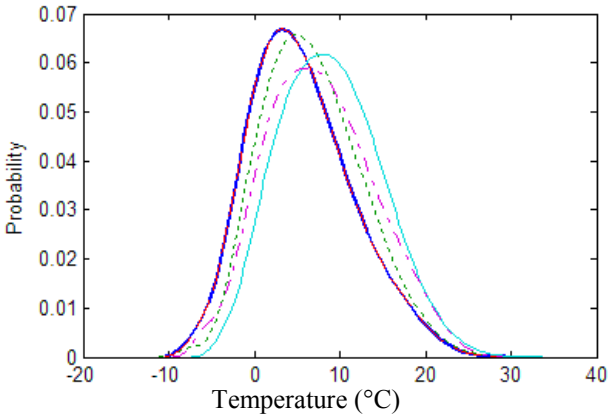
Probability
Temperature (°C)

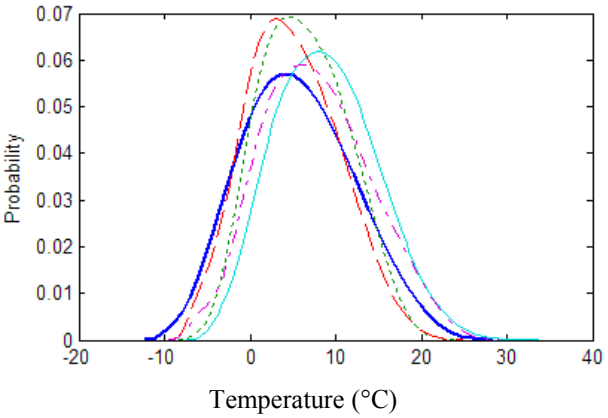
Probability
Temperature (°C)

Dec

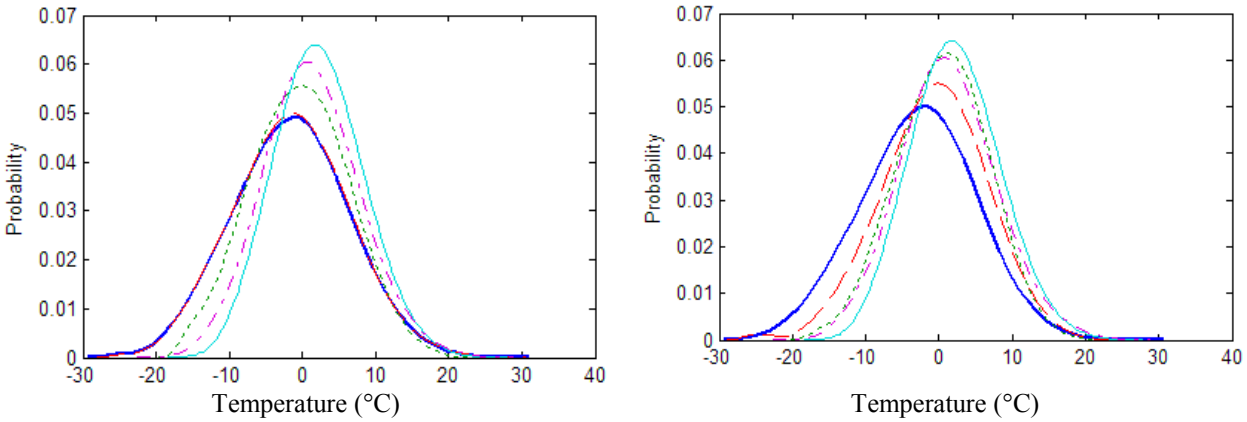

Figure B.2 Empirical monthly PDF of observed, raw, and corrected CRCM maximum temperature in the historical period (1961-2001) as well as future raw and corrected CRCM maximum temperature (2041-2081) over two periods: (a) calibration (left side) and (b) validation (right side) of Ottawa Airport station.

(c) Calibration **(d) Validation**

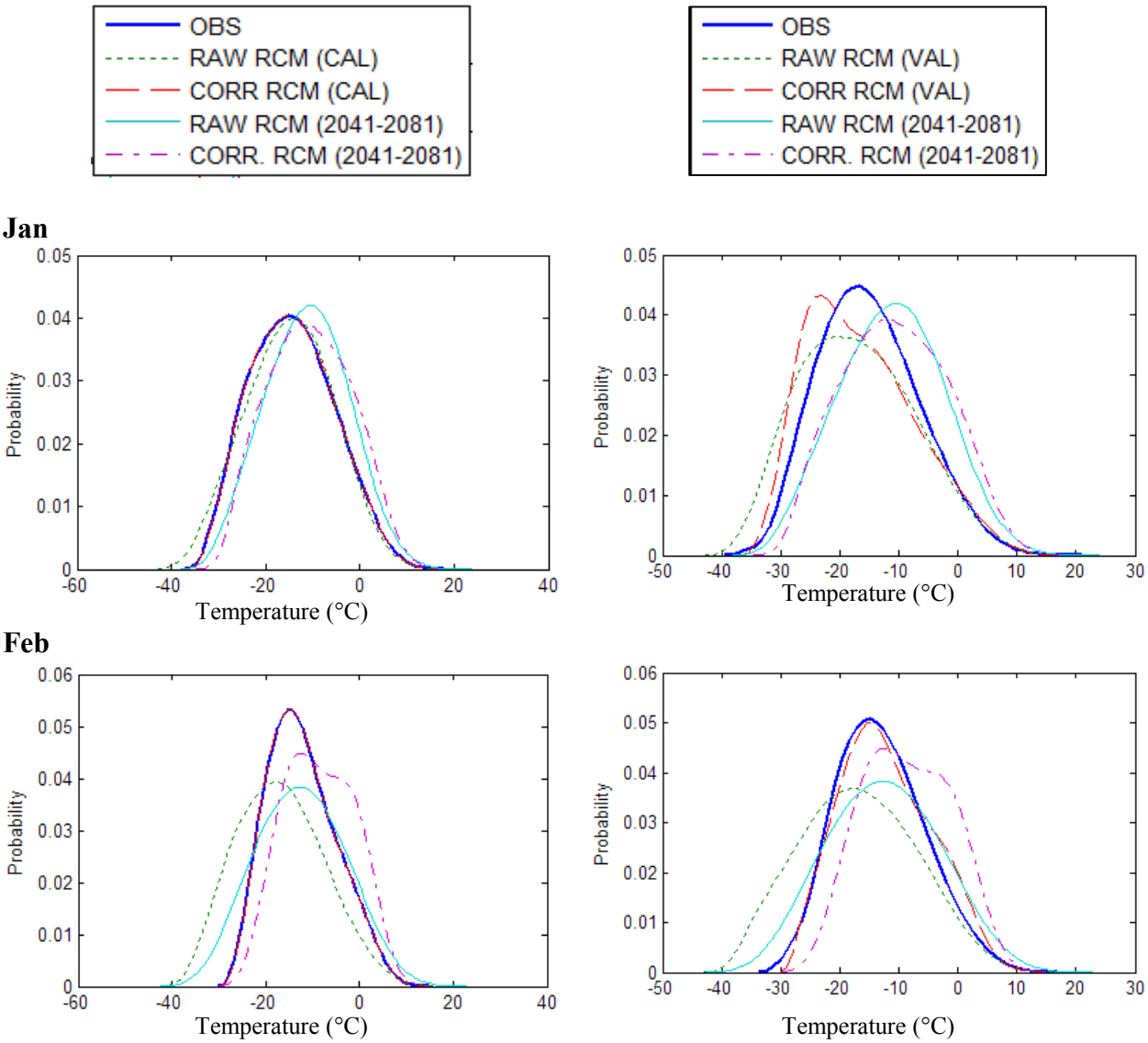

March

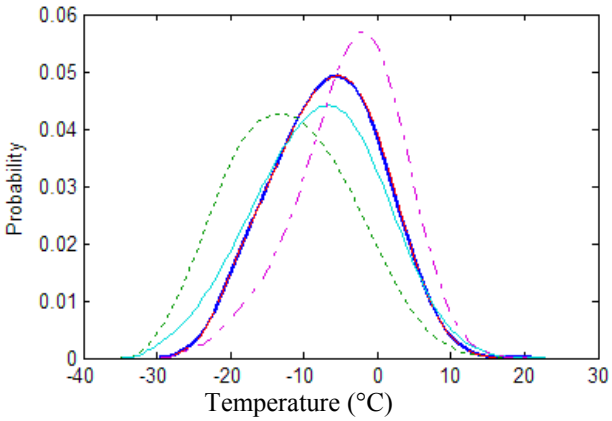

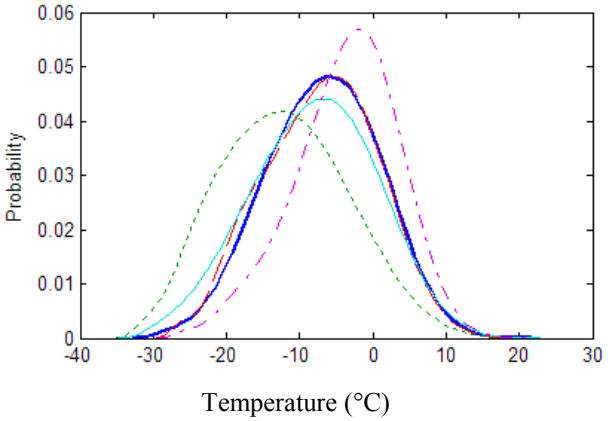

April

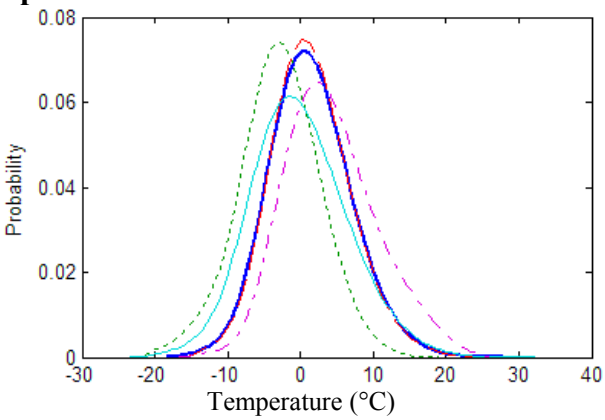

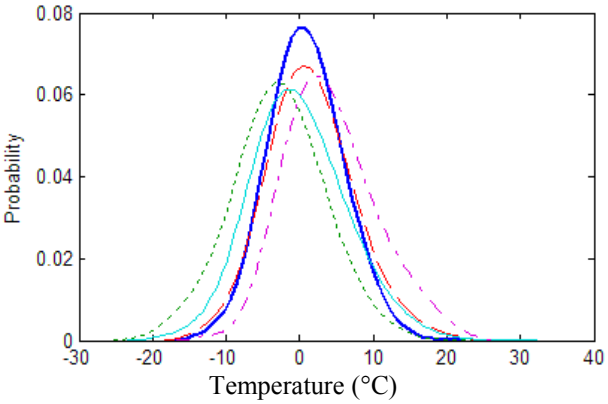

May

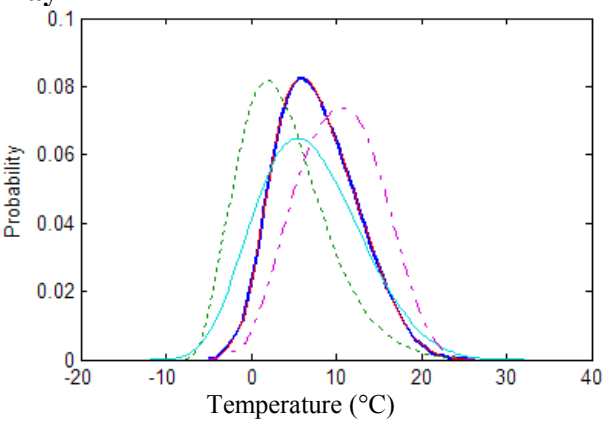

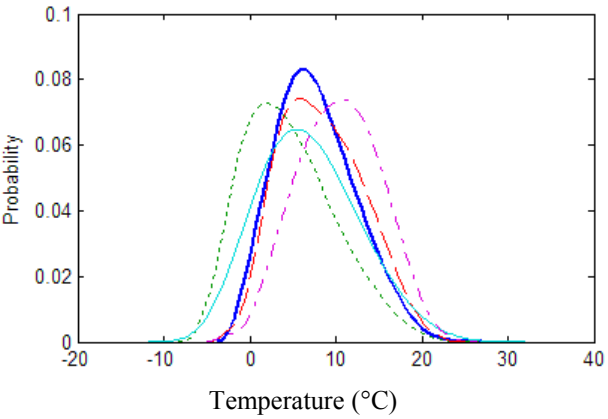

June

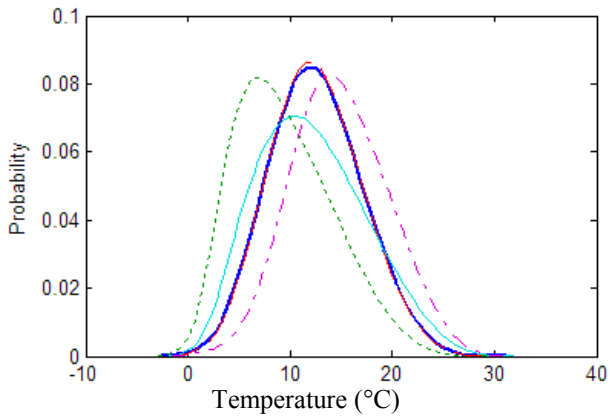

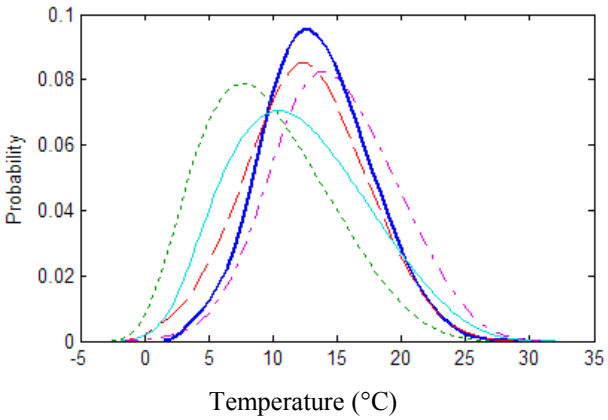

July

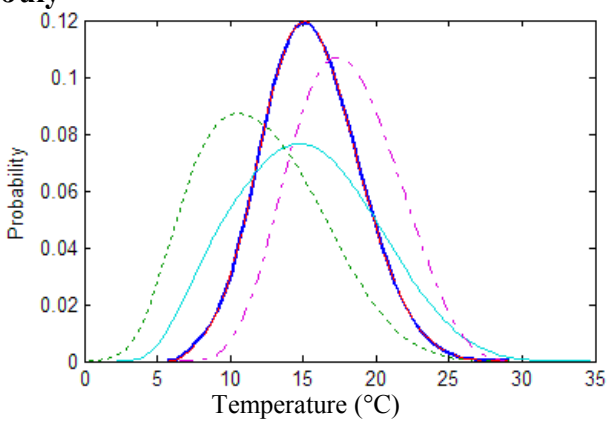

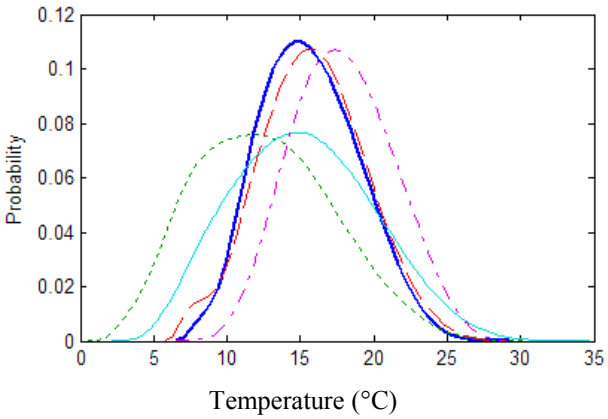

Aug

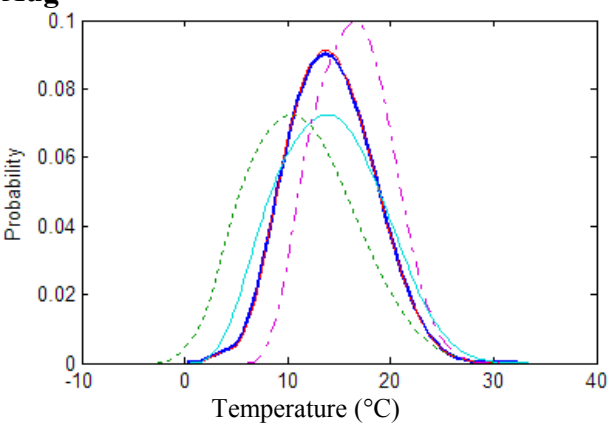

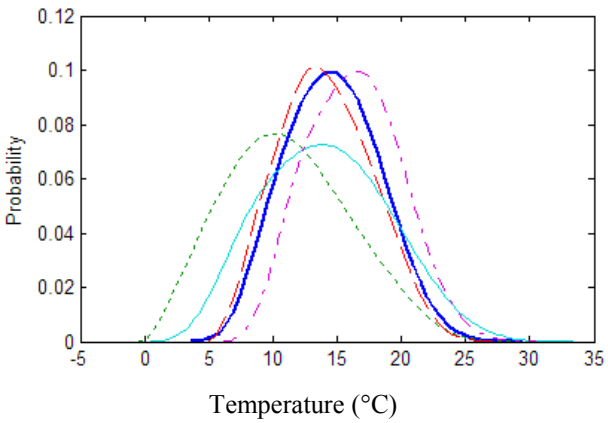

Sep

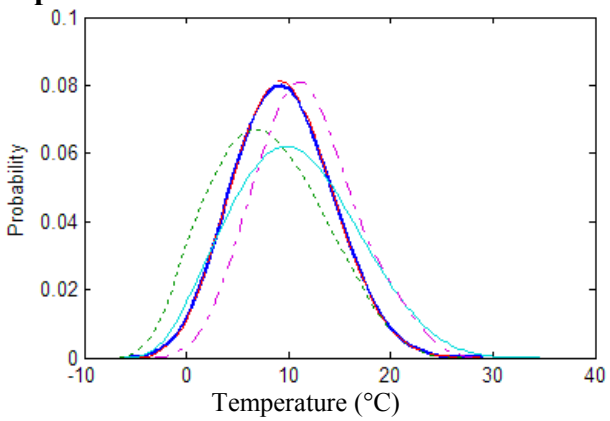
Probability
Temperature (°C)

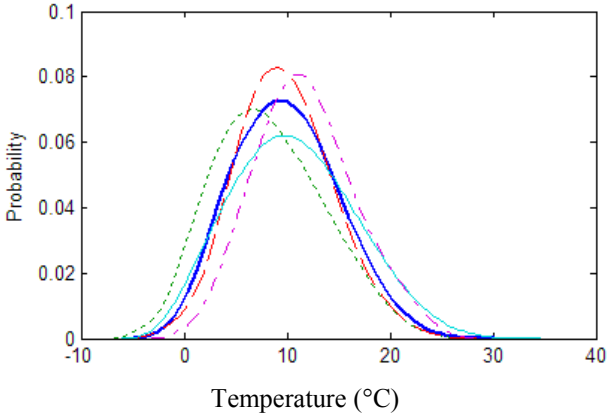
Probability
Temperature (°C)

Oct

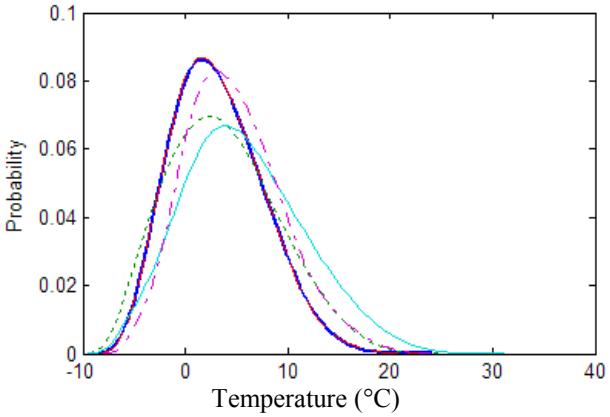
Probability
Temperature (°C)

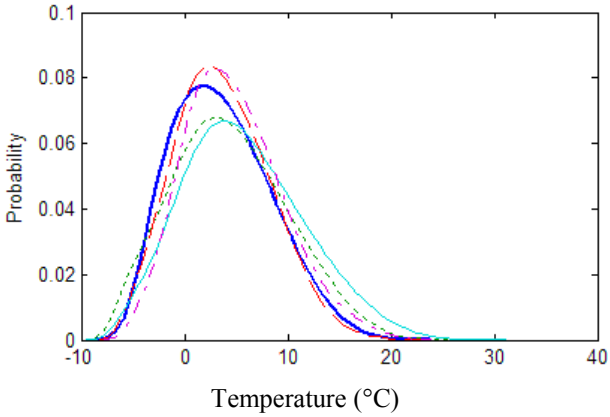
Probability
Temperature (°C)

Nov

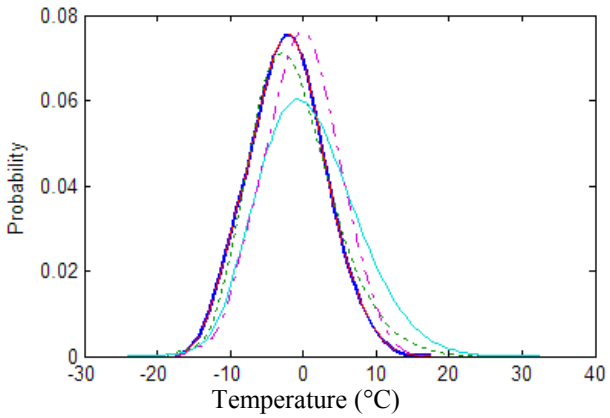
Probability
Temperature (°C)

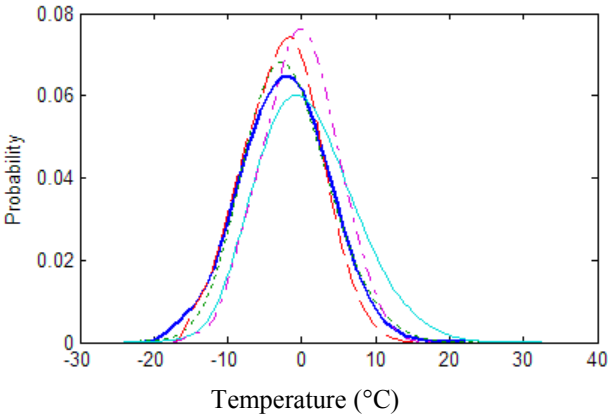
Probability
Temperature (°C)

Dec

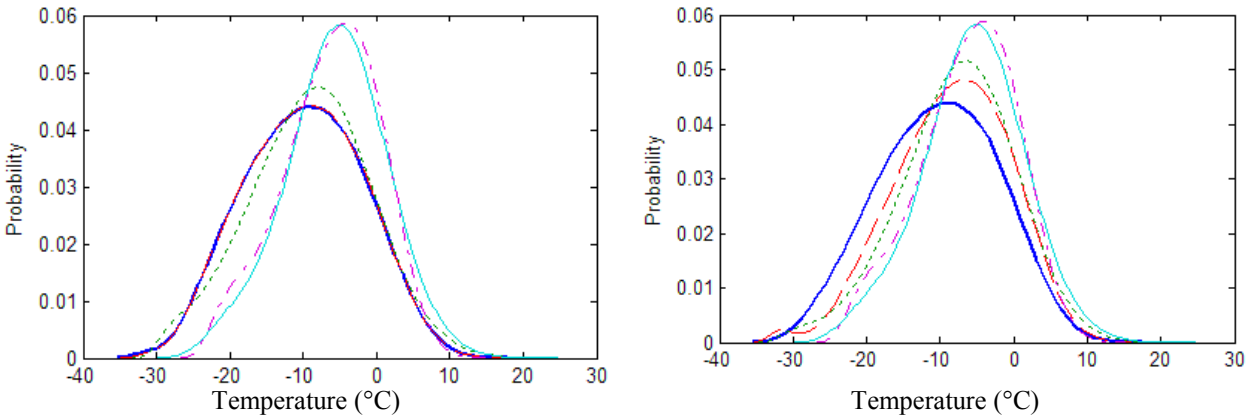

Figure B.3 Empirical monthly PDF of observed, raw, and corrected CRCM minimum temperature in the historical period (1961-2001) as well as future raw and corrected CRCM minimum temperature (2041-2081) over two periods: (a) calibration (left side) and (b) validation (right side) of Ottawa Airport station.

(c) Calibration **(d) Validation**

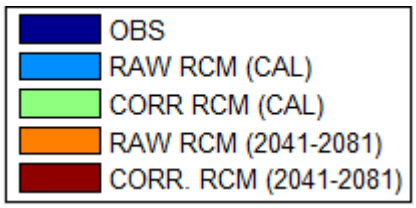

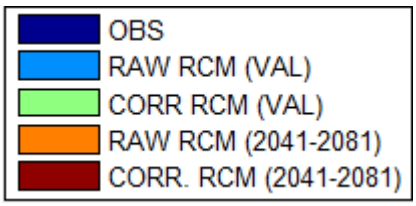

Jan

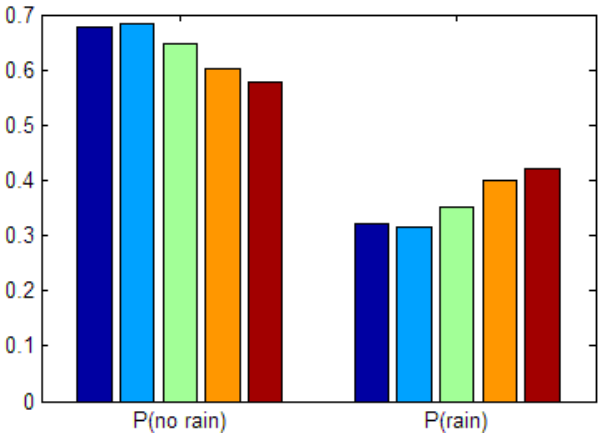

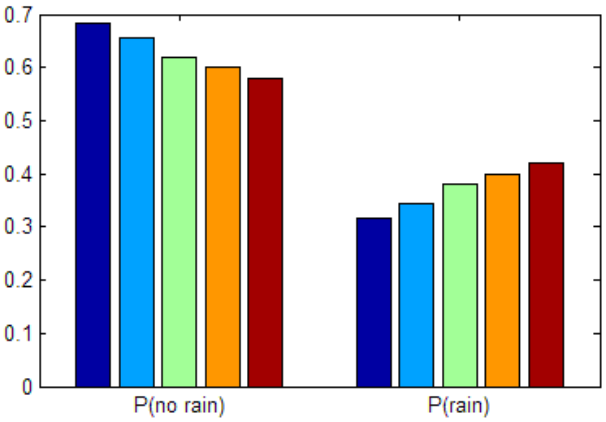

Feb

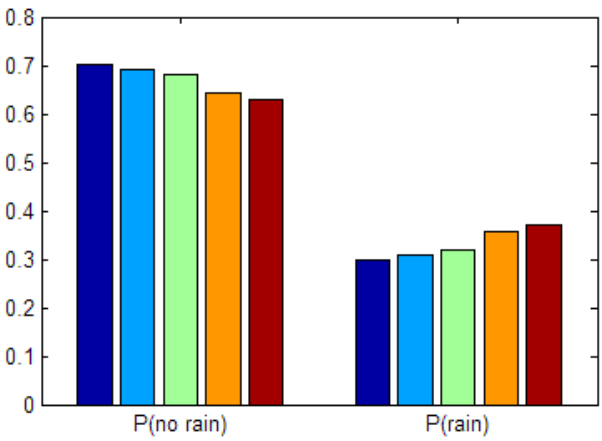

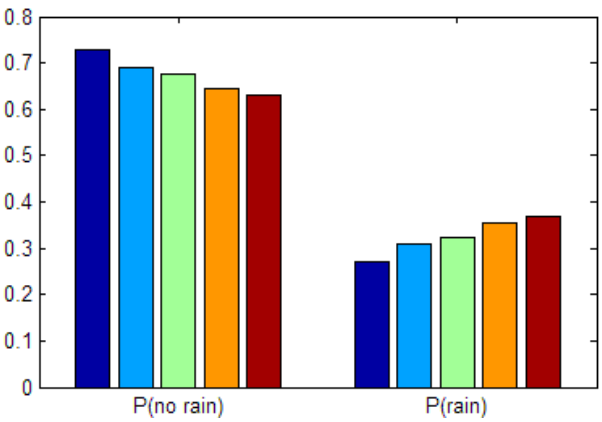

March

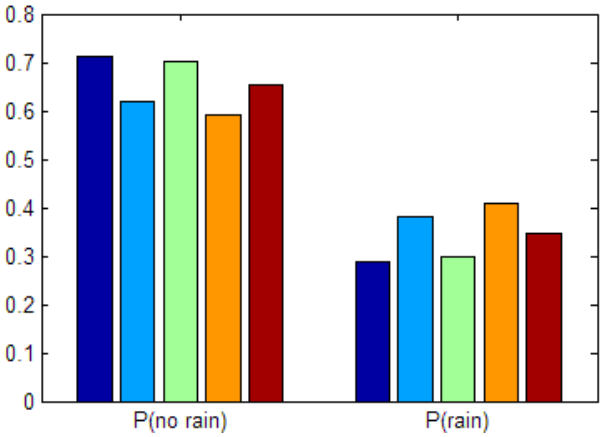

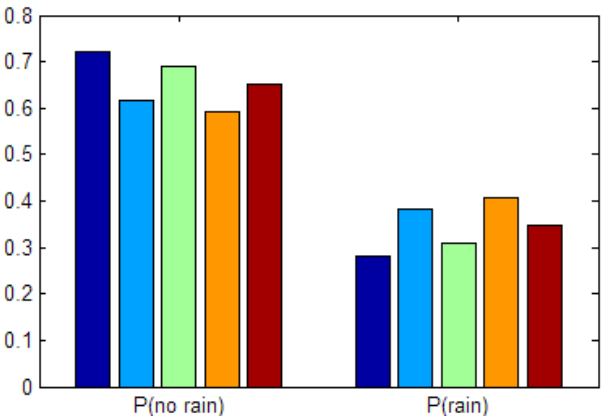

April

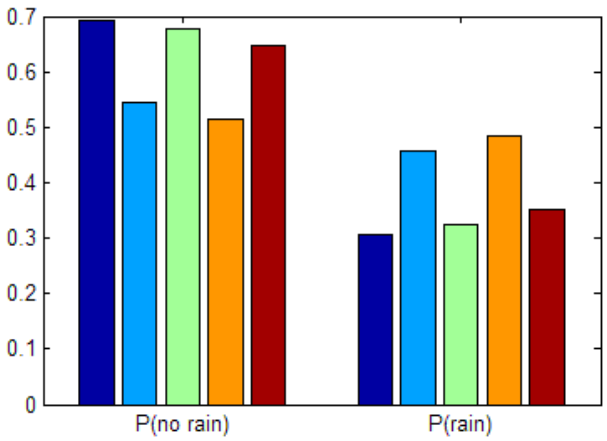

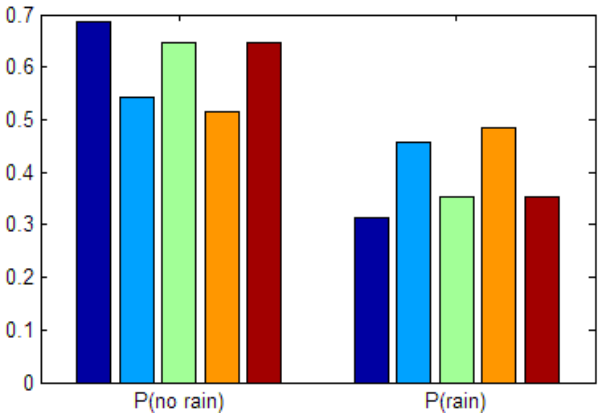

May

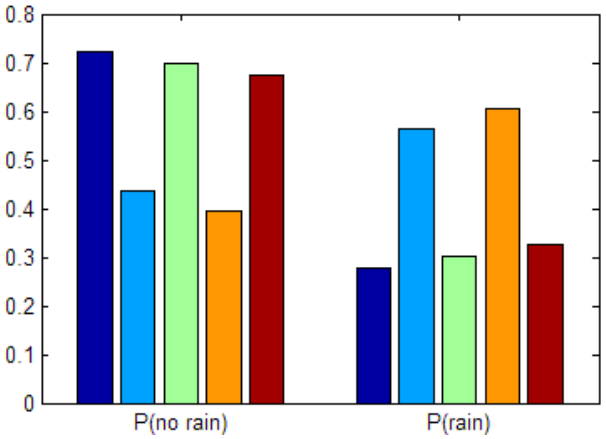

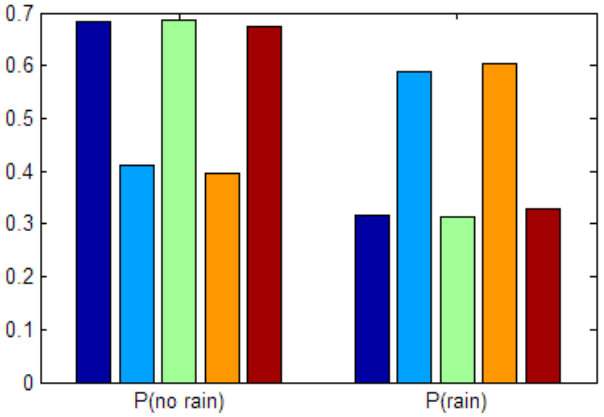

June

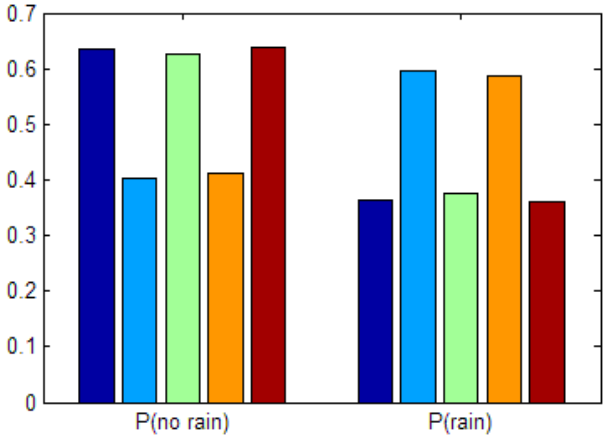

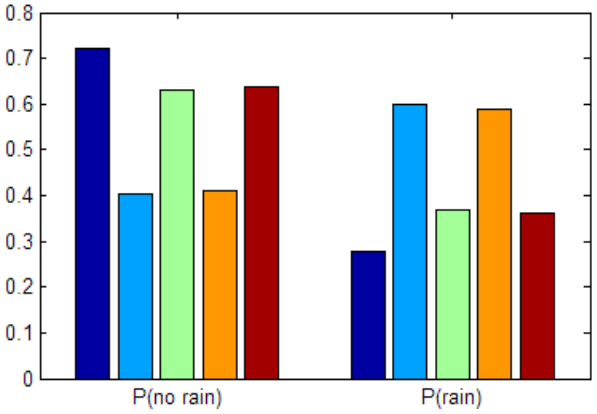

July

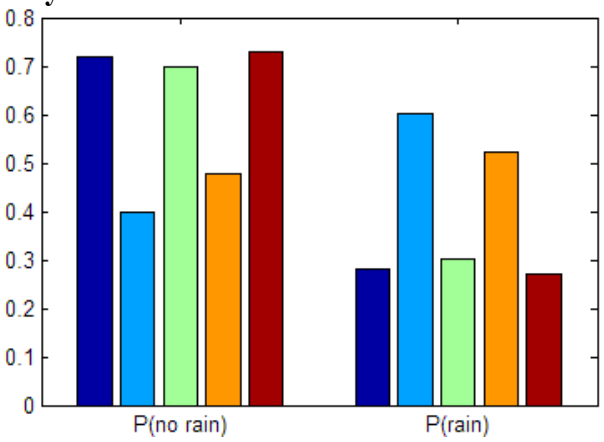

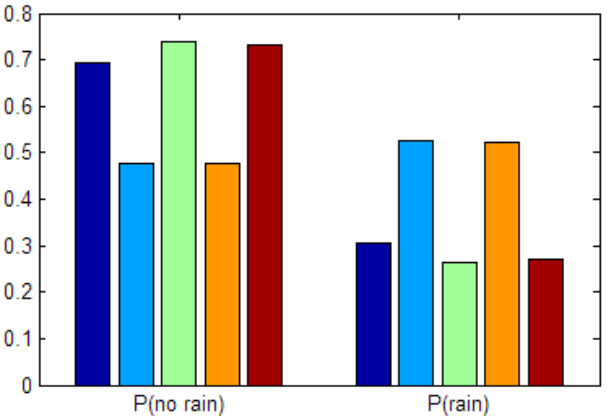

Aug

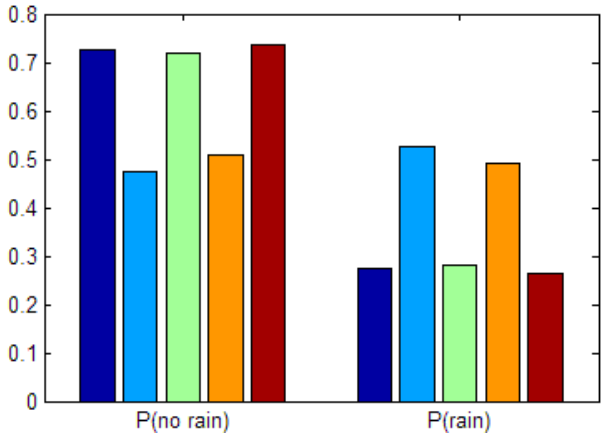
0.8
0.7
0.6
0.5
0.4
0.3
0.2
0.1
0
P(no rain)
P(rain)

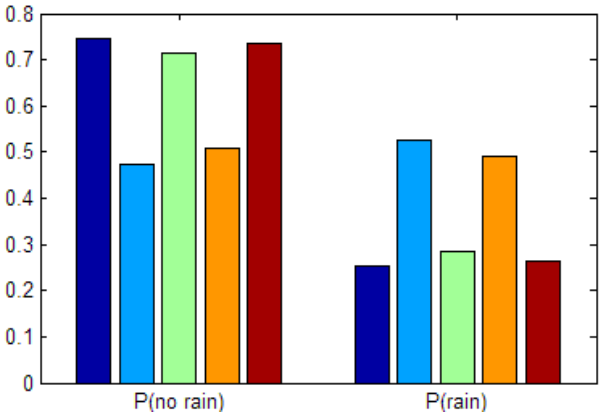
0.8
0.7
0.6
0.5
0.4
0.3
0.2
0.1
0
P(no rain)
P(rain)

Sep

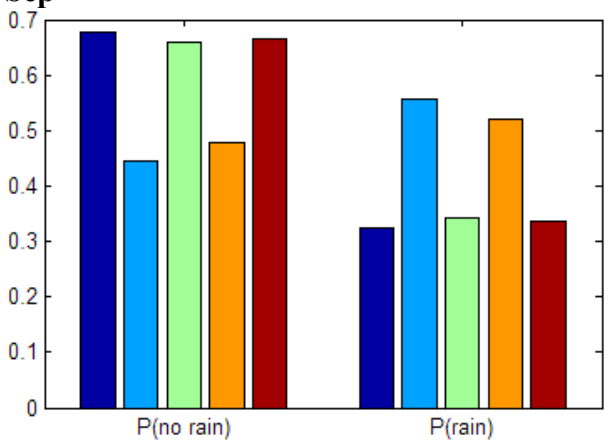
0.7
0.6
0.5
0.4
0.3
0.2
0.1
0
P(no rain)
P(rain)

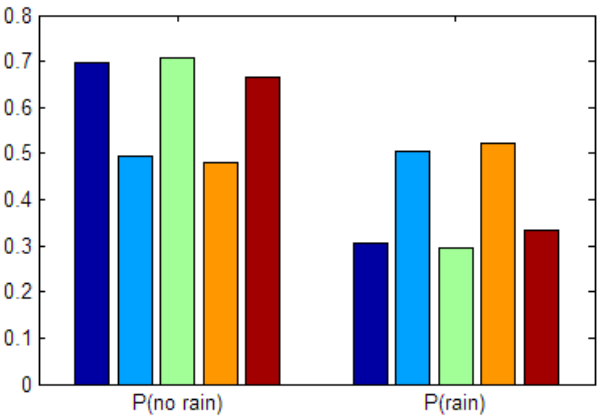
0.8
0.7
0.6
0.5
0.4
0.3
0.2
0.1
0
P(no rain)
P(rain)

Oct

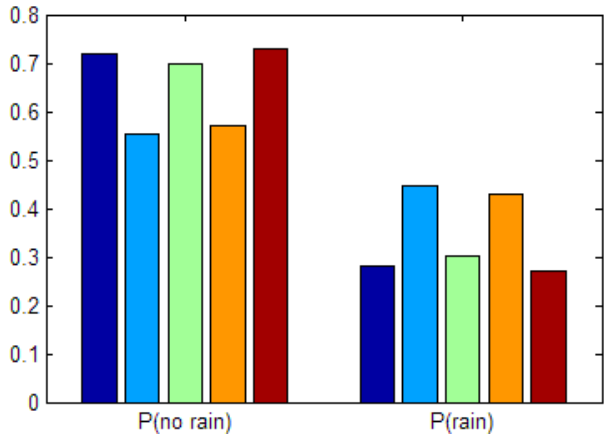
0.8
0.7
0.6
0.5
0.4
0.3
0.2
0.1
0
P(no rain)
P(rain)

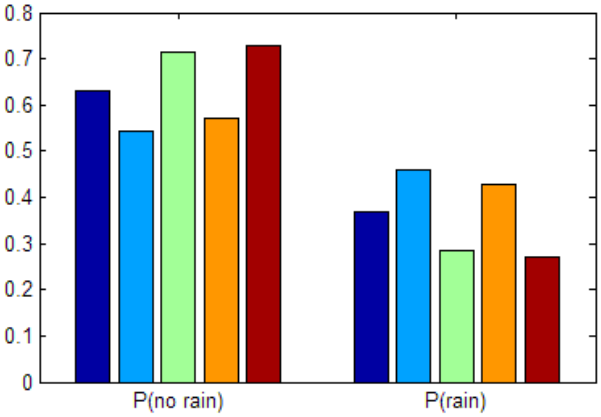
0.8
0.7
0.6
0.5
0.4
0.3
0.2
0.1
0
P(no rain)
P(rain)

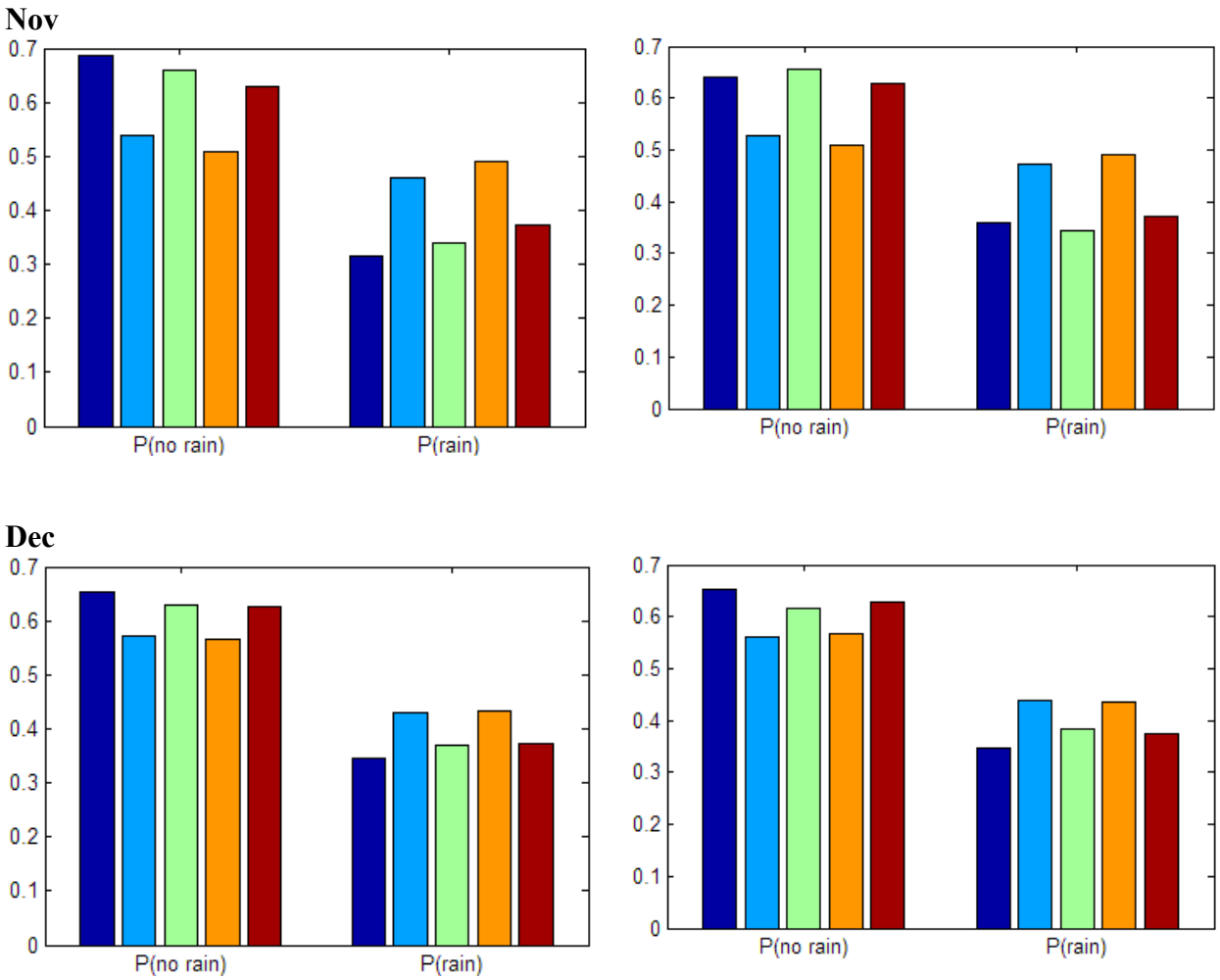

Figure B.4 Probability of 1 mm precipitation of observed, raw, and corrected CRCM in the historical period (1961-2001) as well as future raw and corrected CRCM precipitation occurrence (2041-2081) over two periods: (a) calibration (left side) and (b) validation (right side) of Ottawa Airport station.